Analysis of Protein Interactions Controlling DNA Methyltransferases

Karin Fellinger

München 2009

Analysis of Protein Interactions Controlling DNA Methyltransferases

Karin Fellinger

Dissertation
der Fakultät für Biologie
der Ludwig-Maximilians-Universität
München

vorgelegt von
Karin Fellinger
aus München

München, den 28. Januar 2009

Erstgutachter: Prof. Dr. Heinrich Leonhardt
Zweitgutachter: Prof. Dr. Peter Becker

Tag der mündlichen Prüfung: 20.03.2009

Contents

SUMMARY **1**

1. INTRODUCTION **3**

1.1 Protein-Protein Interactions 4
1.2 Establishment and Maintenance of DNA Methylation 13
1.3 The Epigenetic Protein Network 18

2. RESULTS **25**

2.1 A Mutagenesis Strategy Combining Systematic Alanine Scanning with Larger Mutations to Study Protein Interactions 27
2.2 Biochemical Analysis of Intramolecular N-C Terminal Dnmt1 Interactions 36
2.3 Dimerization of DNA Methyltransferase 1 is Mediated by its Regulatory Domain 41
2.4 Np95 Controls Maintenance of DNA Methylation by Interaction with DNA Methyltransferase 1 68
2.5 Np95 Interacts with *de novo* DNA Methyltransferases Dnmt3a and 3b and Mediates Epigenetic Silencing 77

3. DISCUSSION **101**

3.1 Mutagenesis Strategies to Study Protein-Protein Interactions 101
3.2 Biochemical Analysis of N-C Terminal Dnmt1 Interactions 104
3.3 The N-Terminal TS Domain Mediates Dnmt1 Dimerization 109
3.4 Np95 is a Key Regulator of DNA Methyltransferases 111

4. ANNEX **117**

4.1 References 117
4.2 Contributions 129
4.3 Declaration According to the "Promotionsordnung der LMU München für die Fakultät Biologie" 131
4.4 Abbreviations 133
4.5 List of Expression Constructs 135
4.6 Acknowledgements 139

5. CURRICULUM VITAE **143**

Summary

Epigenetic mechanisms control a multitude of processes in mammalian development such as X-chromosome inactivation, genomic imprinting and cellular differentiation, but if misregulated they also cause diseases as cancer. Complex molecular networks regulate patterns of DNA methylation and histone modifications that give rise to distinct gene expression profiles.

In this study we analyzed the family of DNA methyltransferases (Dnmts) that are responsible for the establishment and maintenance of DNA methylation patterns. To elucidate their role and regulation in the epigenetic protein network we identified and characterized intra- and intermolecular interactions of Dnmts. For this purpose, we first developed a fast and robust alanine scanning mutagenesis method that allowed the streamlined generation of point, deletion and insertion mutants and the establishment of a Dnmt protein variant library as basis for further analysis.

As the methyltransferase activity of Dnmt1 requires allosteric activation of the C-terminal catalytic domain through its regulatory N-terminal domain, we determined the relevant regions for this interaction within the N-terminal domain. While the CXXC zinc finger (amino acids (aa) 648-694) and phosphorylation of serine 515 were dispensable, a major part of the N-terminal regulatory domain was necessary for interaction with the catalytic domain. These results point to the importance of structural integrity of the regulatory domain for allosteric activation of Dnmt1. Moreover, we observed that Dnmt1 forms stable dimers through its N-terminal regulatory domain. Mutational analyses mapped the dimerization domain to a bipartite interaction surface in the targeting sequence domain (TS, aa 310-629) that is also known to be responsible for recruiting Dnmt1 to heterochromatin.

Similar to the targeted disruption of the *dnmt1* gene, knockout of Np95 was reported to result in global hypomethylation in ES cells (ESCs). Therefore, we examined the role of Np95 in the regulation of DNA methylation. We mapped and characterized the interaction between Dnmt1 and Np95 and found that the TS domain of Dnmt1 mediates this interaction and a small deletion within the highly conserved core region of the TS domain abolished the interaction with Np95. This Np95 interaction mutant showed catalytic activity on oligonucleotide DNA in a radioactive methyltransferase assay. However, it failed to restore methylation patterns in *dnmt1*$^{-/-}$ ESCs. These results indicate that Np95 facilitates access of Dnmt1 to DNA target sites in chromatin.

In addition, we found an interaction of Np95 with the N-terminal domains of the *de novo* DNA methyltransferases Dnmt3a and Dnmt3b which is even stronger than the interaction with Dnmt1. Interestingly, we observed no transgene silencing in *np95*$^{-/-}$ or *dnmt1*$^{-/-}$*3a*$^{-/-}$*3b*$^{-/-}$ (TKO) ESCs in contrast to wildtype or *dnmt1*$^{-/-}$ ESCs indicating that both, Np95 and the *de novo* DNA methyltransferases are required for promoter silencing in ESCs. These results assign a crucial role to Np95 in epigenetic silencing and make it an interesting target for epigenetic reprogramming.

In summary, we developed a versatile mutagenesis strategy that allows efficient generation of protein variant libraries. We mapped and characterized intra- and intermolecular interactions of DNA methyltransferases. The TS domain of Dnmt1 that is located in the center of the N-terminus harbors several regulatory functions: It is necessary for allosteric activation of the catalytic domain, mediates dimerization of Dnmt1 and its interaction with Np95 recruits Dnmt1 to pericentric heterochromatin. Beside a complex regulation of Dnmts through interactions within the Dnmt family, other chromatin factors such as Np95 function as key regulators for DNA methylation.

1. Introduction

Epigenetics is defined as the study of heritable changes in genome function that occur without a change in DNA sequence. Epigenetic mechanisms are responsible for numerous processes during development such as X-chromosome inactivation, imprinting and cellular differentiation but missregulation can lead to diseases as cancer. A highly complex interplay between chromatin modifying proteins generates distinct patterns of histone modifications and DNA methylation that give rise to specific gene expression profiles. To date, many epigenetic factors that establish, maintain and change the epigenetic landscape in the nucleus have been identified. However, the spatial and temporal coordination of this epigenetic protein network is not yet understood in detail. DNA methylation at CpG dinucleotides is a crucial epigenetic modification associated with gene silencing. We study the role and regulation of the DNA methyltransferase family that establishes and maintains DNA methylation patterns to elucidate the underlying mechanisms.

The aim of this study is a detailed biochemical and cell biological analysis of DNA methyltransferases, focusing on the maintenance DNA methyltransferase1 (Dnmt1), to achieve a better comprehension of the regulation of DNA methyltransferases within the epigenetic protein network. The first goal of this study was the development of a fast and reliable mutagenesis method that allows mapping of interacting protein regions from protein domains to single amino acids. Consequently, specific interaction mutants can be characterized to determine their functional consequences. The second objective was a detailed biochemical analysis of Dnmt1 to identify and characterize intramolecular and intermolecular interactions that regulate the enzyme. Dnmt1 contains a unique regulatory N-terminal domain. The intramolecular interaction between the regulatory N-terminal domain and the catalytic C-terminal domain is indispensable for the allosteric activation of Dnmt1. Therefore, we determined the parts of this N-terminal domain that are necessary for N-C-terminal interaction and hence Dnmt1 catalytic activity. Moreover, biochemical analysis of Dnmt1 revealed that Dnmt1 forms stable dimers via the central part of the N-terminal regulatory domain. Third, we aimed for the identification and characterization of new interaction partners of DNA methyltransferases. We found that Np95 interacts not only with the maintenance DNA methyltransferase1 but also with the *de novo* DNA methyltransferases3a and 3b and functions as key regulator of DNA methylation.

1.1 Protein-Protein Interactions

Protein-protein interactions play a central role in biological processes such as DNA replication, transcription, translation, splicing, secretion, cell cycle control or signal transduction. To understand the molecular mechanisms regulating the establishment and maintenance of DNA methylation, we study the protein network around DNA methyltransferases. Taking advantage of various methods, we identify interacting proteins, map interacting domains and respective amino acids and characterize the function of these interactions.

1.1.1 Mutagenesis Strategies to Generate Protein Variants

Site-directed mutagenesis (SDM) is a fundamental approach to study the contribution of single amino acid side chains to the properties of proteins. Alanine-scanning mutagenesis has been successfully used to assess protein structure function relationships and systematically map functional binding sites (Ashkenazi et al., 1990; Cunningham and Wells, 1989; Matthews, 1996). Many commercially available site-directed mutagenesis kits offer fast protocols that are based on PCR-primers harboring the mutation (Hogrefe et al., 2002; Zhu et al., 2007). However, those strategies contain one or more disadvantages: First, they either lack a marker to select mutant clones (Invitrogen, Genetailor SDM system), or, if it is included, the procedure gets more time-consuming: Either prior transfer to a special vector or two rounds of transformation in different *E.coli* strains are necessary (Clontech, Transformer SDM Kit; (Andrews and Lesley, 1998; Deng and Nickoloff, 1992). Second, mutations are placed in oligonucleotide primers and the complete vector DNA has to be amplified risking the acquisition of additional unwanted mutations. In some cases the template DNA has to be eliminated by an additional digestion step, e.g. with *DpnI* (Stratagene, QuikChange SDM kit; Clontech, Transformer SDM kit). Third, the creation of single point mutants, deletions and insertions is not only limited to a certain number of bases but also the size of the target vector is restricted to 8-10 kb for high efficiency of the protocols (Invitrogen, Genetailor SDM system; NEB, Phusion SDM kit). Therefore, we developed a fast and robust alanine-scanning mutagenesis strategy that is not restricted by the limitations mentioned above and most importantly allows simultaneous generation of a large set of substitution, deletion and insertion mutants (see Results 2.1).

1.1.2 Methods to Study Protein-Protein Interactions

Various methods focusing on different aspects are available to study protein-protein interactions and protein complexes. Major methods comprising different advantages and disadvantages are described in the following chapter.

Table 1.1 Schematic overview of methods to study protein-protein interactions that are described in the following chapter in detail.

Method	Major Advantage	Major Disadvantage
Large Scale Screens for the Identification of Protein-Protein Interactions		
Yeast Two-Hybrid	cheap	high error rate
Mass-Spectrometry	identify protein complex composition	expensive
Protein Chip	high throughput screen	results limited by experimental conditions
Small Scale Assays for the Analysis of Protein-Protein Interactions		
Fluorescence Based *Protein-Protein Interaction* Methods		
Fluorescence Resonance Energy Transfer	*in vivo* and *in vitro*	technically demanding
Bimolecular Fluorescence Complementation	*in vivo*	irreversible fluorophore assembly
Fluorescence Two-Hybrid	*in vivo*, simple to use	requires cell line with *lac* operator array
Biochemical Methods		
Analytical Ultracentrifugation	complex characterization possible	requires pure protein fractions
Surface Plasmon Resonance	sensitive measurements possible	expensive
Affinity Purification	detects direct interactions	might miss posttranslational modifications
GFP-Nanotrap	fast, quantitative pulldown	"large" GFP-tag necessary

1.1.2.1 Large Scale Screens for the Identification of Protein-Protein Interactions

Genetic Yeast Two-Hybrid Screen

A classical genetic method to identify interacting proteins is the yeast two-hybrid screen (Y2H, (Fields and Song, 1989)). This method is based on two functional domains of a yeast transcription factor (e.g. GAL4): First, a DNA binding domain directs the transcription factor to an upstream activator sequence (UAS) of a transcriptional unit and second, an activator domain initiates transcription by recruiting the RNA polymerase II complex. For a Y2H

interaction screen, the protein of interest is fused to the DNA-binding domain that targets the protein to the UAS sequence of a reporter gene and serves as bait. Potentially interacting candidate proteins taken from a cDNA library are fused to the transcriptional activator domain and serve as prey. Only if the bait and prey proteins interact, the DNA binding domain and the activator domain form a complex, reconstitute the transcription factor and switch on the reporter gene. Commonly used reporter genes are leucine (Leu2) or histidine (HIS3) that allow screening with auxothrophic media. Another marker is LacZ, a ß-galactosidase that catalyzes the conversion of X-Gal to 5'5-dibrom-4,4'-dichlorindigo leading to a blue coloration of the yeast cells (Durfee et al., 1993; Fields and Song, 1989; Vojtek et al., 1993). In summary, the interaction of two proteins can be detected by the reconstitution of a transcription factor that initiates the expression of reporter genes. Y2H screens have been successfully applied to identify protein-protein interactions in large-scale studies (Boxem et al., 2008; Vidal, 2005). However, they also have some disadvantages. A high rate (up to 50%) of the results is false-positive or false-negative (Deane et al., 2002). Besides, prior to screening self-activation of the bait fusion protein has to be excluded. In addition, yeast cells cannot spatially or dynamically resolve protein-protein interactions that take place in distinct cell compartments in higher eukaryotic cells. Furthermore, not only the limited chaperone diversity in yeast might affect proper folding of mammalian proteins but also posttranslational modifications that could be crucial for certain interactions might be absent. The standard Y2H has been modified to achieve a better reliability (Vidal and Legrain, 1999). For further functional analyses, identification of mutations that specifically disrupt the interaction is important. For this purpose, modified yeast two-hybrid systems such as reverse two-hybrid screens have been developed (Jin et al., 2007; Vidal et al., 1996a; Vidal et al., 1996b). In any case, interactions initially identified by Y2H should be confirmed in an independent protein-protein interaction assay such as affinity-purification. Bacterial two-hybrid screens (B2H) can be carried out analogously to Y2H. B2H allows interaction screens of large libraries ($<10^8$) due to higher transformation efficiency and faster expansion of *E.coli* (Hu et al., 2000; Joung et al., 2000).

Mass-Spectrometry

Mass-spectrometry is an important tool for analyzing and characterizing biological samples of varying complexity. The technology allows getting insights into the composition, regulation and function of molecular complexes and pathways (Aebersold and Mann, 2003;

Ong and Mann, 2005). To analyze protein complexes, the protein of interest is used as bait for affinity purification to isolate interacting proteins. If specific antibodies are available, the endogenous protein can be immunoprecipitated and protein over-expression that might result in non-physiological levels and subsequent artifacts is not necessary. A multitude of mass spectrometers with different characteristics are available (reviewed in (Domon and Aebersold, 2006)). In general, after affinity purification of a protein complex, samples are separated by SDS-PAGE, protein bands are excised, digested by trypsin and the peptide mixture is separated by high-pressure liquid chromatography in very fine capillaries. Subsequently, the peptides are eluted to an ion source (e.g. electrospray ionization (ESI)) where they get incorporated into small highly charged droplets. After evaporation, the mass spectrometer records a mass spectrum of the peptides (according to their mass-to-charge ratios). Tandem (MS/MS) mass spectrometers have more than one analyzer and allow structural and sequencing studies. A MS/MS spectrum is recorded after peptide fragmentation and matched against the protein sequence database. Data analysis reveals the identity of the peptides, the proteins and hence the composition of the initially isolated protein complex. One major advantage of this technology is that the bait protein can be isolated from its native environment, i.e. fully processed and modified in living cells. However, proteins identified in one complex reflect only a fraction of the occurring protein-protein interactions, as low affinity or transient interactions can be lost during the affinity purification of the protein complex. In summary, mass spectrometry provides high-content, quantitative information about highly complex biological samples.

Protein Chip

Protein chips allow the identification and quantification of protein-protein interactions in large scale. The major advantages of protein chips are highly sensitive measurements and the possibility to analyze a large number of parameters in one experiment (Kung and Snyder, 2006; Templin et al., 2003). To setup a protein chip, antibodies, proteins or cell lysates are spotted on a surface and serve as bait. After incubation of the chip with a prey protein mixture, bound proteins are detected either by radioactivity, fluorescently or chemiluminescently labeled antibodies. The high sensitivity of protein chips is due to building of a protein complex at maximal concentration of the bait protein. In addition, bait-prey protein complexes are formed at a small, defined spot resulting in high local signal intensity (Ekins and Chu, 1992). However, proteins vary significantly in terms of solubility, charge and

stability. Moreover, protein-protein interactions are dependent on buffer conditions as pH, salt concentrations and cofactors. Thus, as a global protein-protein interaction chip cannot meet the requirements of all different kinds of proteins, the results have to be evaluated under consideration of the experimental conditions. Nonetheless, protein chips are an important tool for high throughput analysis of protein-protein interactions (Jones et al., 2006; MacBeath and Schreiber, 2000).

1.1.2.2 Small Scale Assays for the Analysis of Protein-Protein Interactions

Fluorescence Based Protein-Protein Interaction Methods

The fusion of fluorophores to proteins allows the analysis of protein distribution, dynamics and interactions in their natural environment – in living cells (Phair and Misteli, 2001). Further modeling of kinetic data provides insights into biophysical properties of molecules. However, over-expression of fluorescent fusion proteins is artificial and therefore correct localization should be controlled first. This can be done by comparing the distribution of the fusion protein with antibody stainings of the endogenous protein.

Fluorescence Resonance Energy Transfer

Fluorescence resonance energy transfer (FRET), discovered 1946 by Theodor Förster is a physical process where energy of an excited donor fluorophore is transferred without emission of a photon to an acceptor fluorophore. This effect can be observed *in vitro* and *in vivo*. Importantly, the donor fluorophore must have an emission spectrum overlapping with the excitation spectrum of the acceptor fluorophore. A well suited donor-acceptor pair is the cyan fluorescent protein (CFP) and the yellow fluorescent protein (YFP). Only if the two fluorophores are in close proximity (1-10 nm), energy can be transferred and excite the acceptor fluorophore. To analyze protein-protein interactions, two candidate proteins are fused to CFP and YFP respectively and expressed in cells. Upon interaction of the two proteins, FRET between CFP and YFP can be measured and the donor fluorescence is quenched while the acceptor fluorescence signal increases (Periasamy, 2001). Signal intensity of FRET is dependent on the distance between the two fluorophores. Therefore, N- or C-terminal fusions of the fluorophores can result in a protein complex where the distance between them is too large to detect FRET. In addition, depending on the orientation, a fluorescent fusion can prevent an interaction that could occur between endogenous proteins. Hence, a set of controls is needed to avoid false-negative results. Recently, photobleaching of

YFP was reported to lead to photoconversion of the protein and to produce a byproduct with CFP-like fluorescence (Kirber et al., 2007; Valentin et al., 2005). For this reason this classic FRET pair needs additional controls for the use in protein-protein interaction studies or newly developed FRET pairs should be considered (Ai et al., 2008).

Bimolecular Fluorescence Complementation

Bimolecular fluorescence complementation (BiFC) is also used to analyze protein-protein interactions *in vivo*. This method is based on the reconstitution of a fluorophore such as the green fluorescent protein GFP (Magliery et al., 2005) or the monomeric red fluorescent protein mRFP1 (Jach et al., 2006). Two nonfluorescent halves of a fluorescent protein are fused to two candidate proteins. If the candidate proteins interact, the fluorophore is reconstituted by assembly of the two parts and the fluorescent signal can be observed (Hu et al., 2002). However, the association of the fluorescent protein fragments is irreversible (Kerppola, 2006) and fluorescent protein fragments have a natural capability to interact independent of fused proteins. In addition, chemical reactions of fluorophore reconstitution are too slow to be monitored in real time. Therefore, bimolecular fluorescence complementation is a technically demanding assay that if applied with the appropriate controls can be a versatile method to monitor protein-protein interactions.

Fluorescence Two-Hybrid

The fluorescence two-hybrid assay (F2H) allows direct visualization of protein-protein interactions in single living cells (Zolghadr et al., 2008). The F2H assay monitors the interaction of e.g. a red fluorescent bait with a green fluorescent prey protein as co-localization at a defined nuclear spot. To anchor the fluorescent bait, transgenic cells that contain a chromosomally integrated *lac* operator array are used and provide a defined binding platform for Lac repressor fusion proteins. The protein of interest (X) is fused to the Lac repressor and a fluorescent protein (e.g. mRFP) and serves as bait. Binding of the triple fusion protein (X-LacI-RFP) to the *lac* operator array can directly be visualized by fluorescence microscopy as nuclear spot in living cells. Interaction of green fluorescent prey proteins with red fluorescent protein X leads to co-localization at the anchor point and is visible in an overlay image as orange/yellow spot. To exclude false positive or false negative results appropriate controls have to be performed. In summary, the F2H assay provides a simple optical read-out to visualize protein-protein interactions. If a cDNA library is cloned into the

bait vector (cDNA-LacI-RFP), large-scale screenings of protein-protein interactions can be performed in 96 well formats by high throughput microscopy and automated image analysis.

Biochemical Methods

Biochemical methods are often used to validate and characterize protein-protein interactions that were initially identified by large scale screens as with the methods described above.

Analytical Ultracentrifugation

Analytical ultracentrifugation is used to determine the molecular weight, hydrodynamic and thermodynamic properties of a protein or macromolecule and even short-lived complexes can be detected. Sedimentation and diffusion coefficients and ligand binding can all be analyzed using this versatile instrument. An analytical ultracentrifuge provides sample rotation at a controlled speed (up to 250,000 g) and temperature under vacuum and periodically records the spatial distribution of protein concentration. The protein sample is placed in a cell that contains two windows of quartz or sapphire to allow measurements at different radial positions and at different times. The data obtained from sedimentation velocity experiments is a record of the concentration distribution including the sedimentation constant, the diffusion and friction co-efficient. In sedimentation-equilibrium experiments the density of the protein complex is determined (Lebowitz et al., 2002). Sucrose gradient experiments lead to accumulation of the protein fraction at a point in the sucrose gradient where its density matches with the surrounding sucrose and allows purification and further analysis of the protein complex fraction.

Surface Plasmon Resonance

Surface plasmon resonance (SPR) spectroscopy allows the determination of binding constants, enzyme-substrate interactions, DNA/RNA-protein interactions and others. SPR instruments such as Biacore measure the refractive index near a sensor surface (300 nm), that represents the basis of a flow cell through which an aqueous solution passes in continuous flow. The SPR field is very sensitive to any change such as the adsorption and dissociation of molecules. To analyze (protein) interactions a ligand is immobilized on the sensor surface and the analyte is injected in the same aqueous solution under constant flow into the flow cell. Binding of the analyte to the immobilized ligand leads to a change in the refractive index that is measured in real time. Hence, time constants as well as equilibrium constants can be calculated. Measurements have to be performed under constant optical conditions, in the

same buffer system to accurately detect binding of molecules. SPR offers several advantages: High sensitivity, time resolution, specificity and label-free detection but it is cost-intensive (Anker et al., 2008; Phillips and Cheng, 2007).

Affinity Purification

Affinity purification allows the enrichment and purification of interacting proteins. After immobilization of one ligand to a matrix, a complex mixture of proteins can be loaded and only the interacting protein is specifically bound. Pull-down assays are one kind of affinity purification to test physical interaction between proteins *in vitro*. The glutathione-S-transferase (GST) pulldown is commonly used and well suited to either perform an initial interaction screening or to confirm predicted protein-protein interactions. A protein of interest is fused to GST (bait), expressed in *E.coli* and purified using sepharose beads coated with glutathione. The immobilized bait protein is then incubated with a prey protein that can be either a purified protein or part of a whole cell lysate. After several washing steps bound proteins are eluted by denaturing sample buffer or glutathione and proteins are separated according to their molecular mass by SDS polyacrylamide electrophoresis (PAGE). Interacting proteins can be visualized by coomassie staining or after protein transfer to a membrane by specific antibodies (immunoblotting). For (co-)immunoprecipitation assays, antibodies are coupled to beads and specifically enrich native antigen-complexes from a cell lysate. New interaction partners can be identified by mass spectrometry and immunoblotting. To distinguish between direct or indirect interactions purified proteins have to be used. Nonetheless, to analyze protein-protein interactions biochemical methods are important accepted standard techniques (Cho et al., 2004).

GFP-Nanotrap

In our group, we also use a modified co-immunoprecipitation approach to detect and map protein-protein interactions. It is based on an antibody fragment of a single-chain antibody of *camelidae*. Camelids have not only conventional antibodies but also single chain antibodies that are composed exclusively of single truncated H-chains (Hamers-Casterman et al., 1993). The smallest antigen-binding fragment consists of the heavy chain variable domain (V_HH), has a molecular size of 15 kDa and binds to its antigen with nanomolar affinity (Muyldermans et al., 1994; Muyldermans and Lauwereys, 1999; Muyldermans and Travers, 1994). We use a GFP-binding antibody fragment (GBP; GFP-Nanotrap) that was developed in

our group for biochemical interaction studies (Rothbauer et al., 2008). GFP is fused to a protein of interest, the fusion protein is expressed and enriched with the GFP Nanotrap from a crude cell extract. Interacting proteins are further analyzed by immunoblotting. Compared to a classical co-immunoprecipitation approach using conventional antibodies, the GFP-Nanotrap offers several advantages: First, the small GBP (13 kDa) is coupled covalently through a NHS ester bond to agarose beads providing a binding platform for GFP. Second, incubation of one to two hours is enough to quantitatively enrich a GFP fusion protein from a cell lysate. Third, we do not have any disturbing signals of antibody light and heavy chains on coomassie stained PAGE gels or immunoblots as the GBP fragment is covalently coupled by a NHS-ester bond to sepharose beads. In summary, the GFP Nanotrap provides a versatile and time efficient co-immunoprecipitation assay to study protein-protein interactions. A further advantage of this system is that one and the same GFP fusion protein can be analyzed both by biochemical methods and by fluorescence microscopy to study localization, dynamics and interactions in living cells.

1.2 Establishment and Maintenance of DNA Methylation

DNA methylation is established and maintained by the family of DNA methyltransferases (Dnmts). These enzymes transfer methyl groups from S-adenosyl-L-methionine (SAM) to cytosines (at carbon 5) in the context of CpG sites (Wu and Santi, 1987). CpG methylation occurs in all vertebrates, flowering plants, some fungal, invertebrate and protist taxa and many bacteria. In bacteria, DNA methylation is part of the restriction modification system that protects the host genome against foreign DNA such as bacteriophages (Wilson and Murray, 1991). In vertebrates, it has a repressive effect on gene expression. DNA methylation patterns are reprogrammed by waves of demethylation and remethylation during early mammalian embryogenesis. During pre-implantation development, maternal and paternal methylation patterns are erased except for imprinted loci and retroviral elements (e.g. intracisternal A-type particles, IAPs). After implantation, methylation patterns are established through lineage-specific *de novo* methylation by Dnmt3a and 3b and maintained in somatic cells by Dnmt1 (Howlett and Reik, 1991; Li, 2002; Santos et al., 2002).

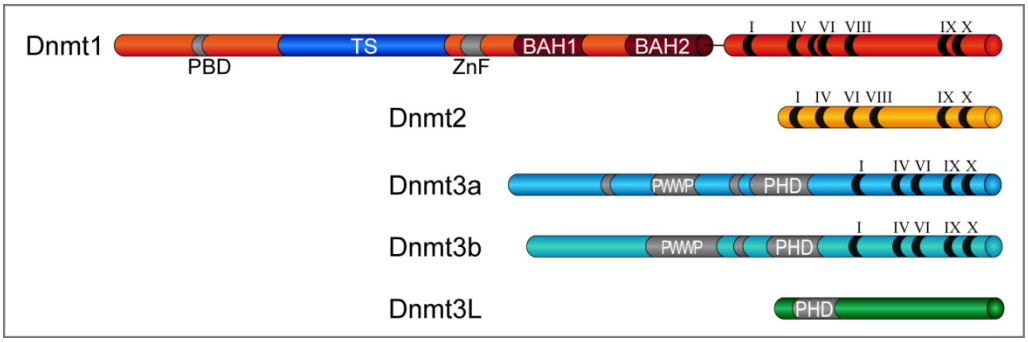

Figure 1.1 Schematic overview of the mammalian DNA methyltransferase family. Subdomains are indicated: PBD, PCNA binding domain; TS, targeting sequence; ZnF, CXXC-type zinc finger; BAH1+2, bromo adjacent homology domain 1+2; I-X, catalytic methyltransferase motifs; PWWP, domain with conserved pro-trp-trp-pro motif; PHD, plant homeo domain.

The family of DNA methyltransferases comprises five members (Figure 1.1). Dnmt1 is the maintenance methyltransferase, it associates with replication sites and copies methylation patterns from the parental to the newly synthesized daughter DNA strand (Chuang et al., 1997; Leonhardt et al., 1992). Dnmt2 was described as RNA methyltransferase for $tRNA_{Asp}$ (Goll et al., 2006) and shown to act through a DNA methyltransferase-like catalytic mechanism (Jurkowski et al., 2008). Dnmt3a and 3b are *de novo* DNA methyltransferases that are responsible for the establishment of methylation patterns early in development (Okano et al., 1998). Although Dnmt3L lacks crucial methyltransferase motifs and is not catalytically active, it plays an essential role in the regulation of Dnmt3a and 3b (Aapola et al., 2002; Hata et al., 2002; Jia et al., 2007; Suetake et al., 2004).

1.2.1 Maintenance DNA Methyltransferase 1

Dnmt1 is ubiquitously expressed and responsible for the inheritance of DNA methylation patterns. Homozygous knockout of the *dnmt1* gene in mice leads to genome-wide loss of DNA methylation and embryonic lethality (Lei et al., 1996; Li et al., 1992). Reduction of cellular Dnmt1 levels severely affects development and genome stability (Gaudet et al., 2003; Gaudet et al., 2004). Dnmt1 consists of two major domains: A regulatory N-terminal domain that is unique among the family of DNA methyltransferases and a C-terminal catalytic domain. The two parts of the enzyme are linked via a glycine-lysine linker $(GK)_7$. The large N-terminal domain of Dnmt1 contains several subdomains: The PCNA binding domain (PBD, (aa) 159-178) targets Dnmt1 to the replication machinery during S phase where it associates with the loading platform PCNA. It was described recently, that this interaction enhances methylation efficiency by twofold but is not strictly required for methylation maintenance (Chuang et al., 1997; Schermelleh et al., 2007; Spada et al., 2007). The N-terminal targeting sequence (TS, aa 310-629) recruits Dnmt1 to heterochromatin in a process that is independent of replication, the presence of H3K9 trimethylation, the interacting histone methyltransferase SUV39H1 and HP1 (Easwaran et al., 2004; Leonhardt et al., 1992). Besides, the TS contains a zinc finger motif (Bestor, 1992; Chuang et al., 1996). The prominent N-terminal CXXC zinc-finger (ZnF, aa 648-694) of Dnmt1 was described to be essential for allosteric activation of the catalytic domain of Dnmt1 (Fatemi et al., 2001). The structure of a very similar zinc-finger from the mixed-lineage leukemia protein (MLL) was solved by nuclear magnetic resonance spectroscopy (NMR) (Allen et al., 2006). Both, the MLL zinc finger and the homolog zinc-finger of the CpG binding protein (CGBP) bind to unmethylated CpG DNA (Birke et al., 2002; Lee et al., 2001). The respective zinc motif of MBD1 was shown to bind both methylated and unmethylated CpG sites (Jorgensen et al., 2004). In addition, the Dnmt1 N-terminus comprises two bromo adjacent homology domains (BAH1+2; aa 758-884 and 935-1103) whose functions are still unknown (Liu et al., 1998). BAH domains have also been found in other proteins where they are involved in protein-protein interactions specialized in gene silencing as in the yeast Orc1p – Sir1p (origin recognition complex 1 – silent information regulator 1) interaction (Callebaut et al., 1999). At least three nuclear localization signals (NLS) have been identified in the Dnmt1 N-terminus (Leonhardt and Cardoso, 2000). In contrast to the unique regulatory N-terminal domain of Dnmt1, the catalytic domain is very well conserved among DNA methyltransferases. Even though it contains all typical conserved methyltransferase motifs

necessary for catalysis, the catalytic domain of Dnmt1 per se lacks catalytic activity. Thus, the intramolecular interaction between the regulatory N-terminus and the catalytic C-terminus is essential for the catalytic activity of Dnmt1 (Fatemi et al., 2001; Margot et al., 2000; Margot et al., 2003). In addition, Dnmt1 is the only methyltransferase with a preference for hemi-methylated CpG sites (Stein et al., 1982) that assures correct transmission of cytosine methylation not only during DNA replication but also during DNA repair (Mortusewicz et al., 2005). It is still unknown, how the activity and specificity of Dnmt1 are regulated. To address these questions we performed detailed analyses of Dnmt1: We mapped subdomains of the regulatory N-terminus that are indispensible for N-C terminal interaction and therefore catalysis to receive a minimal active Dnmt1 enzyme (Results, 2.2). DNA methyltransferases seem to have no sequence specificity beyond CpG recognition (Dodge et al., 2002; Okano et al., 1998; Yoder et al., 1997). Interactions with chromatin factors may direct Dnmts to target sites or help Dnmts to access target cytosines (Bird, 2002).

The goal of this work was to identify subdomains of Dnmt1 and interacting proteins that contribute to functional specialization of the enzyme. Interaction of Dnmt1 with the chromatin factors Np95, LSH and EZH2 was shown to be essential for maintenance of DNA methylation (Bostick et al., 2007; Myant and Stancheva, 2008; Sharif et al., 2007; Vire et al., 2006). However, the molecular mechanisms of these multiple interactions controlling the activity of Dnmt1 and the recognition of hemi-methylated target sites are still largely unknown. To understand this epigenetic protein network involved in the regulation of DNA methylation we studied Dnmt domains to identify interaction partners; we further mapped and mutated the interacting domains to study their function.

1.2.2 *De novo* DNA Methyltransferases 3a and 3b

Dnmt3a and 3b establish DNA methylation patterns *de novo* in early development. They are highly expressed in ES cells, early embryos and developing germ cells and are downregulated after differentiation in somatic cells (Okano et al., 1998). Dnmt3a and Dnmt3L are essential for the establishment of methylation imprints during gametogenesis (Bourc'his 2001, Hata 2002, Kaneda 2004). Targeted disruption of both, *dnmt3a* and *dnmt3b* genes inhibits *de novo* methylation in ES cells and early embryos. *dnmt3a*$^{-/-}$ mice are runted but survive until adulthood. Global methylation levels seem to be normal (Okano et al., 1999), however studies of a conditional knockout of *dnmt3a* in germ cells reported that Dnmt3a is required in male germ cells for the methylation of differentially methylated regions (DMRs) of imprinted genes like *H19* and *Gtl2-Dlk1* (Kaneda et al., 2004). *dnmt3b*$^{-/-}$ mice die at 9.5 days post coitum exhibiting loss of methylation at minor satellite repeats. In humans, point mutations in DNMT3b cause a rare autosomal recessive disorder called the ICF (immunodeficiency, centromere instability and facial anomalies) syndrome (Xu et al., 1999). Methylation of pericentromeric regions of chromosomes 1, 9 and 16 is missing, leading to chromosomal instability. Altogether, these studies demonstrate that correct function of Dnmt3a and 3b is vital for normal development. In addition to their function as *de novo* methyltransferases, Dnmt3a and 3b play also a role in the maintenance of methylation patterns. Inactivation of *dnmt3a* and *dnmt3b* in ES cells by targeted disruption leads to a progressive decrease of global DNA methylation levels (Chen et al., 2003; Liang et al., 2002), although Dnmt3a and 3b show no preference for un- or hemimethylated CpG sites *in vitro* (Aoki et al., 2001; Okano et al., 1998). Dnmt3a and 3b differ only in their regulatory N-terminal domains, while their catalytic domains are highly homologous. The N-terminal variable region contains 280 amino acids for Dnmt3a and 220 amino acids for Dnmt3b. Both contain an N-terminal PWWP domain named after the characteristic pro-trp-trp-pro motif (Dnmt3a aa 289-246, Dnmt3b aa 228-363 (Qiu et al., 2002; Stec et al., 2000)). The PWWP domain was described to be responsible for targeting Dnmt3a and 3b to pericentric heterochromatin (Chen et al., 2004; Ge et al., 2004). Moreover, Dnmt3a and 3b comprise an ATRX homology domain that includes a C2-C2 zinc finger and a PHD-like domain (plant homeo domain (Okano et al., 1998; Xie et al., 1999)). This domain has been described to interact with various chromatin proteins like histone deacetylases (HDACs), heterochromatin protein 1 (HP1) and the histone

methyltransferase suppressor of variegation 3-9 homolog 1 (SUV39H1) (Fuks et al., 2001). Still, the regulation of Dnmt3a and 3b remains largely unknown.

In this work, we identified Np95 as one common regulatory factor for Dnmt1, 3a, 3b and characterized its interactions and role in gene silencing. (see Results 2.4, 2.5)

1.3 The Epigenetic Protein Network

A multitude of epigenetic proteins is responsible for large chromatin diversity including DNA methylation marks and histone modifications such as methylation, acetylation, phosphorylation, ribosylation, ubiquinylation and others (Kouzarides et al., 2007). Positively charged histone tails are target for modifications and preferentially lysines and arginines are subjected to mono-, di-, tri-methylation or acetylation. Different modifications and combinations of modifications lead to complex packaging mechanisms and a differential accessibility of the DNA e.g. for transcription factors. Moreover, in such a crowded environment chromatin remodeling factors play a fundamental role to provide chromatin flexibility and access to DNA (Becker and Horz, 2002; Varga-Weisz and Becker, 2006). This work is focused on DNA methyltransferases – the other hall mark of epigenetic modifications besides histone modifiations. Thus, in the following interactions among DNA methyltransferase enzymes and the interface between DNA methylation and histone modifications will be elucidated and the role in development, disease and reprogramming will be discussed.

1.3.1 Interactions within the Mammalian DNA Methyltransferase Family

Several DNA methyltransferases participate in the establishment and maintenance of DNA methylation patterns (Figure 1.2). Cooperation of *de novo* and maintenance methyltransferases ensures proper methylation patterns while deficiency of one or more methyltransferases results in hypomethylation.

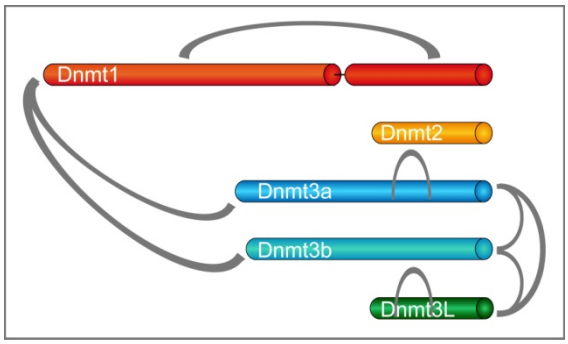

Figure 1.2 Interactions within the Dnmt family. Grey lines indicate interactions. Dnmt1 interacts with Dnmt3a and 3b and the Dnmt1 N-terminal domain allosterically activates the C-terminal domain. Dnmt3a and Dnmt3L can form dimers and together a Dnmt3L-3a-3a-3L tetramer. Dnmt3a and 3b interact with each other and with Dnmt3L.

Dnmt1 interacts with both, Dnmt3a and Dnmt3b (Kim et al., 2002). These interactions are mediated by the N-terminal regulatory domains of Dnmt1 and Dnmt3a/b. Dnmt3a and Dnmt3b function synergistically in the methylation of Oct4 and Nanog in embryonic stem cells and mouse postimplantation embryos through direct interaction (Li et al., 2007). Dnmt3L

stimulates the catalytic activity of both, Dnmt3a and Dnmt3b, by interacting with their catalytic domains (Chedin et al., 2002; Gowher et al., 2005; Kareta et al., 2006; Suetake et al., 2004). Expression of Dnmt3L was reported to be controlled by Dnmt3L promoter methylation during embryonic development (Hu et al., 2008). Mechanistic insights provided the crystal structure of a Dnmt3L-3a-3a-3L tetramer (Jia et al., 2007). The crystal structure of the C-terminal domains revealed that the Dnmt3L-Dnmt3a interface stabilizes the conformation of the active site loop of Dnmt3a and hence suggested a model for *de novo* methylation of imprinted genes. Mutation of either the Dnmt3a-Dnmt3a or the Dnmt3a-Dnmt3L interface disrupted catalytic activity. The central Dnmt3a dimer in the tetramer methylated two CpG dinucleotides that are 8-10 bp apart in one binding event and this spacing was preferentially found in imprinting control regions. In addition, a whole human genome search revealed a high over-representation of CpG dinucleotides with an 8-10 base pair periodicity, indicating potential target sites for 3a-3L tetramers throughout the genome (Ferguson-Smith and Greally, 2007). Interestingly, the Dnmt3a homolog in plants DRM2 (domains rearranged methylase 2) methylates DNA genome-wide with a comparable periodicity (Cokus et al., 2008). Moreover, Dnmt3a-3L complexes were shown to multimerize on DNA, forming protein-DNA filaments. CpG methylation in a distance of 8-10 bp on opposite DNA strands was observed by *in vitro* studies, correlating with the geometry and distance of the two active sites in one Dnmt3a-3L tetramer (Jurkowska et al., 2008).

These interdependencies indicate that DNA methylation is coordinated by a complex interplay between the members of the DNA methyltransferase family. Moreover, the molecular mechanisms of the regulation of Dnmts by interacting chromatin factors such as histone modifying enzymes are not yet understood in detail.

1.3.2 Interface between DNA Methyltransferases and Histone Modifying Enzymes

DNA methyltransferases interact with various histone modifying enzymes but so far, only one DNA methyltransferase was described to interact directly with a histone modification. Dnmt3L binds to unmethylated lysine 4 of histone H3 (H3K4) through its N-terminal PHD domain, thereby Dnmt3a is recruited or activated to induce *de novo* methylation (Ooi et al., 2007). The crystal structure of Dnmt3L revealed C-terminal to the PHD domain a classical methyltransferase fold. The co-crystal structure of the Dnmt3L and the H3 tail showed a specific binding of unmethylated but not methylated H3K4. Dnmt3L seems to respond to states of histone modification to regulate *de novo* DNA methylation.

In addition to the interactions within the DNA methyltransferase family, numerous other interacting chromatin factors are involved in the regulation of DNA methylation. To illustrate this complexity the cellular factors reported to interact with Dnmt1 are outlined in Figure 1.3.

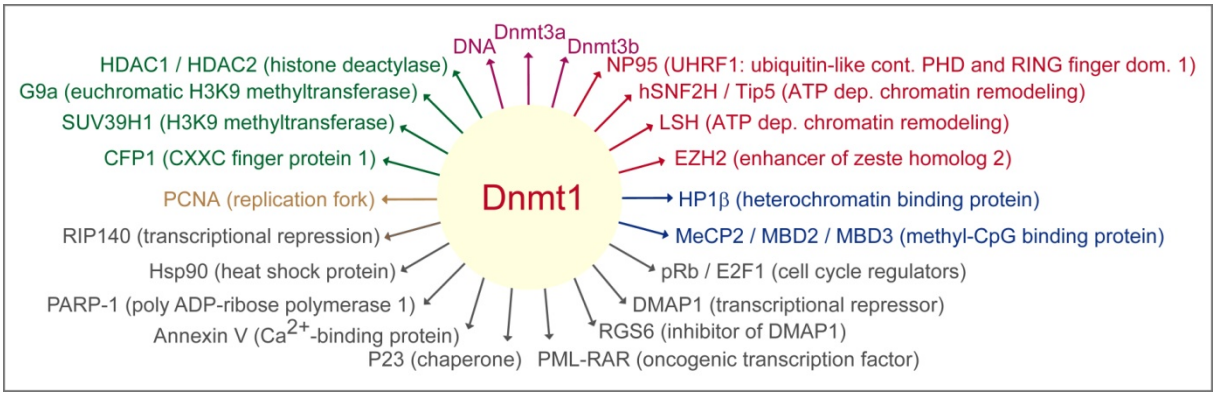

Figure 1.3 Reported interacting factors of Dnmt1: Dnmt3a and Dnmt3b (Kim et al., 2002); Np95 (Bostick et al., 2007; Sharif et al., 2007); hSNF2H / Tip5 (Zhou and Grummt, 2005); LSH (Myant and Stancheva, 2008); EZH2 (Vire et al., 2006); HP1β (Fuks et al., 2003); MeCP2 (Kimura and Shiota, 2003); MBD2 / MBD3 (Tatematsu et al., 2000); pRb / E2F1 (Robertson et al., 2000); DMAP1 (Rountree et al., 2000); RGS6 (Liu and Fisher, 2004); PML-RAR (Di Croce et al., 2002); P23 (Zhang and Verdine, 1996); Annexin V (Ohsawa et al., 1996); PARP-1 (Reale et al., 2005); Hsp90 (Zhou et al., 2008); RIP140 (Kiskinis et al., 2007); PCNA (Chuang et al., 1997); CFP1 (Butler et al., 2008); SUV39H1 (Fuks et al., 2003); G9a (Esteve et al., 2006); HDAC1/2 (Robertson et al., 2000; Rountree et al., 2000).

These interactions of Dnmt1 represent only a small section of this rather complex epigenetic protein network. The underlying molecular mechanisms and their interplay in the genome-wide epigenetic regulation of gene expression is subject of intense research. Histone deacetylation correlates with transcriptional repression and the responsible histone deacetylase enzymes can also recruit Dnmts to establish DNA methylation marks. HDAC1 interacts with Dnmt1, 3a, 3b and 3L while HDAC2 interacts only with Dnmt1 and 3b (Bachman et al., 2001; Deplus et al., 2002; Fuks et al., 2001; Geiman et al., 2004; Robertson et al., 2000; Rountree et al., 2000). The histone methyltransferase SUV39H1 binds HDAC1 and HDAC2 and is responsible for trimethylation of lysine 9 at histone H3 (H3K9) in heterochromatic regions. Moreover, SUV39H1 interacts with Dnmt1, 3a and 3b. SUV39H1 or the resulting H3K9

trimethylation can further recruit HP1 which also binds Dnmts (Fuks et al., 2003; Geiman et al., 2004; Lehnertz et al., 2003). HP1α and HP1β are found only at heterochromatin while HP1γ is found at hetero- and euchromatin (Minc et al., 2000). G9a is also a H3K9 methyltransferase but acts on euchromatic DNA. G9a associates with Dnmt1, 3a and 3b (Epsztejn-Litman et al., 2008; Esteve et al., 2006). A recent report suggests that the noncoding RNA *Air* recruits G9a to chromatin (Nagano et al., 2008). SETDB1 (suppressor of variegation, enhancer of zest and trithorax domain bifurcated 1) is another H3K9 methyltransferase that specifically trimethylates H3K9 and interacts with HDAC1 and 2 (Schultz et al., 2002; Yang et al., 2003; Yang et al., 2002). It mainly functions in euchromatic regions and plays a central role in the silencing of euchromatic promotors. SETDB1 interacts with *de novo* methyltransferases Dnmt3a and 3b but not with Dnmt1 (Li et al., 2006). LSH is a member of the SNF2H chromatin remodeling family and was shown to be essential for both types of epigenetic information – DNA methylation and histone tail methylation (De La Fuente et al., 2006; Dennis et al., 2001; Huang et al., 2004; Myant and Stancheva, 2008). LSH serves as a recruiting factor for Dnmts and HDACs to establish transcriptionally repressive chromatin that might be further stabilized by DNA methylation at targeted loci (Myant & Stancheva, 2008). Methyl CpG binding domain (MBD) proteins such as MeCP2, MBD1 and MBD2 bind to 5-methyl cytosine residues in CpG dinucleotides and are involved in transcriptional silencing. MeCP2, MBD2 and MBD3 interact with Dnmt1 (Kimura and Shiota, 2003; Tatematsu et al., 2000). There are many more chromatin binding factors involved in gene silencing that are not mentioned here. In general, it is very likely that repressive factors are able to recruit each other. The exact order of events has not been resolved so far. The clustering of epigenetic factors and the establishment of repressive chromatin modifications lead to gene silencing. In addition, RNA directed DNA methylation was first described in plants and latest research revealed the existence of similar mechanisms in mammals (Aravin et al., 2008; Kanno et al., 2008; Kuramochi-Miyagawa et al., 2008; Tam et al., 2008; Watanabe et al., 2008).

1.3.3 Epigenetic Mechanisms in Gene Silencing – a Crucial Process in Development and Disease

Epigenetic modifications control gene expression profiles and therefore play a fundamental role in development, disease and gene therapy. Early in development pluripotent stem cells have the potential to specialize in various different lineages. During the process of differentiation, expression of pluripotency genes is epigenetically silenced through DNA

methylation and repressive histone modifications. Depending on the developmental program, distinct sets of genes are activated and lead to functional specialization of a cell. During this process, epigenetic marks are changed and are stably maintained in differentiated somatic cells. While histone modifications are flexible and can be reversed to allow expression of a respective gene, silencing of transposons and imprinted genes is long-term and requires DNA methylation that has to be maintained.

Various diseases are caused or accompanied by drastic changes in the epigenetic landscape. The best studied example involving both genetic and epigenetic alterations is cancer. In general, cancer cells exhibit global hypomethylation and local hypermethylation of promoter regions of tumor suppressor genes. It was shown that silencing can occur at early stages during tumorigenesis and mostly involved disruption or over-activation of key signal pathways (Feinberg and Tycko, 2004; Yamada et al., 2005). These issues were extensively studied in the human colon cancer cell line HCT116. Methylation of the *sfrp* genes, the antagonists of the Wnt pathway was found, causing over-activation of the Wnt-pathway and therefore increased proliferation and expansion of stem-cell populations (Taketo, 2004). Treatment of the cells with DNA demethylating agents or disruption of the DNA methyltransferase genes could reactivate epigenetically silenced genes. Re-expression of these growth control genes resulted in phenotypic changes, ranging from decreased proliferation to induction of apoptosis or senescence (Bachman et al., 2003; Herman et al., 1998; Suzuki et al., 2004).

Understanding the molecular mechanisms that initiate and maintain epigenetic gene silencing could help to develop strategies for epigenetic cancer therapies to reverse the silencing process and reactivate critical genes.

1.3.4 Epigenetic Reprogramming and Transgene Silencing

Major epigenetic changes have to occur during the reprogramming of a differentiated somatic cell into a pluripotent stem cell-like state. Reprogramming of somatic cells to induced pluripotent stem cells (IPS) has been achieved after virus-mediated transduction of the four transcription factors Oct4, Sox2, Klf4 and c-*myc* and subsequent selection for activation of the Oct4 target gene *Fbx15 (Takahashi and Yamanaka, 2006)*. Recently, the dispensability of the proto-oncogene c-*myc* for this transition was shown, but the process required more time and was less efficient (Nakagawa et al., 2008; Wernig et al., 2008; Yu et al., 2007). Exogenous expression of the three or four factors leads to the activation of the endogenous counterparts that is further maintained by an autoregulatory loop by binding of the transcription factors to their promoters (Boyer et al., 2005). After selection of the IPS by activation of endogenous Oct4 or Nanog, the cells exhibited a pluripotent ES cell state by indistinguishable global gene expression, chromatin configuration and they generated postnatal chimeras and contributed to the germline (Maherali et al., 2007; Okita et al., 2007; Wernig et al., 2007). During the reprogramming process *de novo* methyltransferases Dnmt3a and Dnmt3b are activated and cause silencing of moloney virus vectors through methylation (Okano et al., 1999). It is important to understand the sequence of key events in the reprogramming process in order to be able to explore the potential of nuclear reprogramming as a source of patient-specific cells. In addition, the consequences of silencing and re-activation of viral vectors should be elucidated to enable the development of stable expressing vectors that are suitable for gene therapy.

CpG islands are generally located in the promoter region of housekeeping genes, have a CG content of at least 55% and most importantly they are inherently resistant to *de novo* methylation (Bestor et al., 1992; Bird, 1986; Caiafa and Zampieri, 2005). CpG islands are protected from methylation to ensure gene expression. In addition, a CpG island fused to a provirus sequence had the capacity to confer transcriptional activity to the provirus (Hejnar et al., 2001). The shielding mechanism from methylation has not been elucidated so far, but it is damaged in cancer cells where methylation of CpG islands leads to gene silencing of tumor suppressor genes (Palii and Robertson, 2007).

Transgene silencing is a common issue occurring in stable cell lines or transgenic mice (Mehta et al., 2009). The strong viral cytomegalie virus major immediate early (CMV) promoter is routinely used in expression vectors. Transgenic mice using CMV promoter

driven expression showed either reproducible expression patterns in different tissues or silencing of the transgene a few weeks after gene transfer (Fitzsimons et al., 2002; Schmidt et al., 1990; Villuendas et al., 2001). *In vivo* silencing of the CMV promoter has been associated with DNA methylation (Brooks et al., 2004), reduced histone tail acetylation (Murphy et al., 2002) and could be reversed by treatment with inhibitors of DNA methylation and histone deacetylation (Choi et al., 2005; Grassi et al., 2003; Meier, 2001). In addition, depending on the integration in euchromatic or heterochromatic regions of the host genome, the CMV driven transgene was expressed or not, respectively (Mehta et al., 2009).

Viral or bacterial promoter regions containing unmethylated CpG dinucleotides have an immunstimulatory effect and rapidly induce the innate immune system through toll-like receptor 9 (TLR9) (Sawamura et al., 2005). CpG methylation of the promoter regions of transgenes impedes stable, long lasting expression which would be required for successful gene therapy. To circumvent silencing through CpG DNA methylation CpG-free expression vectors have been generated, are commercially available and contain CpG-free versions of the mouse CMV enhancer and the human EF1 promoter to allow stable transgene expression (Invivogen, pCpG-vitro). Moreover, a mouse model was described were the use of a CpG-free expression vector reduced CpG mediated inflammation and resulted in stable *in vivo* transgene expression (Hyde et al., 2008). CpG-free vectors seem to be one possibility to avoid methylation dependent transgene silencing. However, other epigenetic events such as repressive histone marks still may arise and lead to silencing.

Understanding of the sequence of epigenetic key events in gene silencing that shut down transgene expression would help to circumvent repressive mechanisms to obtain stable transgene expression. Moreover, this understanding would advance research in cancer and epigenetic reprogramming.

2. Results

Table 2.1 Overview of the subsections described in chapter 2. Most of the data are summarized in the publications listed below. The contributions are explained in chapter 4.2.

Chapter	Title	Data	Page
2.1	A Mutagenesis Strategy Combining Systematic Alanine Scanning with Larger Mutations to Study Protein Interactions	publication in "Analytical Biochemistry"	27
2.2	Biochemical Analysis of Intramolecular N-C Terminal Dnmt1 Interactions	unpublished data	36
2.3	Dimerization of DNA Methyltransferase 1 is Mediated by its Regulatory Domain	accepted publication at the "Journal of Cellular Biochemistry"	41
2.4	Np95 Controls Maintenance of DNA Methylation by Interaction with DNA Methyltransferase 1	unpublished data	68
2.5	Np95 Interacts with *de novo* DNA Methyltransferases Dnmt3a and 3b and Mediates Epigenetic Silencing	publication under revision at "EMBO Reports"	77

2.1 A Mutagenesis Strategy Combining Systematic Alanine Scanning with Larger Mutations to Study Protein Interactions

Available online at www.sciencedirect.com
ScienceDirect
Analytical Biochemistry 373 (2008) 176–178
ANALYTICAL BIOCHEMISTRY
www.elsevier.com/locate/yabio

Notes & Tips

A mutagenesis strategy combining systematic alanine scanning with larger mutations to study protein interactions

Karin Fellinger, Heinrich Leonhardt, Fabio Spada *

Department of Biology and Munich Center for Integrated Protein Science, Ludwig Maximilians University Munich, 82152 Planegg-Martinsried, Germany

Received 13 September 2007
Available online 18 October 2007

Site-directed mutagenesis (SDM)[1] of target DNA is an invaluable tool to study protein structure–function relationships. Alanine-scanning mutagenesis has been successfully applied to systematically map functional binding epitopes [1–3]. Substitution of target amino acids with alanine removes all side chain atoms past the β-carbon and does not introduce unusual backbone dihedral angle preferences. Therefore, alanine scanning is particularly useful for assessing the contribution of charged residues on the protein surface without disrupting the folding of its core. This approach requires the production of large numbers of point mutants by SDM. Numerous SDM methods have been described (reviewed in Refs. [4,5]), and commercially available kits offer fast protocols based on oligonucleotide primers harboring the mutation [6]. However, most strategies do not include a selectable marker to distinguish mutant clones from wild-type clones and when they do so the procedure becomes significantly more laborious and time-consuming, as it requires either two cycles of transformation in different bacterial strains [7,8] or transfer of the target DNA sequence to and from a specialized vector. In addition, most of these procedures are not suited to generate large sequence alterations. Methods based on type IIs restriction enzymes allow precise replacement of individual nucleotides or codons [9] and either selection for mutant clones [10] or generation of larger mutations [11], but not both possibilities together. Again, when selection for mutant clones is possible, multiple restriction, ligation, fill-in and transformation reactions are necessary and suitable restriction sites relatively close to the mutagenesis site are required [10]. Other PCR-based approaches allow generation of point and larger mutations and rapid screening for mutant clones but involve amplification of the entire plasmid with consequent risk of introducing additional mutations [12]. Here we describe a simple, fast and inexpensive strategy to generate alanine substitutions as well as deletions, duplications, insertions or larger replacements while retaining the ability to screen for mutant clones by restriction analysis.

The three major steps of our mutagenesis strategy are outlined in Fig. 1. Single, double or triple alanine substitutions are introduced at multiple sites of a defined DNA region by performing (i) two independent sets of PCR reactions (PCR1 and PCR2 in Fig. 1A), (ii) restriction of the PCR fragments and (iii) triple ligation of the two sets of PCR fragments into a suitable vector and transformation. For each mutation, both a reverse and a forward mutagenic primer are required. The 3′ regions of these primers match the sequence directly upstream and downstream to the codons coding for the residues to be exchanged to alanine, respectively, while the overlapping 5′ tails of the primers harbor a *Sac*II or *Not*I site that encodes the alanine residue(s) (Fig. 1). In addition, both a forward and a reverse primer are designed flanking the entire sequence where the set of mutations are to be introduced. These shared flanking primers have 5′ tails harboring distinct restriction sites (designated E1 and E2 in Fig. 1A) to be used for subsequent cloning in a suitable vector. In one set of PCR reactions, the flanking forward primer is combined with distinct reverse mutagenic primers, whereas in the other set of amplifications, the forward mutagenic primers and the reverse flanking primer are employed. The two sets of PCR reactions may be performed simultaneously depending on the annealing temperature of the primers. The two sets of PCR fragments are then digested with the restriction enzyme corresponding to the mutagenic restriction site and the respective enzyme whose site is present at the opposite end

* Corresponding author. Fax: +49 89 2180 74236.
E-mail address: f.spada@lmu.de (F. Spada).

[1] *Abbreviations used:* SDM, site-directed mutagenesis; Dnmt1, DNA methyltransferase 1.

0003-2697/$ - see front matter © 2007 Elsevier Inc. All rights reserved.
doi:10.1016/j.ab.2007.10.016

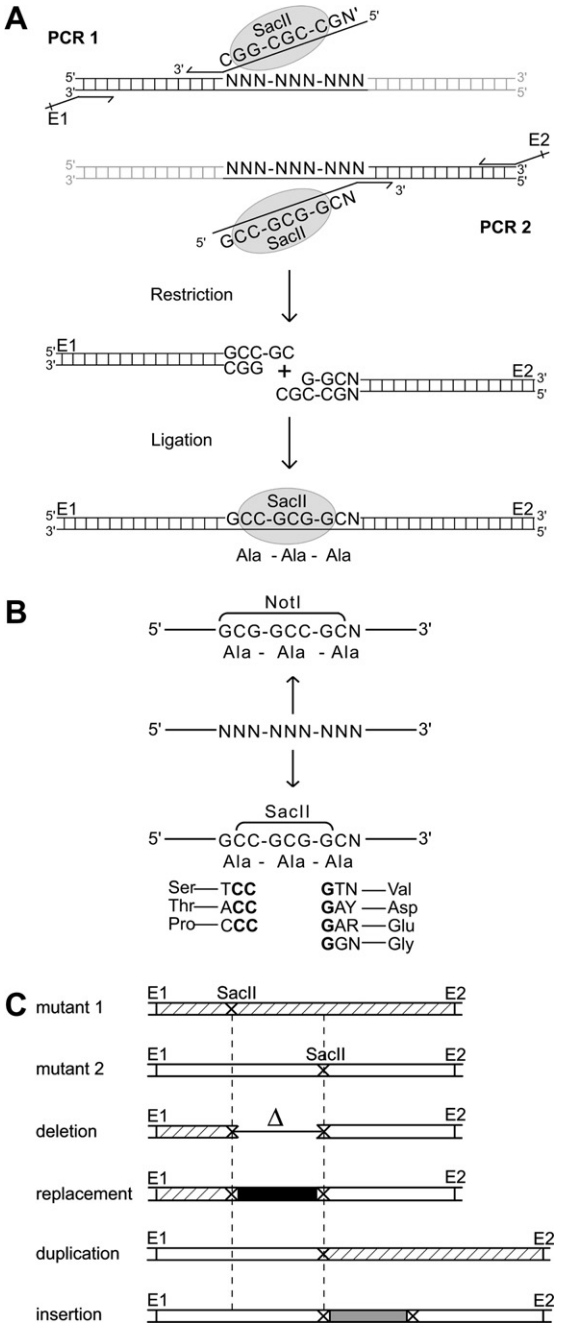

Fig. 1. Outline of the mutagenesis strategy. (A) Schematic representation of the three steps involved in the procedure. E1 and E2 represent restriction endonuclease sites of choice. The use of the *Sac*II restriction site coding for three alanine residues is exemplified. (B) Illustration of the introduction of the *Not*I and *Sac*II restriction sites in the reading frame to generate triple, double, or single alanine substitutions with all possible choices of adjacent residues. (C) Schematic drawing of the derivation of deletion, replacement, duplication, and insertion mutants from PCR fragments used to generate individual (alanine) substitutions. E1 and E2 represent the restriction sites in the flanking primers.

of each fragment. Fragment pairs to generate a given substitution are then joined into an appropriate vector by a three-fragment ligation. After transformation, randomly selected clones can be screened by simple restriction analysis, with the enzyme recognizing the mutagenic site and one or more suitable enzymes (Fig. 2).

When a *Not*I site is used three adjacent residues are exchanged to alanines, whereas when a *Sac*II site is used it is possible to accommodate codons for alanine, serine, threonine or proline in the first position and alanine, glycine, glutamine, valine aspartate in the third position (Fig. 1B).

With the same approach other restriction sites may be employed according to the specific amino acid substitutions required. A major advantage of this strategy is that fragments used to introduce the same mutagenic restriction site at different positions can be combined to generate deletions and duplications (Fig. 1C). The residues chosen for the mutagenesis will replace the deleted region and be present at the junction between the repeats, respectively. When several mutagenic sites are planned a large number of deletions can be generated covering different parts of the region. In addition, insertions or larger substitutions can be generated at one or between two mutagenic sites by introducing a DNA fragment whose ends are compatible with the chosen mutagenic restriction site(s). Such fragments may be easily obtained by annealing complementary synthetic oligonucleotides or by PCR. In addition, when mutations are introduced in different members of a protein family it is possible to generate chimeric proteins where domains or peptide elements are swapped.

We used our mutagenesis strategy as part of an effort to characterize potential inter- and intramolecular interactions mediated by the TS domain [13,14] of the murine DNA methyltransferase 1 (Dnmt1). Eight triple alanine substitutions were designed at positions corresponding to either peaks or minima in the hydrophilicity plot of the target region (Figs. 2A and 2B and Supplementary Table 1). The restriction analysis of these mutants is shown in Fig. 2C. The mutants were generated in parallel and more than 90% of the clones tested positive by *Sac*II restriction analysis in each case. In addition, we generated a deletion where aa 553–578 were replaced by three alanine residues by combining the PCR fragments upstream and downstream to the $EDS_{(553–555)}AAA$ and $DDE_{(576–578)}AAA$ mutations, respectively. The sites at the endpoints of the deletion correspond to consecutive hydrophilic peaks (Fig. 2A) and were selected with the aim of not disrupting the overall folding of the domain. We found that the postreplicative methyltransferase activity of this deletion mutant in living cells is comparable to that of wild-type Dnmt1 (Supplementary Fig. 1). Interestingly, a set of less specifically targeted deletions in this region was described previously [15], where all of the deletions either overlapping or immediately adjacent to the one described here had deleterious effects on the catalytic activity, suggesting that the integrity of structural motifs in this region is crucial for correct protein folding. Thus, our strategy allowed precise deletion of a distinct structural element without disrupting the overall folding of the protein. This method proved to be very robust in that it was successfully applied not only in our hands but also by inexperienced biology students in the context of a practical course in molecular biology.

In conclusion, our mutagenesis approach offers a simple method for systematic generation of alanine mutants and

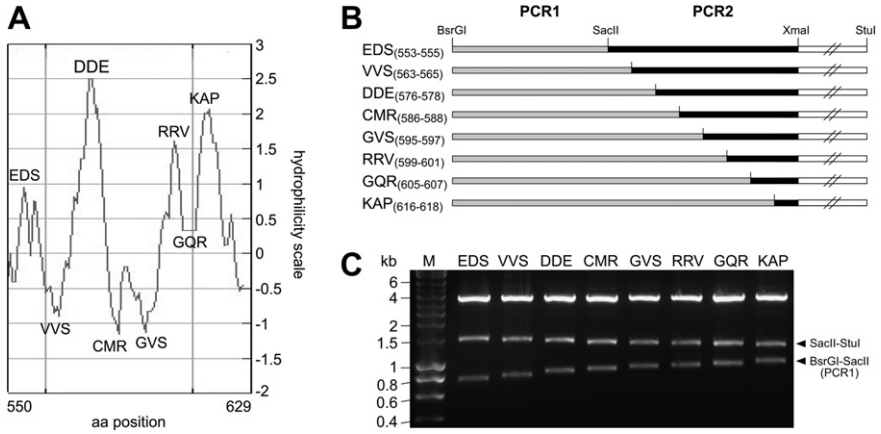

Fig. 2. Generation of an alanine-scanning set of mutants across the C-terminal part of the TS domain in Dnmt1. (A) Hydrophilicity plot of the C-terminal part of the TS domain from Dnmt1. The triplets of amino acids selected for mutagenesis reported in Supplementary Table 1 are shown here above and below the corresponding hydrophilic peaks and minima, respectively. The plot was generated with the ProtScale tool of the ExPASy proteomics server (http://www.expasy.ch/tools/protscale.html), selecting the Hopp and Woods algorithm [16] with linear weight variation model and a 7-aa window. (B) Schematic drawing of the eight triple alanine mutations. Fragments derived by the PCR1 and PCR2 amplification sets are shown as light gray and black rectangles, respectively. Restriction sites introduced with the primers are indicated at the top. The double forward slash indicates that the *Xma*I–*Stu*I vector fragment (open rectangles) is not represented on the scale. (C) Restriction analysis of the mutants. Fragments derived from the PCR1 set of amplifications (*Bsr*GI–*Sac*II) and containing the PCR2 fragment set (*Sac*II–*Stu*I) are indicated on the right and sizes of molecular weight standard (M) bands are indicated on the left.

fast and inexpensive screening of clones. In addition, sets of larger mutations, such as deletions, insertions, replacements and duplications can be generated in parallel with the same reagents used for generation of alanine mutations. This strategy allows rapid construction of well-designed sets of mutants for systematic protein analysis.

Acknowledgments

We thank Ulrich Rothbauer for the construction of $pEGmTS_{310–629}$ and thank members of the Leonhardt laboratory for critical reading of this manuscript and suggestions. This work was supported by grants from the Deutsche Forschungsgemeinschaft to H.L.

Appendix A. Supplementary data

Supplementary data associated with this article can be found, in the online version, at doi:10.1016/j.ab.2007.10.016.

References

[1] B.W. Matthews, Structural and genetic analysis of the folding and function of T4 lysozyme, FASEB J. 10 (1996) 35–41.
[2] A. Ashkenazi, L.G. Presta, S.A. Marsters, T.R. Camerato, K.A. Rosenthal, B.M. Fendly, D.J. Capon, Mapping the CD4 binding site for human immunodeficiency virus by alanine-scanning mutagenesis, Proc. Natl. Acad. Sci. USA 87 (1990) 7150–7154.
[3] B.C. Cunningham, J.A. Wells, High-resolution epitope mapping of hGH–receptor interactions by alanine-scanning mutagenesis, Science 244 (1989) 1081–1085.
[4] T.M. Ishii, P. Zerr, X.M. Xia, C.T. Bond, J. Maylie, J.P. Adelman, Site-directed mutagenesis, Methods Enzymol. 293 (1998) 53–71.
[5] M.M. Ling, B.H. Robinson, Approaches to DNA mutagenesis: An overview, Anal. Biochem. 254 (1997) 157–178.
[6] B. Zhu, G. Cai, E.O. Hall, G.J. Freeman, In-fusion assembly: Seamless engineering of multidomain fusion proteins, modular vectors, and mutations, BioTechniques 43 (2007) 354–359.
[7] C.A. Andrews, S.A. Lesley, Selection strategy for site-directed mutagenesis based on altered β-lactamase specificity, BioTechniques 24 (1998) 972–978.
[8] W.P. Deng, J.A. Nickoloff, Site-directed mutagenesis of virtually any plasmid by eliminating a unique site, Anal. Biochem. 200 (1992) 81–88.
[9] M. Tomic, I. Sunjevaric, E.S. Savtchenko, M. Blumenberg, A rapid and simple method for introducing specific mutations into any position of DNA leaving all other positions unaltered, Nucleic Acids Res. 18 (1990) 1656–1659.
[10] D.M. Kegler-Ebo, C.M. Docktor, D. DiMaio, Codon cassette mutagenesis: A general method to insert or replace individual codons by using universal mutagenic cassettes, Nucleic Acids Res. 22 (1994) 1593–1599.
[11] J-K. Ko, J. Ma, A rapid and efficient PCR-based mutagenesis method applicable to cell physiology study, Am. J. Physiol. Cell Physiol. 288 (2005) C1273–C1278.
[12] F. Allemandou, J. Nussberger, H.R. Brunner, N. Brakch, Rapid site-directed mutagenesis using two PCR-generated DNA fragments reproducing the plasmid template, J. Biomed. Biotechnol. 2003 (2003) 202–207.
[13] H. Leonhardt, A.W. Page, H.U. Weier, T.H. Bestor, A targeting sequence directs DNA methyltransferase to sites of DNA replication in mammalian nuclei, Cell 71 (1992) 865–873.
[14] H.P. Easwaran, L. Schermelleh, H. Leonhardt, M.C. Cardoso, Replication-independent chromatin loading of Dnmt1 during G2 and M phases, EMBO Rep. 5 (2004) 1181–1186.
[15] J.B. Margot, A.M. Aguirre-Arteta, B.V. Di Giacco, S. Pradhan, R.J. Roberts, M.C. Cardoso, H. Leonhardt, Structure and function of the mouse DNA methyltransferase gene: Dnmt1 shows a tripartite structure, J. Mol. Biol. 297 (2000) 293–300.
[16] T.P. Hopp, K.R. Woods, Prediction of protein antigenic determinants from amino acid sequences, Proc. Natl. Acad. Sci. USA 78 (1981) 3824–3828.

Fellinger *et al.*, A mutagenesis strategy combining systematic alanine-scanning with larger mutations to study protein interactions.

SUPPLEMENTARY DATA

Supplementary table 1. Oligonucleotide primers used in this study for the triple alanine-scanning mutagenesis of the TS domain from murine Dnmt1.

Mutation	PCR1 Reverse mutagenic Primers	PCR2 Forward mutagenic primers
EDS$_{(553-555)}$AAA	TG**C CGC GG**C TGT GAA CCG GTT CAC-3'	G**CC GCG G**CA CTC TTA CGC CAC GCC CAG-3'
VVS$_{(563-565)}$AAA	GTAT TG**C CGC GG**C AAA CTG GGC GTG GCG	GAAG G**CC GCG G**CA CAG GTA GAG AGT TAC GAC
DDE$_{(576-578)}$AAA	GAAG TG**C CGC GG**C GTC CTT GGC TTC GTC G	GAAG G**CC GCG G**CA ACC CCC ATC TTC TTG
CMR$_{(586-588)}$AAA	GAAG TG**C CGC GG**C GGG AGA CAA GAA GAT GGG	GAAG G**CC GCG G**CA GCC CTG ATC CAT TTG GC
GVS$_{(595-597)}$AAA	GGGG TG**C CGC GG**C AGC CAA ATG GAT CAG GG	GAAT G**CC GCG G**CA CTG GGA CAG AGG CGA GC
GQR$_{(599-601)}$AAA	GTAT TG**C CGC GG**C CAG GGA GAC ACC AGC	GAAT G**CC GCG G**CA CGA GCA ACA AGG CGC G
RRV$_{(605-607)}$AAA	GAAG TG**C CGC GG**C TGT TGC TCG CCT CTG	GAAG G**CC GCG** GCA ATG GGT GCT ACC AAG G
KAP$_{(616-618)}$AAA	GGGG TG**C CGC GG**C GTC CTT CTC CTT GGT AG	GGGG G**CC GCG G**CA ACG AAA GCC ACC ACC AC
	Forward flanking primer (G_{310}-D_{315}) GGGG **TG TAC A**AG GCG ATC GCA *GAG GAC AGA GAC GAG G*	**Reverse flanking primer** (T_{624}-Q_{629}) GAAG **CC CGG G**GC GGC CGC TTA *CTG ATA GAC CAG CTT G*

For each reverse and forward mutagenic primer the exchanged amino acids and their positions are indicated (left column) and the sequence encoding the three alanines is underlined and the sacII site is in bold face. The sequences complementary to the plasmid template in the forward and reverse flanking primers are italicized and the positions of the corresponding amino acids are indicated, while the BsrGI and XmaI sites used for subcloning are in bold face.

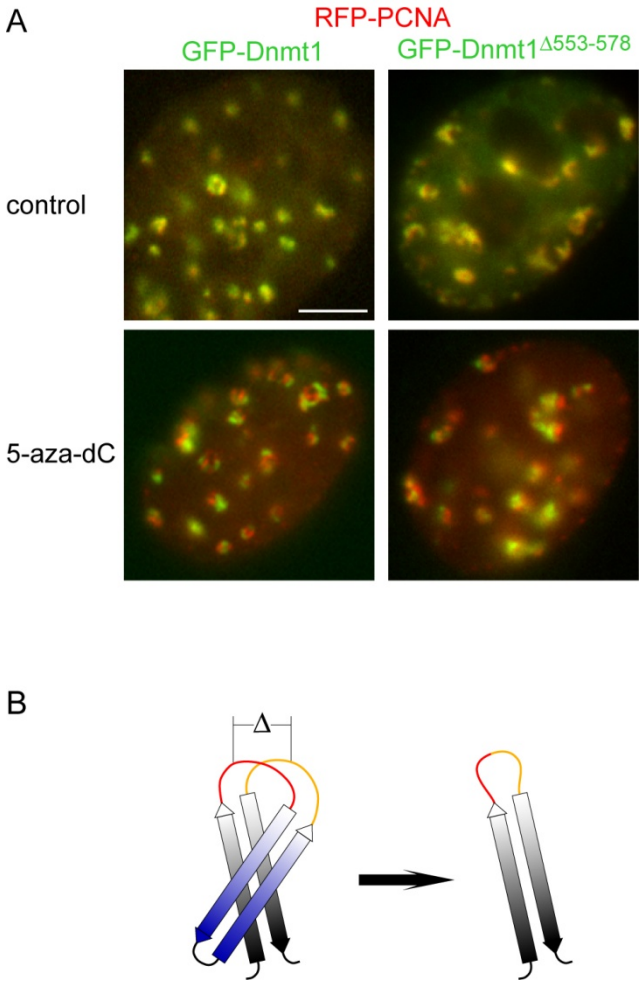

Supplementary Figure 1. GFP-Dnmt1$^{\Delta 553\text{-}578}$ is catalytically active *in vivo*. (**A**) A GFP-Dnmt1 fusion construct where aa 553-578 of Dnmt1 were substituted with three alanine residues (GFP-Dnmt1$^{\Delta 553\text{-}578}$) or the corresponding wild type construct (GFP-Dnmt1^{wt}) were co-expressed in C2C12 mouse myoblasts with a RFP-PCNA construct as a replication foci (RF) marker (red;1). The postreplicative methyltransferase activity of the two Dnmt1 constructs (green) was compared using a simplified variation of our live cell trapping assay (3,4). Briefly, transfected cultures were incubated with and without (control) the mechanism based inhibitor 5-aza-2'-deoxycytidine (5-aza-dC) prior to fixation. This deoxycytidine (dC) analogue is incorporated into newly synthesized DNA at RF. Dnmt1 interacts directly but transiently with PCNA at RF (yellow signal) and is engaged in methylation of hemi-methylated CpG sites as they are generated during DNA replication (2). As part of its catalytic mechanism Dnmt1 forms a transient covalent bond with the cytidine ring which is released after methylation, but when dC is replaced by 5-aza-dC this covalent bond cannot be resolved and Dnmt1 is permanently "trapped" at the site of action. This leads to complete

immobilization of the GFP-Dnmt1 pool in about 40 min (2). Thus, while RFP-PCNA dissociates from fully replicated replicons and associates at new, adjacent RF (5), all GFP-Dnmt1 remains trapped at sites that are distinct from current RF, resulting in separation of red RF from green GFP-Dnmt1 foci. As immobilization is strictly dependent on enzymatic activity (3), the similar separation of green and red foci observed with GFP-Dnmt1^{wt} and GFP-Dnmt1$^{\Delta 553\text{-}578}$ indicates that they are comparably active. Scale bar 5 µm.

(**B**) Model of how deletion between two hydrophilic patches may result in precise removal of a distinct structural element without disrupting the overall protein folding.

Supplementary References

1. **Easwaran, H.P., H. Leonhardt and M.C. Cardoso.** 2005. Cell Cycle Markers for Live Cell Analyses. Cell Cycle *4*: 453-455.
2. **Schermelleh, L., A. Haemmer, F. Spada, N. Rosing, D. Meilinger, U. Rothbauer, M. Cristina Cardoso and H. Leonhardt.** 2007. Dynamics of Dnmt1 interaction with the replication machinery and its role in postreplicative maintenance of DNA methylation. Nucl. Acids Res.:10.1093/nar/gkm1432.
3. **Schermelleh, L., F. Spada, H.P. Easwaran, K. Zolghadr, J.B. Margot, M.C. Cardoso and H. Leonhardt.** 2005. Trapped in action: direct visualization of DNA methyltransferase activity in living cells. Nat Methods *2*:751-756.
4. **Schermelleh, L., F. Spada and H. Leonhardt.** 2007. Visualization and Measurement of DNA Methyltransferase Activity in Living Cells. *In* M. Dasso (Ed.), Current Protocols in Cell Biology. Wiley and Sons, Hillsborough, NJ. In Press.
5. **Sporbert, A., A. Gahl, R. Ankerhold, H. Leonhardt and M.C. Cardoso.** 2002. DNA polymerase clamp shows little turnover at established replication sites but sequential de novo assembly at adjacent origin clusters. Mol Cell *10*:1355-1365.

2.2 Biochemical Analysis of Intramolecular N-C Terminal Dnmt1 Interactions

2.2 Biochemical Analysis of Intramolecular N-C Terminal Dnmt1 Interactions

Among the family of DNA methyltransferases Dnmt1 is the only enzyme that possesses a large regulatory N-terminal domain of 1111 amino acids which is connected via a $(GK)_7$ linker to the catalytic domain. This unique N-terminal region is indispensable for the allosteric activation of the catalytic domain as the catalytic domain alone is not enzymatically active even though it contains all conserved methyltransferase motifs known from bacterial enzymes (Fatemi et al., 2001; Margot et al., 2003).

2.2.1 A Major Part of the N-Terminal Regulatory Domain is Necessary for Interaction with the C-Terminal Catalytic Domain

To understand the intramolecular regulation of Dnmt1 we mapped subdomains within the N-terminus that are essential for the interaction with the catalytic domain and therefore catalysis. To this end we performed co-immunoprecipitation experiments using the GFP-Nanotrap (Rothbauer et al., 2008). GFP-N-terminal Dnmt1 fragments were co-expressed with Cherry-C-terminal domain, precipitated with GFP-Nanotrap and input and bound fractions were analyzed by SDS-PAGE and immunoblotting (Figure 2.1; procedure as described in Fellinger et al, 2009).

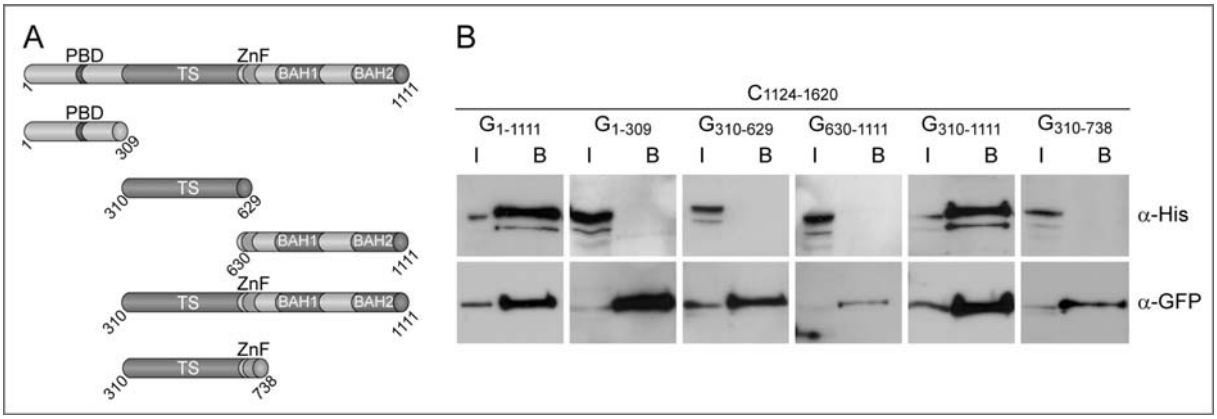

Figure 2.1 N-C terminal interactions of Dnmt1 were tested by co-immunoprecipitation experiments. (A) Schematic outline of N-terminal constructs used, subdomains are indicated: PBD, PCNA binding domain; TS, targeting sequence; ZnF, CXXC-type zinc finger; BAH1+2, bromo adjacent homology domain 1+2. Numbers in subscript denote first and last amino acids in Dnmt1. All depicted constructs contain a N-terminal GFP tag and were co-expressed with Cherry-C-terminus ($C_{1124-1620}$) that contains a C-terminal His_6 tag. (B) 1% of input (I) and 30% of bound (B) fractions were subjected to SDS-PAGE and immunoblot analysis with antibodies against His and GFP.

GFP-N-terminus G_{1-1111} precipitated quantitatively Cherry-C-terminus $C_{1124-1620}$ while the three parts of the N-terminus G_{1-309}, $G_{310-629}$ and $G_{630-1111}$ did not interact with $C_{1124-1620}$. Moreover, the N-terminal region containing the TS domain and the zinc finger $G_{310-738}$ was not sufficient for interaction with the C-terminus. Deletion of the N-terminal 309 amino acids of the N-

terminus ($G_{310-1111}$) did not impair the interaction between N- and C-terminus of Dnmt1. As single subdomains of the N-terminus were not sufficient to interact with the C-terminus, the interaction very likely involves the major part of the N-terminus (aa 310-1111). These results indicate that the overall folding of the N-terminus is crucial for interaction and allosteric activation of the C-terminal catalytic domain. These results are in line with previously published data that showed aa 228-1111 as minimal N-terminal domain of Dnmt1 interacting with the catalytic domain in a Y2H screen (Margot et al., 2003). In addition, *in vitro* activity tests of Dnmt1 deletion mutants showed that the N-terminal 425 amino acids were dispensable for enzymatic activity of Dnmt1 while more C-terminal deletions within the N-terminus disrupted the catalytic activity (Margot et al., 2000).

2.2.2 The CXXC Zinc Finger is Dispensable for Dnmt1 N-C Terminal Interaction

As part of our effort to determine the region of the Dnmt1 N-terminus that is essential for interaction and allosteric activation of the catalytic domain, we tested whether the zinc finger plays a role in that process as it was indicated by previous publications (Fatemi et al., 2001; Pradhan et al., 2008). The Dnmt1 N-terminus contains a CXXC type zinc finger (C is cysteine, X is any amino acid; aa 655-696). The mixed lineage leukemia protein (MLL) contains a CXXC zinc finger motif that is highly similar to the one in Dnmt1 (Figure 2.2A). Based on the structural information of the MLL zinc finger (Allen et al., 2006) we precisely removed this distinct zinc finger structure from Dnmt1 without affecting the surrounding protein regions. To this end, we performed deletion mutagenesis according to the mutagenesis strategy described in chapter 2.1 (Fellinger et al., 2008). Then, we analyzed Dnmt1 N-C terminal interactions by co-immunoprecipitation experiments. GFP and Cherry tagged Dnmt1 domains were expressed in HEK293T cells; GFP fusions were precipitated with the GFP Nanotrap (Rothbauer et al., 2008) and bound proteins were analyzed by SDS-PAGE and immunoblotting (procedure as described in Fellinger et al, 2009, Figure 2.2B/C).

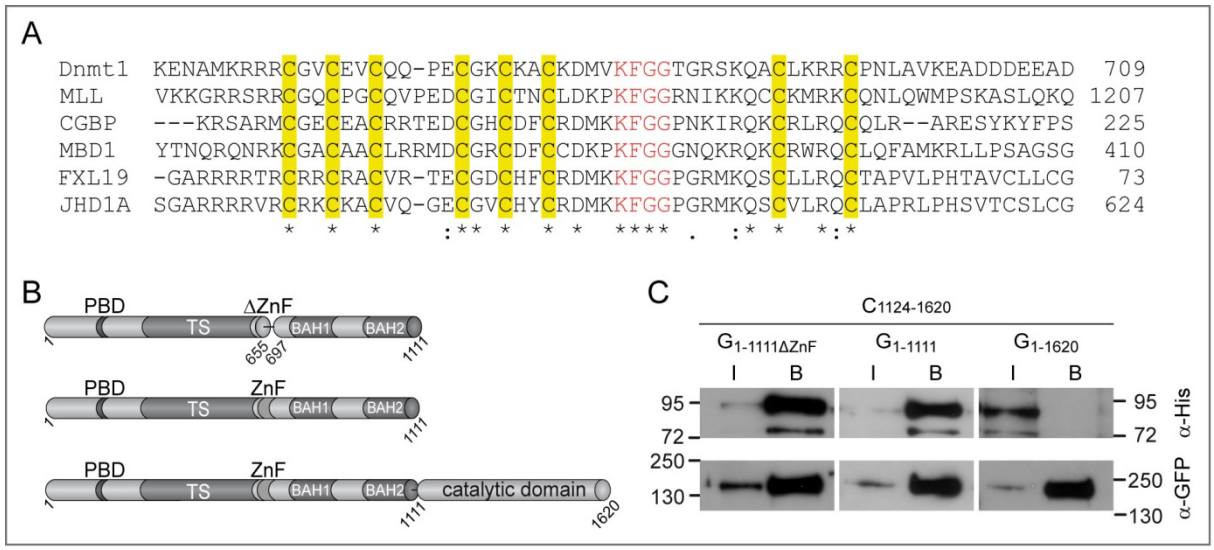

Figure 2.2 Analysis of the CXXC zinc finger in the Dnmt1 N-C-terminal interaction. (A) Alignment of the CXXC zinc finger domain. Cysteines are highlighted in yellow, KFGG motif in red, asterisks mark identical amino acids. Numbers signify the amino acid position within the respective protein. NCBI accession numbers are as follows: Dnmt1 (NP_034196); MLL (mixed lineage leukemia, NP_001074518); CGBP (CpG binding protein, NM_028868); MBD1 (methyl binding domain protein 1, AF120978); FXL19 (F-box and leucine-rich repeat protein 19, Q6PB97); JHD1A (JmjC domain-containing histone demethylation protein 1A, P59997). (B) Schematic outline of Dnmt1 constructs used for co-immunoprecipitation experiments. Subdomains are indicated: PBD, PCNA binding domain; TS, targeting sequence; ZnF, CXXC-type zinc finger; BAH1+2, bromo adjacent homology domain 1+2. Numbers in subscript denote first and last amino acids in Dnmt1. All depicted constructs contain a N-terminal GFP tag and were co-expressed with Cherry-C-terminus ($C_{1124-1620}$) that contains a C-terminal His_6 tag. (C) 1% of input (I) and 30% of bound (B) fractions of the co-immunoprecipitation experiments were subjected to SDS-PAGE and immunoblotting with antibodies against His and GFP. Deletion of the ZnF does not affect N-C-terminal interaction. Molecular size markers are indicated on both sides.

Cherry-C-terminus $C_{1124-1620}$ was efficiently co-precipitated with the N-terminal domain $G_{1-1111}\Delta Zn$ as well as with G_{1-1111} full-length. Moreover, GFP-Dnmt1 wt (G_{1-1620}) did not interact with the isolated catalytic domain indicating that the intramolecular N-C terminal interaction within full-length Dnmt1 is favored.

These results show that the CXXC zinc finger does not play a role in the intramolecular N-C-terminal interaction of Dnmt1.

2.2.3 Impact of Serine 515 Phosphorylation on Dnmt1 N-C Terminal Interaction

Phosphorylation of serine 515 (S515) was described to be a common posttranslational modification of Dnmt1 (Glickman et al., 1997; Goyal et al., 2007). As this S515 is located within the TS domain, in the center of the N-terminus, we tested whether this phosphorylation has an influence on N-C-terminal interaction of Dnmt1. Thus, we compared a Dnmt1 "P off" mutant containing a S515A (alanine) substitution and a "P on" mutant comprising a S515D (aspartic acid) substitution with the wt N-terminal domain. The carboxyl group of aspartic acid mimics the phosphate group. Again, we performed co-immunoprecipitation experiments using the GFP Nanotrap (Figure 2.3; (Rothbauer et al., 2008) by the standard procedure described in Fellinger et al, 2009).

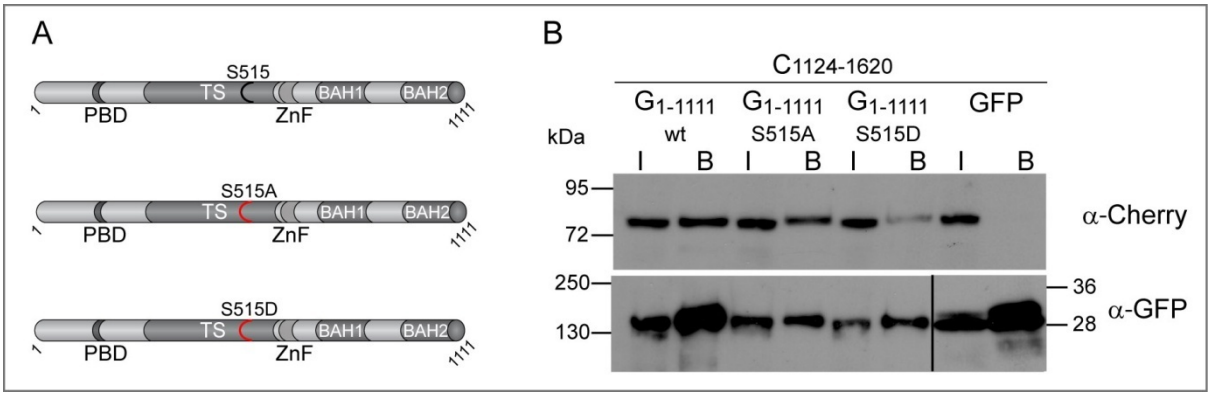

Figure 2.3 Co-immunoprecipitation experiments to study the role of S515A phosphorylation in the N-C-terminal Dnmt1 interaction. (A) Schematic outline of N-terminal Dnmt1 constructs used, subdomains are indicated: PBD, PCNA binding domain; TS, targeting sequence; ZnF, CXXC-type zinc finger; BAH1+2, bromo adjacent homology domain 1+2. Numbers in subscript denote first and last amino acids in Dnmt1, S515 mutations are marked by red lines. All depicted constructs contain a N-terminal GFP tag. (B) G_{1-1111} wt, S515A and S515D were co-expressed with Cherry-C-terminus ($C_{1124-1620}$) that contains a C-terminal His_6 tag. 1% of input (I) and 30% of bound (B) fractions of the co-immunoprecipitation experiments were subjected to SDS-PAGE and immunoblotting with antibodies against Cherry (Rottach et al., 2008) and GFP. In contrast to S515D mutation, S515A substitution does not affect N-C-terminal interaction. Molecular size markers are indicated on both sides.

Both GFP-N-terminus wt and S515A co-precipitated the catalytic domain $C_{1124-1620}$ while the N-terminal domain containing the "P on" mutant S515D only weakly interacted with the catalytic domain. To date, it is unknown how the phosphorylation of Dnmt1 is regulated. However, comparing the wildtype and S515A mutation we did not observe any differences in N-C terminal interaction. The S515D substitution, mimicking a phosphate group even had a negative effect on N-C-terminal interaction pointing to a tight regulation of this transient posttranslational modification. In addition, normal catalytic activity of both S515 mutants in the context of full-length Dnmt1 was confirmed using the *in vivo* trapping assay (unpublished data from A. Rottach).

The results indicate that phosphorylation of serine 515 is not crucial for the interaction between the regulatory N-terminal and the catalytic C-terminal domain of Dnmt1.

2.3 Dimerization of DNA Methyltransferase 1 is Mediated by its Regulatory Domain

Dimerization of DNA Methyltransferase 1 is Mediated by its Regulatory Domain

Karin Fellinger[1], Ulrich Rothbauer[1], Max Felle[2], Gernot Längst[2], Heinrich Leonhardt[1]*

[1]Center for Integrated Protein Science at the Department of Biology II, Ludwig Maximilians University Munich, 82152 Planegg-Martinsried, Germany

[2]Institute for Biochemistry, Genetics and Microbiology, University of Regensburg, 93053 Regensburg, Germany

*Correspondence to: Heinrich Leonhardt, [1]Department of Biology II, Ludwig Maximilians University Munich, 82152 Planegg-Martinsried, Germany; Tel. +49 89 2180-74232; Fax +49 89 2180-74236; E-mail: h.leonhardt@lmu.de

Running Title: Dnmt1 forms a stable dimer

Key Words: dimer; methylation; DNA methyltransferase1; Dnmt1; targeting sequence

ABSTRACT

DNA methylation is a major epigenetic modification and plays a crucial role in the regulation of gene expression. Within the family of DNA methyltransferases (Dnmts), Dnmt3a and 3b establish methylation marks during early development, while Dnmt1 maintains methylation patterns after DNA replication. The maintenance function of Dnmt1 is regulated by its large regulatory N-terminal domain that interacts with other chromatin factors and is essential for the recognition of hemi-methylated DNA. Gelfiltration analysis showed that purified Dnmt1 elutes at an apparent molecular weight corresponding to the size of a dimer. With protein interaction assays we could show that Dnmt1 interacts with itself through its N-terminal regulatory domain. By deletion analysis and co-immunoprecipitations we mapped the dimerization domain to the targeting sequence TS that is located in the center of the N-terminal domain (amino acids 310-629) and was previously shown to mediate replication independent association with heterochromatin at chromocenters. Further mutational analyses suggested that the dimeric complex has a bipartite interaction interface and is formed in a head-to-head orientation. Dnmt1 dimer formation could facilitate the discrimination of hemi-methylated target sites as has been found for other palindromic DNA sequence recognizing enzymes. These results assign an additional function to the TS domain and raise the interesting question how these functions are spatially and temporarily co-ordinated.

INTRODUCTION

DNA methylation at cytosine residues of CpG dinucleotides is a crucial epigenetic modification that regulates gene expression and chromatin structure and is required for X chromosome inactivation and imprinting [Bird, 2002; Leonhardt and Cardoso, 2000]. In early development new methylation patterns are established by *de novo* methyltransferases Dnmt3a and 3b and are subsequently maintained by DNA methyltransferase1 (Dnmt1) [Goll and Bestor, 2005; Hermann et al., 2004]. Dnmt1 is the only methyltransferase with a preference for hemi-methylated DNA [Bestor and Ingram, 1983; Pradhan et al., 1999] generated by DNA replication and repair. Targeted disruption of the *dnmt1* gene leads to genome-wide loss of DNA methylation and embryonic lethality [Li et al., 1992]. Artificial reduction of cellular Dnmt1 levels severely affects development and genome stability [Gaudet et al., 2003; Gaudet et al., 2004]. The crucial role of Dnmt1 was recently also shown in human cells [Easwaran et al., 2004; Egger et al., 2006; Spada et al., 2007]. During S-phase Dnmt1 associates with the replication machinery by interacting with PCNA [Chuang et al., 1997; Leonhardt et al., 1992]. PCNA also targets Dnmt1 to DNA repair sites to restore the epigenetic information [Mortusewicz et al., 2005]. The interaction of Dnmt1 with the replication machinery enhances methylation efficiency by twofold, but is not strictly required for postreplicative maintenance of DNA methylation [Schermelleh et al., 2007; Spada et al., 2007]. The targeting sequence (TS domain) recruits Dnmt1 to pericentric heterochromatin independent of DNA replication, H3K9 trimethylation and the interacting proteins SUV39H1 and HP1 [Easwaran et al., 2004]. Both, the PCNA binding domain PBD and the heterochromatin binding TS domain, reside in the large N-terminal part of Dnmt1, a region of the protein that contains several regulatory functions and is unique among the family of DNA methyltransferases. The intramolecular interaction between the regulatory N-terminus and the catalytic C-terminus is essential for the catalytic activity of Dnmt1. Despite the presence of all typical, conserved methyltransferase motifs, the catalytic domain per se lacks methyltransferase activity [Fatemi et al., 2001; Margot et al., 2000; Margot et al., 2003; Zimmermann et al., 1997]. Also, interaction of Dnmt1 with the chromatin factors Np95, LSH, EZH2 and G9a was shown to be essential for maintenance of DNA methylation [Bostick et al., 2007; Esteve et al., 2006; Myant and Stancheva, 2008; Sharif et al., 2007; Vire et al., 2006]. The molecular mechanism of these multiple interactions controlling the activity of Dnmt1 and the recognition of hemi-methylated target sites remains largely unknown.

Our biochemical characterization shows that Dnmt1 forms a stable dimer. With gelfiltration, co-immunoprecipitation and *in vivo* assays we demonstrate that Dnmt1 dimerization is mediated by the N-terminal TS domain. These results show that the TS domain is not only crucial for recruitment of Dnmt1 to heterochromatin as reported previously, but also for the assembly of stable dimeric Dnmt1 complexes.

MATERIALS AND METHODS

Expression Constructs

The expression construct for GFP-Dnmt1 was described previously [Easwaran et al., 2004]. GFP-Dnmt1 fusion constructs were generated by PCR cloning using eGFP-Dnmt1 as template to clone into pEGFP-N1 (Clontech) employing either the restriction sites XhoI and XmaI or BsrGI and HindIII. GFP was subsequently replaced with mCherry (kindly provided by R.Y. Tsien [Shaner et al., 2004]). Throughout this study we used the enhanced GFP and monomeric Cherry. PCR primers are listed in supplementary table 1. All constructs were sequenced and tested by transient expression in human embryonic kidney (HEK) 293T cells followed by immunoblot analysis. hTS was cloned into pMAL-2cX (NEB) after replacement of factor Xa cleavage site through a TEV cleavage site.

Cell Culture, Transfection and Microscopy

HEK 293T HeLa and BHK cells were cultured in DMEM supplemented with 10% fetal calf serum and 50 µg/ml gentamycine. BHK cells carrying a *lac* operator array were maintained in the presence of 150 µg/ml hygromycin B (PAA Laboratories) [Tsukamoto et al., 2000]. HEK 293T cells were transfected with polyethyleneimine (Sigma). For microscopy, BHK cells were grown to 50-70% confluence on glass coverslips and co-transfected with TS-LacI-RFP and GFP-Dnmt1 constructs using Transfectin (Bio-Rad) according to manufacturer's instructions. Cells were fixed 24 hr after transfection with 3.7% formaldehyde in PBS for 10 min at room temperature. After permeabilization with 0.2% Triton X-100 in PBS for 3 min cells were counterstaind with DAPI and mounted in Vectashield (Vector Laboratories). Microscopy was performed as described [Zolghadr et al., 2008].

Co-Immunoprecipitation and Immunoblotting and Quantification

HEK 293T cells were transiently transfected with expression plasmids as described above. After 24 hr, 60-90% of the cells expressed the constructs as determined by fluorescence microscopy. About ~ 1 x 10^7 cells were harvested in 200 µl of lysis buffer (20 mM Tris/HCl pH 7.5, 150 mM or 1 M NaCl, 0.5 mM EDTA, 2 mM PMSF, 0.5% NP40). After clearing by centrifugation (10 min, 20,000xg, 4°C) supernatants were adjusted to a volume of 500 µl with dilution buffer (lysis buffer without NP40). 50 µl aliquots were prepared in SDS-containing sample buffer (referred to as input (I)). Extracts were incubated with GFP Nanotrap [Rothbauer et al., 2008] (Chromotek) for 2 h at 4°C with constant mixing. Immunocomplexes

were harvested by centrifugation (2 min, 5,000xg, 4°C) and beads were washed twice with 1 ml of dilution buffer containing 300 mM NaCl and resuspended in SDS-PAGE sample buffer (referred to a bound (B)). Proteins were eluted by boiling at 95°C. For immunoblot analysis 1% of the input and 20% of the bound fractions were separated by SDS–PAGE and blotted onto a PVDF-membrane (Millipore). Antigens were detected with a mouse monoclonal anti-GFP antibody (Roche), a rat monoclonal anti-mCherry antibody [Rottach et al., 2008] or a rat monoclonal anti-DNMT1 antibody [Spada et al., 2007]. For quantification mean grey values of band intensities of co-precipitated proteins obtained from westernblots were calculated with the ImageJ software (Version 1.38, http://rsb.info.nih.gov/ij/). The ratios of bound and input signals were determined and the mean value and standard error from three independent experiments were calculated.

Gelfiltration

Reference gelfiltration was carried out with a Superose 6 column and separation properties were determined in a first run with mass standard proteins (thyroglobulin (669kDa), apoferritin (443kDa), BSA (66kDa)). For analysis of endogenous Dnmt1, HeLa cells were lysed in 200 µl of buffer (20 mM Tris/HCl pH 7.5, 50 mM NaCl, 0.5 mM EDTA, 2 mM PMSF, 0.5 mM NP40, 1µg/µl DNase I, 5 mM $MgCl_2$), incubated on ice for 30 min and centrifuged (15 min, 20,000xg, 4°C). The supernatant was adjusted to 500 µl with PBS and applied to a Superose 6 gelfiltration column (GE Healthcare) (Figure1). Recombinant human Dnmt1 and TS proteins were analyzed by a Superdex 200 column (GE Healthcare) (Figure 3) in buffer containing 20 mM Tris, pH 7.5, 150 mM NaCl, 1 mM EDTA, 1 mM DTT. Chromatography was performed with a flow rate of 0.5 ml/min and fractions were analyzed by SDS-PAGE and immunoblotting with an antibody against human DNMT1.

Protein Purification

DNMT1 containing an N-terminal His tag was purified from baculovirus infected Sf21 insect cells and purified by Ni-NTA chromatography as described previously [Yokochi and Robertson, 2002]. The DNMT1 virus was kindly provided by K.D. Robertson. DNMT1 was further purified on a Resource Q column (GE Healthcare) with a linear gradient from 100 – 600 mM NaCl in 20 mM Hepes, pH 7.9; 1 mM EDTA; 1.5 mM $MgCl_2$; 10% Glycerol; 1 mM DTT, 1 mM PMSF. The peak fractions were combined and stored at -80°C. The DNMT1 TS domain (pMAL-TS) was expressed in *E.coli* K12 TB1 cells (NEB) according to the manufacturer's

instructions. Protein expression was induced at an OD_{600} of 0.7 with 0.3 mM IPTG for 2 hours, cells were harvested and washed once with TBS. The cell pellet of 1 l culture was resuspended in 30 ml of buffer CV (20 mM Tris pH 7.5, 200 mM NaCl, 1 mM EDTA, 1 mM PMSF, 1 mM DTT) and cells were lysed (Branson Sonifier). The lysate was cleared (20,000 g, 4°C, 20 min) and incubated with 10 ml amylose resin (NEB). The resin was washed 3x with 50 ml buffer CV and applied to a glass column. The MBP-TS fusion protein was eluted with 30 ml elution buffer (buffer CV + 10 mM Maltose). The peak fractions were combined and the TS domain was cleaved off the MBP moiety by incubation with TEV protease (Invitrogen) at 16°C over night. TEV protease and MBP were removed by a Q FF 5 ml column (GE Healthcare) and the TS domain was eluted with a step gradient.

RESULTS

Dnmt1 Forms Stable Dimers

For biochemical characterization we purified (full-length) DNMT1 using a baculovirus expression system. Purified DNMT1 was loaded on a gelfiltration column and the elution profile was recorded (Figure 1A). Immunoblot analysis of collected fractions showed that DNMT1 was eluted in a fraction corresponding to a molecular mass of about 400kDa. This is approximately two-fold the molecular mass of DNMT1 (183kDa) indicating the presence of a dimeric DNMT1 complex. To analyze DNMT1 complex formation *in vivo*, we analyzed extracts from HeLa cells by gelfiltration and also did not observe a DNMT1 monomer fraction. Instead, the endogenous DNMT1 eluted as part of a higher molecular weight complex of 400-700 kDa which is likely caused by additional protein interactions occuring in living cells. The dimeric complex was stable under high salt buffer conditions up to 1 M NaCl. Dimer formation was further tested by co-immunoprecipitation experiments. GFP-Dnmt1 was expressed in transiently transfected HEK 293T cells and immunoprecipitated using the GFP-Nanotrap [Rothbauer et al., 2008]. Immunoblot analysis of input and bound fractions showed that the endogenous DNMT1 counterpart was efficiently co-precipitated (Figure 1B).

The N-Terminal TS Domain Mediates Dnmt1 Dimerization

The gelfiltration and co-immunoprecipitation experiments both indicated that DNMT1 forms a stable dimeric complex. To test whether this dimerization is related to the previously reported interaction between the N- and C-terminal domain [Fatemi et al., 2001; Margot et al., 2003] and to map the domains involved in this dimerization, we fused various parts of Dnmt1 with GFP and Cherry (Figure 2A) and performed co-immunoprecipitation studies. We found that the TS domain was sufficient to precipitate the endogenous DNMT1 (Figure 1C). To identify the part of Dnmt1 the TS domain binds to we co-expressed different GFP-Dnmt1 subdomains with Cherry-TS ($C_{310-629}$) in HEK 293T cells and performed co-immunoprecipitation. Input and bound fractions were analyzed by immunoblots against GFP and Cherry (Figure 2A). GFP-N-terminus (G_{1-1111}) but not GFP-C-terminus ($G_{1124-1620}$) efficiently precipitated the TS domain $C_{310-629}$ pointing to a dimerization through the N-termini of two Dnmt1 molecules rather than an intermolecular interaction between the N- and C-terminal domain (Figure 2B). Further fine-mapping showed that the TS domain $C_{310-629}$ efficiently co-precipitated with GFP-TS $G_{310-629}$ but not with G_{1-309} or $G_{630-1111}$ (Figure 2b). These results show

that Dnmt1 dimerization is mediated through a homotypic interaction of the N-terminal TS domain.

To independently verify these biochemical data *in vivo*, we performed a fluorescent two-hybrid assay (F2H), that allows direct visualization of protein interactions in single living cells [Zolghadr et al., 2008]. The F2H assay visualizes the interaction of a red fluorescent bait with a green fluorescent prey protein as co-localization at a defined nuclear spot. To anchor the fluorescent bait, we used a transgenic cell-line that contains a chromosomally integrated *lac* operator array and provides a defined binding platform for Lac repressor fusion proteins. We engineered a triple fusion protein comprising the TS domain as bait, the Lac repressor and the red fluorescent protein (RFP). Binding of the fusion protein (TS-LacI-RFP) to the *lac* operator array can directly be visualized as defined nuclear spot in living cells by fluorescence microscopy (Figure 2C). Interaction of green fluorescent prey proteins with the TS domain leads to a co-localization at the anchor point (Figure 2C, right panel) that is visible in the overlay as orange/yellow spot. With this assay we tested different Dnmt1 domains for interaction with the TS domain containing bait construct. We observed a clear co-localization of the N-terminal domain (G_{1-1111}) with the TS-LacI-RFP bait protein while the C-terminal domain ($G_{1124-1620}$) did not co-localize (Figure 2C). To fine-map the interaction with the TS domain three parts of the N-terminal domain were tested and only $G_{310-629}$ showed co-localization with TS-LacI-RFP while the first and the last part (G_{1-309} or $G_{630-1111}$) did not interact and showed a diffuse distribution. These results show that the red labeled TS domain interacts with green labeled TS domain *in vivo*. In summary, biochemical and cellular assays indicate that Dnmt1 dimerization is mediated by a direct intermolecular TS-TS domain interaction.

Dnmt1 Dimerization is Formed by a Rather Hydrophobic TS-TS Interaction

To test the complex formation properties we purified the TS domain that has a calculated molecular weight of about 30 kDa and analyzed it by gelfiltration. Immunoblot analysis of elution fractions showed a distinct peak at about 66 kDa corresponding to a TS dimer and high molecular weight complexes in the size range above 500 kDa indicating multimerization of the TS domain (Figure 3A, lane 2). This supports the conclusion that the TS domain by itself can form a stable dimer and thus drive dimerization of DNMT1.

To analyze the nature and strength of this interaction, we performed co-immunoprecipitions of GFP-TS and Cherry-TS in the presence of increasing salt concentrations. We found that the interaction was stable despite the high ionic strength of the buffer containing 1M NaCl (Figure 3B) arguing for a more hydrophobic interaction. Indeed, the hydrophilicity plot [Hopp and Woods, 1981] of Dnmt1 shows that the TS domain is among the most hydrophobic parts of the regulatory domain of Dnmt1 (Figure 3C). Taken together, these results indicate that the dimerization of Dnmt1 is mediated by a stable and rather hydrophobic interaction of the N-terminal TS domain.

Dnmt1 Dimerization is Mediated by a Bipartite Interface

To fine-map the dimerization interface we generated a series of GFP-TS deletion constructs including N- and C-terminal deletions in steps of about 50 amino acids. HEK 293T cells were co-transfected with GFP-TS deletion constructs and Cherry-TS ($C_{310-629}$) and co-precipitation experiments were performed. Surprisingly, all tested GFP-TS deletion proteins interacted with the Cherry-TS full-length domain (Supplementary Figure 1) indicating a more complex and potentially multipartite interaction interface.

To further investigate the interacting regions of the domain, we generated additional GFP- and Cherry fusion proteins and tested interactions by co-immunoprecipitations (Figure 4A). Pairs of TS subdomain constructs tested are depicted on the left side and their relative co-immunoprecipitation efficiency is shown in the bar graph on the right side. One representative immunoblot is displayed in Figure 4B. We observed no interaction between the N- and C-terminal parts of the TS domain (lane 3) arguing against a head-to-tail interaction. Interestingly, N- and C-terminal parts of the TS domain overlapping by 27 amino acids showed a strong interaction (lane 4) indicating that this middle part plays an important role in the TS-TS interaction. In addition, we found that the N-terminal part but not the C-terminal part of the TS domain can dimerize. These results indicate that dimerization is mediated by a bipartite interface containing the N-terminal (aa 310-409) and the central part (aa 476-502) of the TS domain. It should be noted that the hydrophobic nature of the TS domain makes the fine-mapping of the dimerization interface difficult and may lead to false-positive results. Further alanine scanning mutagenesis [Fellinger et al., 2008] of the TS domain did not yield specific dimerization mutants (data not shown) which is probably due to the large bipartite interaction surface spanning almost 200 amino acids.

Larger deletions within the TS domain were previously shown to abolish catalytic activity of Dnmt1 (Figure 5A, Margot et al, 2000; Zimmermann et al, 1997) emphasizing the importance of the TS domain. However, it is unclear to what extent this is due to disruption of dimerization, since the TS domain also mediates association with heterochromatin [Easwaran et al., 2004] and may also contribute to the allosteric activation of the catalytic domain [Fatemi et al., 2001; Margot et al., 2000].

Interestingly, sequence alignments of Dnmt1 homologs showed that the core region of the TS domain that is involved in dimerization is highly conserved from human to plants (Figure 5A). The crystal structure shows that the conserved core region consists of three β-sheets forming part of a potential binding pocket in the TS domain (Figure 5B). The high conservation and distinct structure of this TS core region suggests an essential role in Dnmt1 regulation.

DISCUSSION

Recent work has shown that DNA methylation is linked with several other nuclear processes and involves numerous protein interactions. Analyzing recombinant and endogenous Dnmt1 protein fractions we found that Dnmt1 forms a stable dimer. We mapped the dimerization domain to the N-terminal TS domain of Dnmt1 using gelfiltration, co-immunoprecipitation and *in vivo* fluorescent two-hybrid assay. Fine-mapping identified a homotypic TS-TS interaction containing a bipartite dimerization interface spanning about 200 amino acids of the TS domain.

Interestingly, dimerization has also been shown for other C5 DNA methyltransferases including the bacteria HhaI and the vertebrate Dnmt3a and Dnmt3L [Dong et al., 2004; Jia et al., 2007]. The crystal structure revealed that the central Dnmt3a dimer is flanked by Dnmt3L forming a 3L-3a-3a-3L tetramer. Disruption of the Dnmt3a dimer by specific point mutations resulted in loss of catalytic activity [Jia et al., 2007]. In contrast to these DNA methyltransferases that dimerize via the catalytic domain, Dnmt1 dimerization is mediated by its unique regulatory, N-terminal domain. Consistent with this difference, the key residues for Dnmt3a dimerization (R881 and D872) are not conserved in Dnmt1. In addition to dimerization, the TS domain of Dnmt1 also seems to contribute to allosteric activation of the catalytic domain [Fatemi et al., 2001; Margot et al., 2000; Zimmermann et al., 1997] and mediates association with heterochromatin [Easwaran et al., 2004]. Further studies are necessary to elucidate the temporal and spatial coordination of these multiple functions of the TS domain.

ACKNOWLEDGEMENTS

We thank Bijàn Montazeri for practical support, Kourosh Zolghadr for introduction to the F2H assay, Andrea Rottach and Fabio Spada for discussion and critical reading of the manuscript. We thank R.Y. Tsien for mCherry DNA and D. Spector for the transgenic BHK cell line. This work has been supported by grants from the Deutsche Forschungsgemeinschaft to HL and GL and the Nanosystems Initiative Munich (NIM). KF is a fellow of the International Max Planck Research School (IMPRS) for Molecular and Cellular Life Sciences.

REFERENCES

Bestor TH, Ingram VM. 1983. Two DNA methyltransferases from murine erythroleukemia cells: purification, sequence specificity, and mode of interaction with DNA. Proc Natl Acad Sci U S A 80:5559-63.
Bird A. 2002. DNA methylation patterns and epigenetic memory. Genes Dev 16:6-21.
Bostick M, Kim JK, Esteve PO, Clark A, Pradhan S, Jacobsen SE. 2007. UHRF1 plays a role in maintaining DNA methylation in mammalian cells. Science 317:1760-4.
Chuang LS, Ian HI, Koh TW, Ng HH, Xu G, Li BF. 1997. Human DNA-(cytosine-5) methyltransferase-PCNA complex as a target for p21WAF1. Science 277:1996-2000.
Dong A, Zhou L, Zhang X, Stickel S, Roberts RJ, Cheng X. 2004. Structure of the Q237W mutant of HhaI DNA methyltransferase: an insight into protein-protein interactions. Biol Chem 385:373-9.
Easwaran HP, Schermelleh L, Leonhardt H, Cardoso MC. 2004. Replication-independent chromatin loading of Dnmt1 during G2 and M phases. EMBO Rep 5:1181-6.
Egger G, Jeong S, Escobar SG, Cortez CC, Li TW, Saito Y, Yoo CB, Jones PA, Liang G. 2006. Identification of DNMT1 (DNA methyltransferase 1) hypomorphs in somatic knockouts suggests an essential role for DNMT1 in cell survival. Proc Natl Acad Sci U S A 103:14080-5.
Esteve PO, Chin HG, Smallwood A, Feehery GR, Gangisetty O, Karpf AR, Carey MF, Pradhan S. 2006. Direct interaction between DNMT1 and G9a coordinates DNA and histone methylation during replication. Genes Dev 20:3089-103.
Fatemi M, Hermann A, Pradhan S, Jeltsch A. 2001. The activity of the murine DNA methyltransferase Dnmt1 is controlled by interaction of the catalytic domain with the N-terminal part of the enzyme leading to an allosteric activation of the enzyme after binding to methylated DNA. J Mol Biol 309:1189-99.
Fellinger K, Leonhardt H, Spada F. 2008. A mutagenesis strategy combining systematic alanine scanning with larger mutations to study protein interactions. Anal Biochem 373:176-8.
Gaudet F, Hodgson JG, Eden A, Jackson-Grusby L, Dausman J, Gray JW, Leonhardt H, Jaenisch R. 2003. Induction of tumors in mice by genomic hypomethylation. Science 300:489-92.
Gaudet F, Rideout WM, 3rd, Meissner A, Dausman J, Leonhardt H, Jaenisch R. 2004. Dnmt1 expression in pre- and postimplantation embryogenesis and the maintenance of IAP silencing. Mol Cell Biol 24:1640-8.
Goll MG, Bestor TH. 2005. Eukaryotic cytosine methyltransferases. Annu Rev Biochem 74:481-514.
Hermann A, Gowher H, Jeltsch A. 2004. Biochemistry and biology of mammalian DNA methyltransferases. Cell Mol Life Sci 61:2571-87.
Hopp TP, Woods KR. 1981. Prediction of protein antigenic determinants from amino acid sequences. Proc Natl Acad Sci U S A 78:3824-8.
Jia D, Jurkowska RZ, Zhang X, Jeltsch A, Cheng X. 2007. Structure of Dnmt3a bound to Dnmt3L suggests a model for de novo DNA methylation. Nature 449:248-51.
Leonhardt H, Cardoso MC. 2000. DNA methylation, nuclear structure, gene expression and cancer. J Cell Biochem Suppl Suppl:78-83.
Leonhardt H, Page AW, Weier HU, Bestor TH. 1992. A targeting sequence directs DNA methyltransferase to sites of DNA replication in mammalian nuclei. Cell 71:865-73.
Li E, Bestor TH, Jaenisch R. 1992. Targeted mutation of the DNA methyltransferase gene results in embryonic lethality. Cell 69:915-26.
Margot JB, Aguirre-Arteta AM, Di Giacco BV, Pradhan S, Roberts RJ, Cardoso MC, Leonhardt H. 2000. Structure and function of the mouse DNA methyltransferase gene: Dnmt1 shows a tripartite structure. J Mol Biol 297:293-300.

Margot JB, Ehrenhofer-Murray AE, Leonhardt H. 2003. Interactions within the mammalian DNA methyltransferase family. BMC Mol Biol 4:7.
Mortusewicz O, Schermelleh L, Walter J, Cardoso MC, Leonhardt H. 2005. Recruitment of DNA methyltransferase I to DNA repair sites. Proc Natl Acad Sci U S A 102:8905-9.
Myant K, Stancheva I. 2008. LSH cooperates with DNA methyltransferases to repress transcription. Mol Cell Biol 28:215-26.
Pradhan S, Bacolla A, Wells RD, Roberts RJ. 1999. Recombinant human DNA (cytosine-5) methyltransferase. I. Expression, purification, and comparison of de novo and maintenance methylation. J Biol Chem 274:33002-10.
Rothbauer U, Zolghadr K, Muyldermans S, Schepers A, Cardoso MC, Leonhardt H. 2008. A versatile nanotrap for biochemical and functional studies with fluorescent fusion proteins. Mol Cell Proteomics 7:282-9.
Rottach A, Kremmer E, Nowak D, Leonhardt H, Cardoso MC. 2008. Generation and characterization of a rat monoclonal antibody specific for multiple red fluorescent proteins. Hybridoma (Larchmt) 27:337-43.
Schermelleh L, Haemmer A, Spada F, Rosing N, Meilinger D, Rothbauer U, Cardoso MC, Leonhardt H. 2007. Dynamics of Dnmt1 interaction with the replication machinery and its role in postreplicative maintenance of DNA methylation. Nucleic Acids Res 35:4301-12.
Shaner NC, Campbell RE, Steinbach PA, Giepmans BN, Palmer AE, Tsien RY. 2004. Improved monomeric red, orange and yellow fluorescent proteins derived from Discosoma sp. red fluorescent protein. Nat Biotechnol 22:1567-72.
Sharif J, Muto M, Takebayashi S, Suetake I, Iwamatsu A, Endo TA, Shinga J, Mizutani-Koseki Y, Toyoda T, Okamura K, Tajima S, Mitsuya K, Okano M, Koseki H. 2007. The SRA protein Np95 mediates epigenetic inheritance by recruiting Dnmt1 to methylated DNA. Nature 450:908-12.
Spada F, Haemmer A, Kuch D, Rothbauer U, Schermelleh L, Kremmer E, Carell T, Langst G, Leonhardt H. 2007. DNMT1 but not its interaction with the replication machinery is required for maintenance of DNA methylation in human cells J. Cell Biol. 176:565-571.
Tsukamoto T, Hashiguchi N, Janicki SM, Tumbar T, Belmont AS, Spector DL. 2000. Visualization of gene activity in living cells. Nat Cell Biol 2:871-8.
Vire E, Brenner C, Deplus R, Blanchon L, Fraga M, Didelot C, Morey L, Van Eynde A, Bernard D, Vanderwinden JM, Bollen M, Esteller M, Di Croce L, de Launoit Y, Fuks F. 2006. The Polycomb group protein EZH2 directly controls DNA methylation. Nature 439:871-4.
Yokochi T, Robertson KD. 2002. Preferential methylation of unmethylated DNA by Mammalian de novo DNA methyltransferase Dnmt3a. J Biol Chem 277:11735-45.
Zimmermann C, Guhl E, Graessmann A. 1997. Mouse DNA methyltransferase (MTase) deletion mutants that retain the catalytic domain display neither de novo nor maintenance methylation activity in vivo. Biol Chem 378:393-405.
Zolghadr K, Mortusewicz O, Rothbauer U, Kleinhans R, Goehler H, Wanker EE, Cardoso MC, Leonhardt H. 2008b. A fluorescent two-hybrid assay for direct visualization of protein interactions in living cells. Mol Cell Proteomics 7:2279-87.

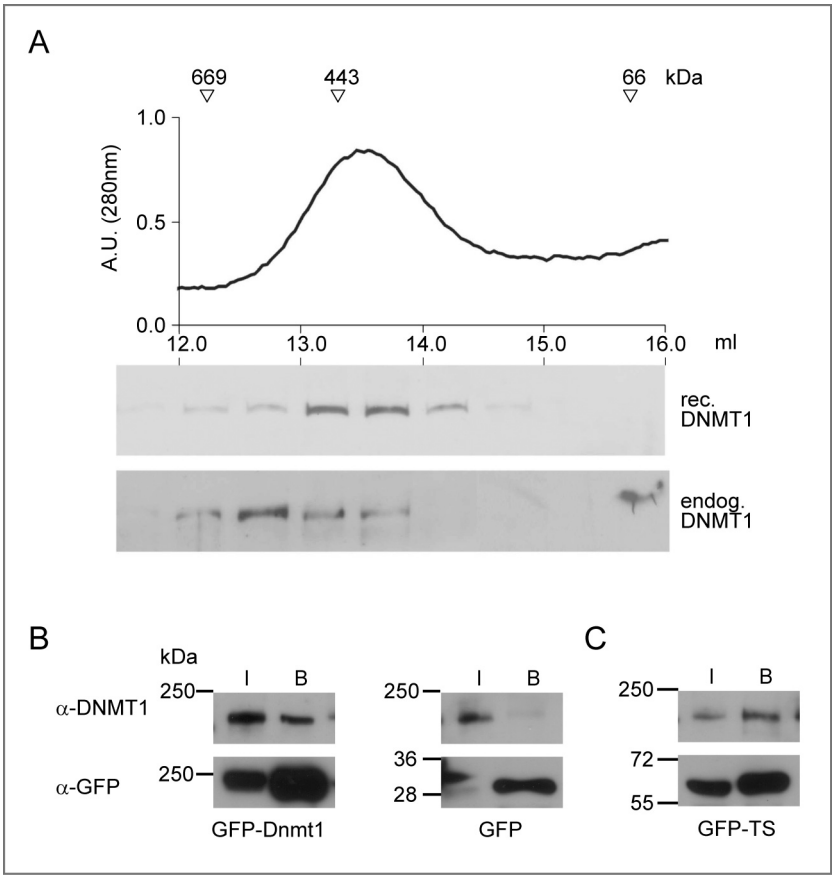

Figure 1

DNMT1 was analyzed by gelfiltration and co-immunoprecipitation. **(A)** Elution profile of recombinant human DNMT1 showing a peak at ~ 400 kDa**,** the x-axis indicates the protein fractions collected in 1 ml steps and the y-axis presents the absorption units (A.U.) at the wavelength of 280 nm. The arrows denote the molecular size of marker proteins applied in a separate run (thyroglobulin: 669 kDa, apoferritin 443 kDa, BSA 66 kDa). Immunoblot of elution fractions confirms the elution profile of recombinant DNMT1 (upper row). Endogenous DNMT1 of a HeLa cell extract is present in a higher molecular weight complex (lower row). **(B)** Immunoblots after co-immunuprecipitations illustrate the interaction between GFP-Dnmt1 and endogenous DNMT1, whereas GFP alone was used as negative control. 1% of input and 30% of bound fractions were subjected to immunoblot analysis. The molecular size of the proteins (kDa) and the antibodies used are indicated. **(C)** Mapping the Dnmt1 dimerization to the TS domain of Dnmt1: Immunoblot after co-immunoprecipitation showing that the N-terminal TS domain of Dnmt1 can co-precipitate endogenous DNMT1.

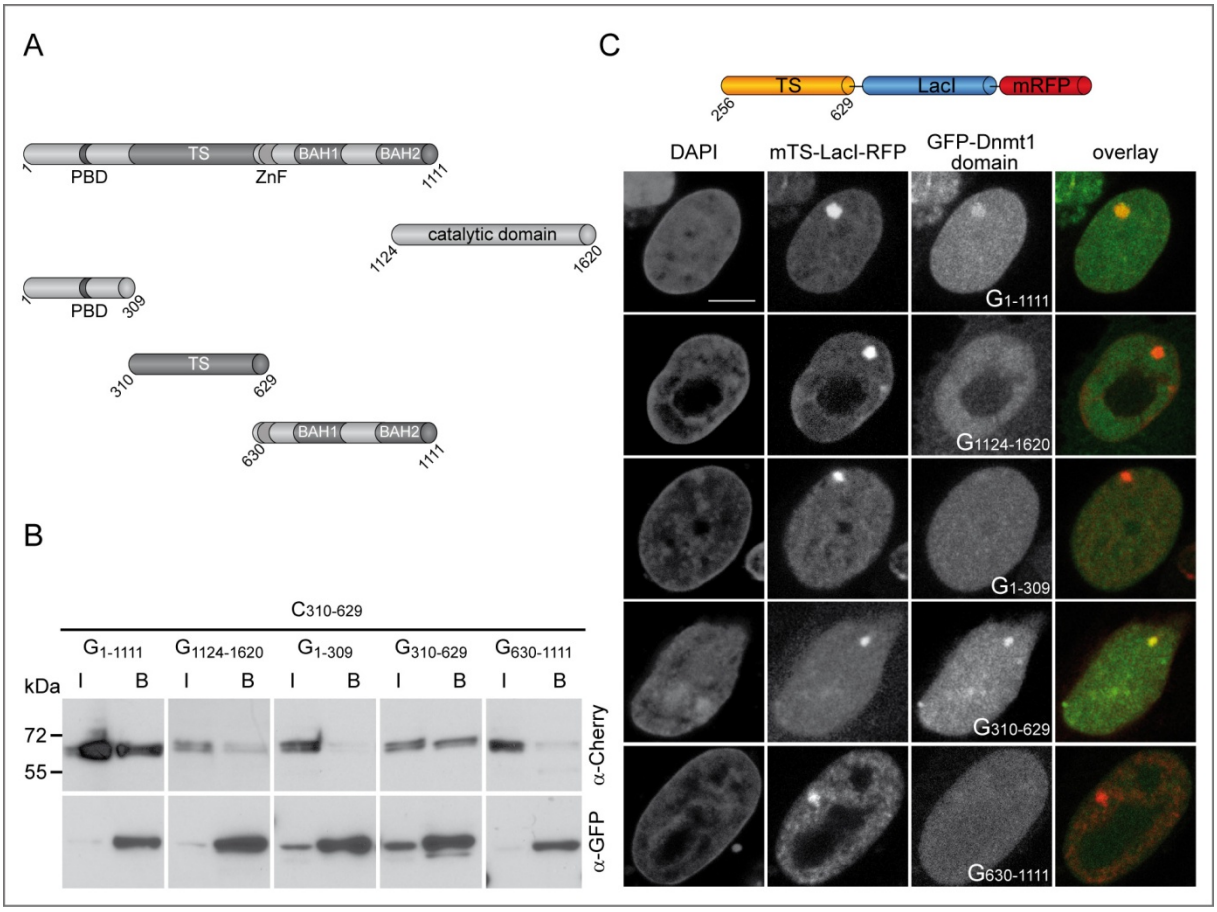

Figure 2

N-terminal TS domain is the Dnmt1 dimerization domain. **(A)** Schematic overview of Dnmt1 constructs used for co-immunoprecipitations. Subdomains are indicated: PBD, PCNA binding domain; NLS nuclear localization signal; TS, targeting sequence; ZnF, zinc finger; BAH1+2, bromo adjacent homology domains 1+2. **(B)** Immunoblots after co-immunoprecipitations of GFP-Dnmt1 domains and Cherry-TS ($C_{310-629}$) with the GFP-Nanotrap. G indicates GFP and C Cherry, numerics in subscript denote the first and last amino acids of Dnmt1 present in these constructs. 1% of input (I) and 20% of bound (B) fractions were subjected to SDS-PAGE, blotted on PVDF membrane (Millipore) and decorated with antibodies against Cherry and GFP. These results are representative of three independent experiments and show that GFP-N-terminus (G_{1-1111}) and GFP-TS ($G_{310-629}$) interact with Cherry-TS ($C_{310-629}$). **(C)** Fluorescent two-hybrid (F2H) assay confirms biochemical interaction data. TS-LacI-RFP (bait, depicted on top) was co-expressed with GFP-Dnmt1 domains (prey) in transgenic BHK cells [Tsukamoto et al., 2000] containing a *lac* operator array. Binding of the TS-LacI-RFP fusion protein is visible as distinct nuclear spot and interaction of a GFP fusion protein leads to co-localizing

fluorescence signals. DAPI, RFP, and GFP were imaged and an overlay image of GFP and RFP fluorescence is presented. The Dnmt1 N-terminus ($G_{1\text{-}1111}$) co-localizes with TS-LacI-RFP but the C-terminus ($G_{1124\text{-}1620}$) does not. From the three parts of the N-terminal domain only the TS domain ($G_{310\text{-}629}$) co-localized with TS-LacI-RFP indicating a specific TS-TS interaction *in vivo*. The scale bar represents 5 µm.

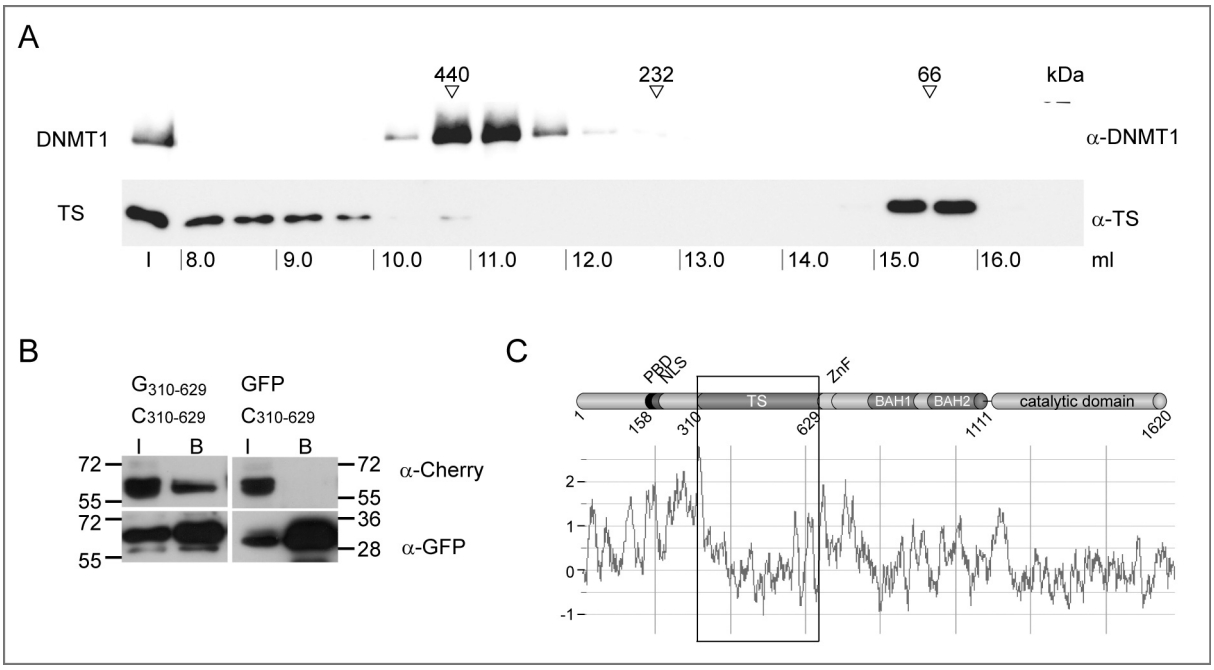

Figure 3

Dnmt1 dimerization is formed by a rather hydrophobic TS-TS interaction. **(A)** DNMT1 and the TS domain were studied by gelfiltration and the respective protein fractions are analyzed by immunoblots. The proteins and the migration of the size standards are indicated (in kDa) as well as the protein fractions loaded in ml and the input fraction (I). **(B)** Hydrophilic or hydrophobic nature of the dimerization interaction was tested by co-immunoprecipitation of GFP-TS ($G_{310-629}$) and Cherry-TS ($C_{310-629}$) in buffer containing 1 M NaCl with subsequent immunoblot analysis. 1% of input (I) and 20% of bound (B) fractions were loaded and immunoblots probed with antibodies against GFP and Cherry. **(C)** Top: Schematic outline of Dnmt1 full-length protein including subdomains: PBD (PCNA binding domain), NLS (nuclear localization signal). TS (targeting sequence), ZnF (zinc finger), BAH 1 + 2 (bromo adjacent homology domains 1 + 2). Bottom: Hydrophilicity plot [Hopp and Woods, 1981] of the Dnmt1 protein sequence generated with the ProtScale tool of the ExPASy proteomics server (http://www.expasy.ch/tools/protscale.html) with the linear weight variation model and a 15 amino acid window. Hydrophobic regions are represented as minima in the plot; a rectangle marks the TS domain which is rather hydrophobic in comparison with the rest of the N-terminus.

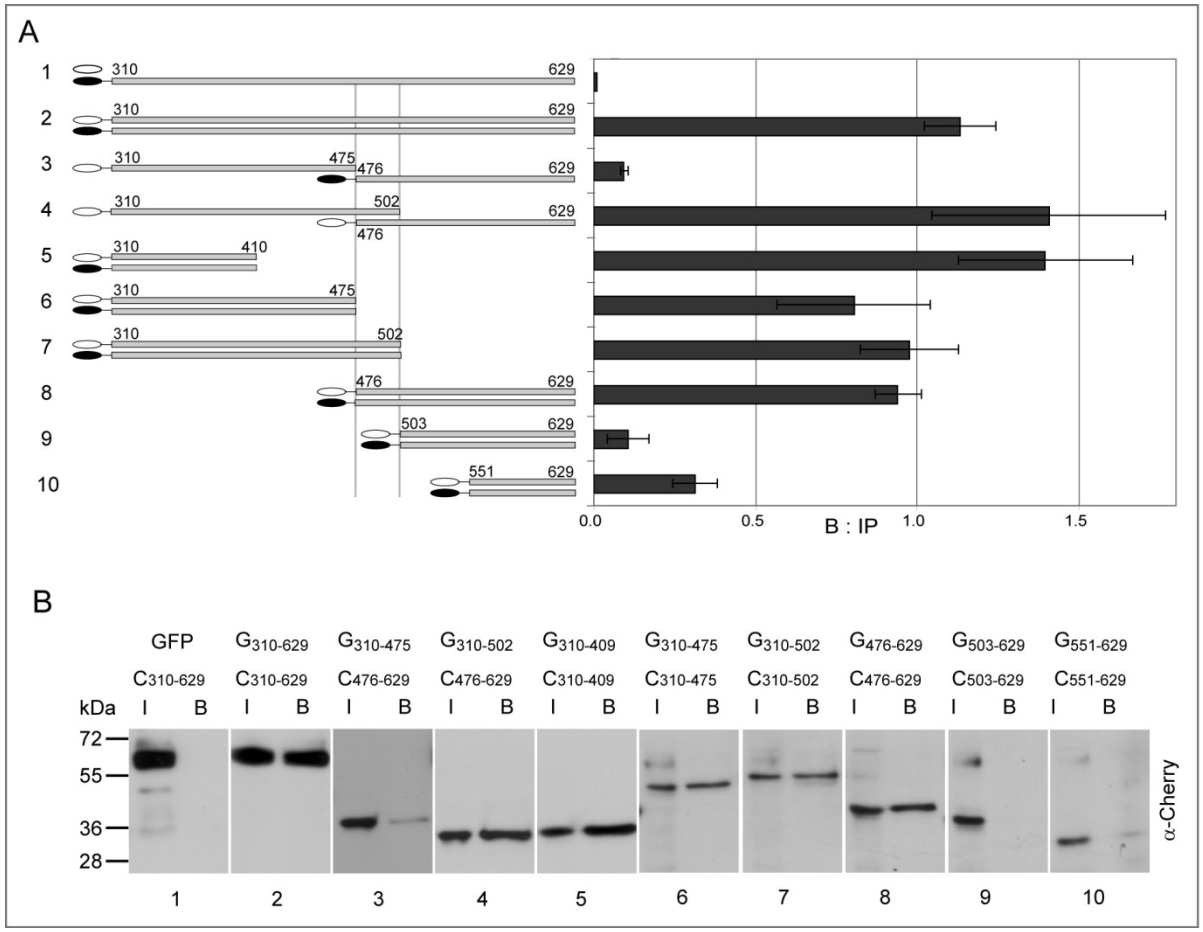

Figure 4

Fine-Mapping of the TS-TS interactions by co-immunoprecipitation analyses. **(A)** Left panel: Scheme of GFP (open elipse) and Cherry (filled elipse) tagged TS deletion constructs used for immunoprecipitation assays: Numbers above the construct refer to respective amino acid positions within Dnmt1. Right panel: Bar graph shows relative co-immunoprecipitation rates. Westernblot signals from input and bound fractions were quantified with ImageJ and mean ratios of three independent experiments +/- standard error (SE) determined. **(B)** Immunoblot from one representative co-immunprecipitation experiment out of three independent experiments. Quantification of all three experiments is shown above in A. G indicates GFP, C Cherry. 1% of input (I) and 20% of bound (B) fractions were subjected to SDS-PAGE and immunoblotting and probed with antibodies against Cherry. Precipitation efficiency of GFP-proteins was checked by immunoblot analysis with antibodies against GFP (not shown). Molecular marker sizes are indicated on the left.

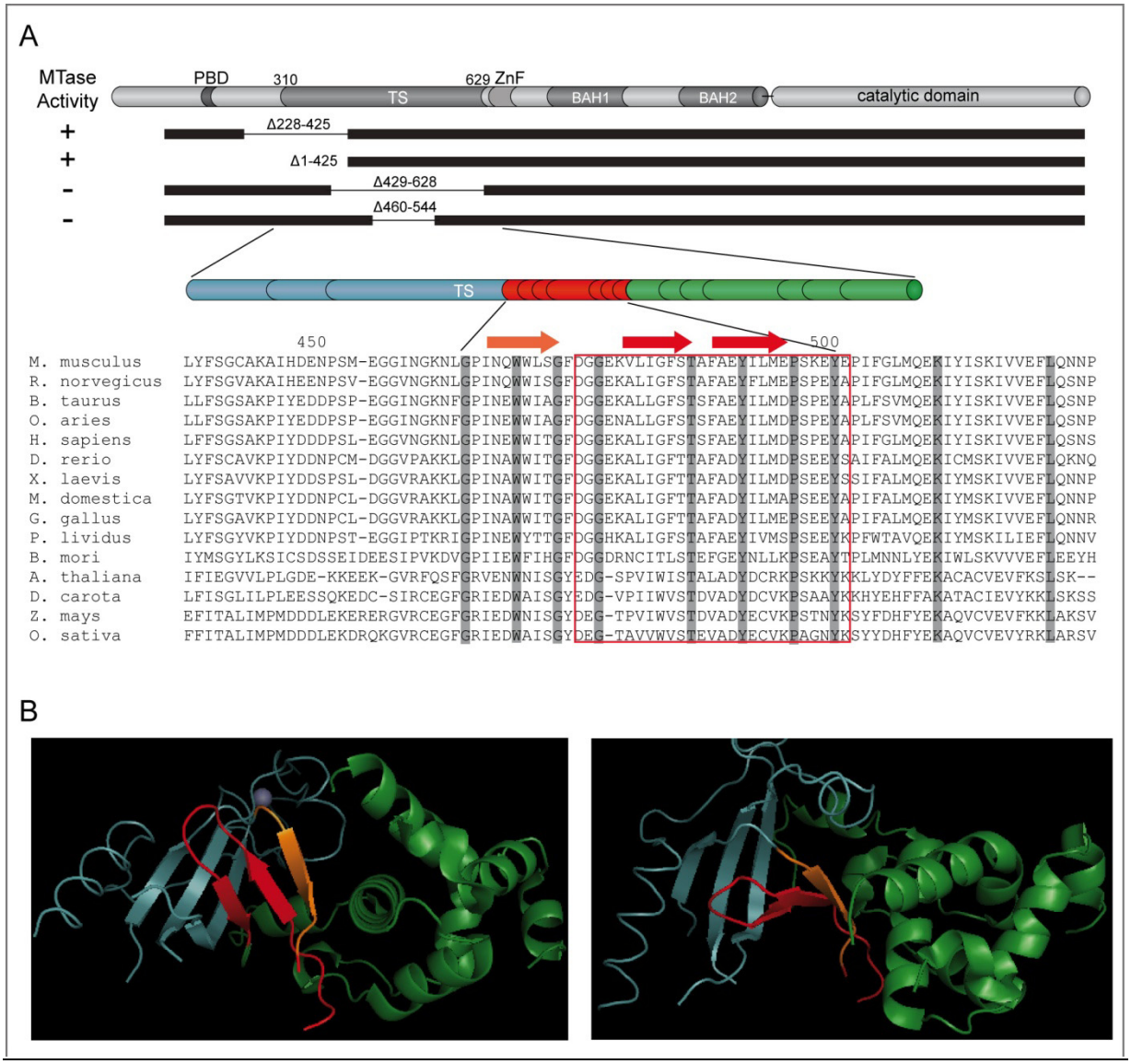

Figure 5

TS domain is crucial for Dnmt1 activity and contains a highly conserved core region.

(A) Schematic overview of Dnmt1 and subdomains (PBD, PCNA binding domain; TS, targeting sequence; ZnF, zinc finger; BAH1+2, bromo adjacent homology domains1+2). Below, Dnmt1 deletion mutants and their *in vitro* activity (left) are shown, results were taken from Margot et al., 2000. Below, a magnified overview of the TS domain is depicted with an N-terminal part (blue), the highly conserved core (red) and the C-terminal part (green). Black lines represent amino acids that are identical in Dnmt1 homologs from human to plants. Below, a ClustalW alignment of the central TS region from selected Dnmt1 homologs is shown. Identical amino acids are marked by dark gray shading. Red rectangle highlights the 27 amino acids which are important for TS-TS dimerization. Accession numbers: M. musculus,

P13864; R. norwegicus, Q9Z330; B. taurus, Q24K09; O. aries, Q865V5; H. sapiens, P26358; D. rerio, Q8QGB8; X. laevis, Q6GQH0; M. domestica, Q8MJ28; G.gallus, Q92072; P. lividus, Q27746; B. mori, Q5W7N6; A. thaliana, Q9SEG3; D. carota, O48867; Z. mays, Q8LPU6; O. sativa, A2XMY1. **(B)** Crystal structure of human TS domain (aa 351-600; Protein Data Bank 3epz). The image was generated using PyMOL (DeLano 2002). The N-terminal part of the TS domain is colored in blue and coordinates a zinc-ion, the highly conserved central region in orange and red and the C-terminal region in green. The view from two angles shows the highly conserved β-sheet structure (orange / red) of the TS domain as part of a potential binding pocket.

SUPPLEMENTARY INFORMATION

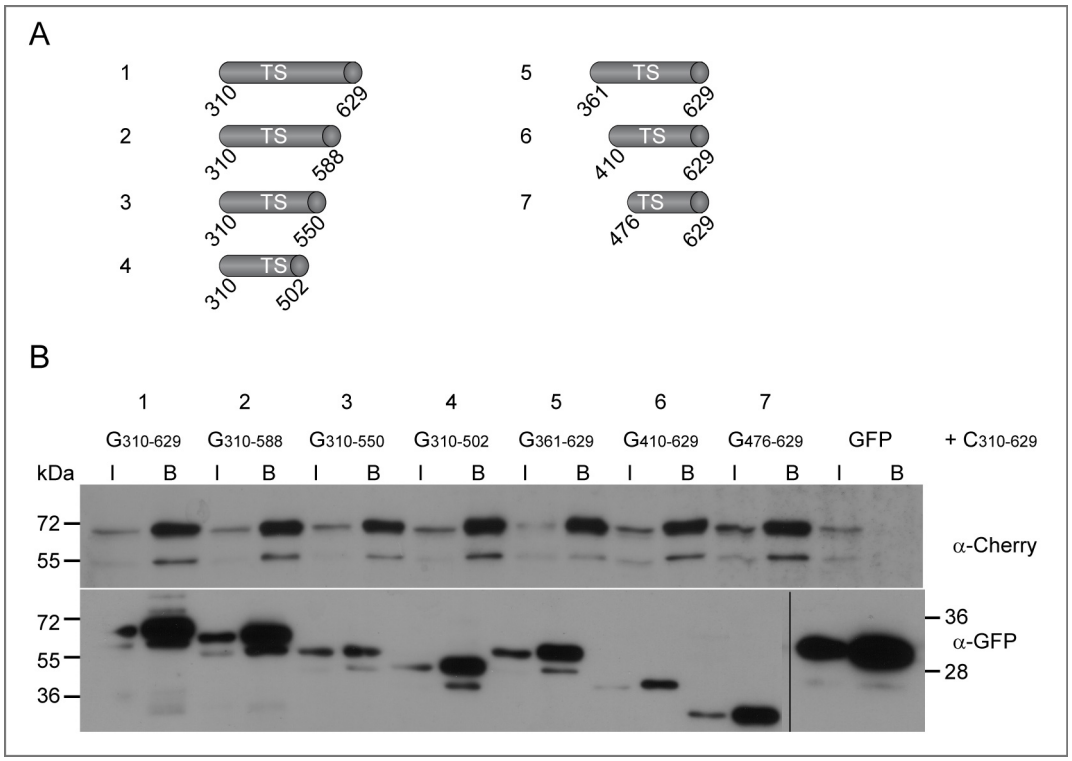

Supplementary Figure 1

TS-TS Interaction studies by co-immunoprecipitation. **(A)** Overview illustrating TS domain constructs used for TS-TS co-immunoprecipitations. Amino acid numbers are indicated. All constructs contain an N–terminal GFP tag and were co-expressed with Cherry-TS ($C_{310-629}$).

(B) Immunoblots of co-immunoprecipitation fractions; 1% of input (I) and 20% of bound (B) fractions were loaded on 10% SDS-PAGE, protein size standard in kDa is indicated; immunoblots were probed with antibodies against Cherry and GFP.

Supplementary Table 1

Oligonucleotide primers applied for PCR cloning of murine Dnmt1 constructs, restriction sites are underlined.

Construct	Forward Primer (5′ – 3′)	Reverse Primer (5′ – 3′)
GFP-N$_{(1-1111)}$	GAGACTCGAGGCGATCGCATGCCAGCGCGAACAG	GAGACCCGGGTTATGCGGCCGCGTTCCCAGGGCTGCG
GFP-C$_{(1124-1620)}$	GAGACTCGAGGCGATCGCAAGCATCAGGTGTCAGAG	GAGACCCGGGTTATGCGGCCGCGTCCTTGGTAGCAGC
GFP-N$_{(1-309)}$	GGGGTGTACAAGGCGATCGCAATGCCAGCGCGAACAG	GGGGAAGCTTGCGGCCGCTTAGGGAGTCTCTGGAGCTAC
GFP-TS$_{(310-629)}$	GAGACTCGAGGCGATCGCGAGGACAGAGACGAGG	GAGACCCGGGTTATGCGGCCGCCTGATAGACCAGCTTGGTG
GFP-N$_{(630-1111)}$	GGGGTGACAAGGCGATCGCAATCTTTGACACTTTCTTCTCAGA	GGGAAGCTTGCGGCCGCTTAGTTCCCAGGGCTGCG
Ch-TS$_{(310-629)}$	GGGGTGTACAAGTCCGGACTCAGATCTGAGGACAGAGACGAGGATG	GGGGTCTAGACTATTACTGATAGACCAGCTTGGTGG
GFP-TS$_{(310-410)}$	GAGACTCGAGGCGATCGCGAGGACAGAGACGAGG	GAGACCCGGGTTATGCGGCCGCGGGAGAATCTTCATAAG
GFP-TS$_{(310-475)}$	see primer above	GAGACCCGGGTTATGCGGCCGCAAAGCCACTGAGCCAC
GFP-TS$_{(310-502)}$	see primer above	GAGACCCGGGTTATGCGGCCGCCTCATACTCTTTGCTGGG
GFP-TS$_{(476-629)}$	GAGACTCGAGGCGATCGCGATGGTGGCGAGAAGG	GAGACCCGGGTTATGCGGCCGCCTGATAGACCAGCTTGGTG
GFP-TS$_{(503-629)}$	GAGACTCGAGGCGATCGCCCAATATTTGGGCTGATGCAG	see primer above
GFP-TS$_{(551-629)}$	GAGACTCGAGGCGATCGCTTCACAGAGGACTCCCTCTTACG	see primer above
MBP-TS	GGCGAATTCATGGACGAGGATGAAAAGGAGGAGA	GCCAAGCTTCTCGAGTTACTTATCGTCGTCATCCTTGTAATCC
Ch-TS$_{(310-409)}$	**Ch-TS$_{(310-475)}$ Ch-TS$_{(310-502)}$ Ch-TS$_{(476-629)}$ Ch-TS$_{(503-629))}$**	**ChTS$_{(551-629)}$**
	GAGAGCTAGCGCCACCATGGCTTCGTGGGGATC	GAGAGGTGTACAGCTCGTCCATGCCG

2.4 Np95 Controls Maintenance of DNA Methylation by Interaction with DNA Methyltransferase 1

2.4 Np95 Controls Maintenance of DNA Methylation by Interaction with DNA Methyltransferase 1

Beside the allosteric activation of Dnmt1 through its N-C-terminal interaction and dimerization, other chromatin factors are important for the regulation of Dnmt1.

Np95 was described to bind to chromatin (histones and HDAC1), to possess ubiquitin E3 ligase activity and to play an important role in cell cycle for S phase entry (Bonapace et al., 2002; Citterio et al., 2004; Jenkins et al., 2005; Unoki et al., 2004). An overview of the nuclear protein (Np) family is provided in Figure 2.4. Several names have been assigned to Np95 such as ICBP90 (inverted CCAAT box binding protein of 90 kDa) and UHRF1 (ubiquitin-like, containing PHD and RING finger domains 1).

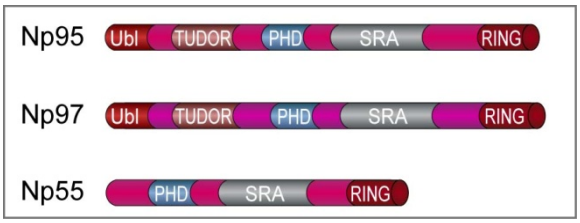

Figure 2.4 Schematic overview of the murine Np protein family. Subdomains are indicated: Ubl, ubiquitin-like domain; TUDOR, tandem tudor domain; PHD, plant homeo domain; SRA, SET and RING associated domain; RING, really interesting new gene, containing ubiquitin E3 ligase activity.

Targeted disruption of the *np95* gene resulted in global hypomethylation of ESCs, embryonic lethality and thus phenocopied the *dnmt1*$^{-/-}$ knockout (Li et al., 1992; Muto et al., 2002; Sharif et al., 2007). Np95 was shown to localize at replication foci (RF) during early and mid S phase and to pericentric heterochromatin (PH) from mid S phase to G2 (Papait et al., 2007; Uemura et al., 2000). Recently, the co-crystal structure of the Np95 SRA domain and hemi-methylated DNA was solved showing the SRA domain flipping out methyl-cytosine from the DNA double helix (Arita et al., 2008; Avvakumov et al., 2008; Hashimoto et al., 2008). DNA base flipping is a conserved mechanism that is known from nucleotide modifying enzymes, including DNA methyltransferases, DNA repair enzymes and RNA modifying enzymes (Cheng and Roberts, 2001; Klimasauskas et al., 1994; Lee et al., 2005; Min and Pavletich, 2007; Parker et al., 2007; Yang et al., 2008). Moreover, Np95 was reported to play a role in methylation maintenance by recruiting Dnmt1 to methylated DNA (Bostick et al., 2007; Sharif et al., 2007). To elucidate how Np95 regulates DNA methylation and Dnmt1 we analyzed the interacting domains and tried to rescue *dnmt1*$^{-/-}$ ECS with a Dnmt1 construct that cannot interact with Np95.

2.4.1 Dnmt1 Interacts with Np95 through its Regulatory Domain

Dnmt1 displays a cell cycle dependent subnuclear distribution that depends on two subdomains of the regulatory N-terminal part: The PBD is responsible for Dnmt1 localization at RF and the TS domain recruits Dnmt1 to PH (Easwaran et al., 2004; Schermelleh et al., 2007). To elucidate the role of Np95 in DNA methylation maintenance, we first determined the region of Dnmt1 that is responsible for the interaction with Np95. As recent studies mapped the interacting regions of Dnmt1 and Np95 to different domains we tried to clarify this point (Achour et al., 2008; Bostick et al., 2007; Sharif et al., 2007). To map the interaction between Dnmt1 and Np95, we expressed individual GFP-Dnmt1 domains together with Np95 in HEK293T cells and performed co-immunoprecipitation experiments with the cell lysates using the GFP-Nanotrap (Figure 2.5A/B; (Rothbauer et al., 2008)).

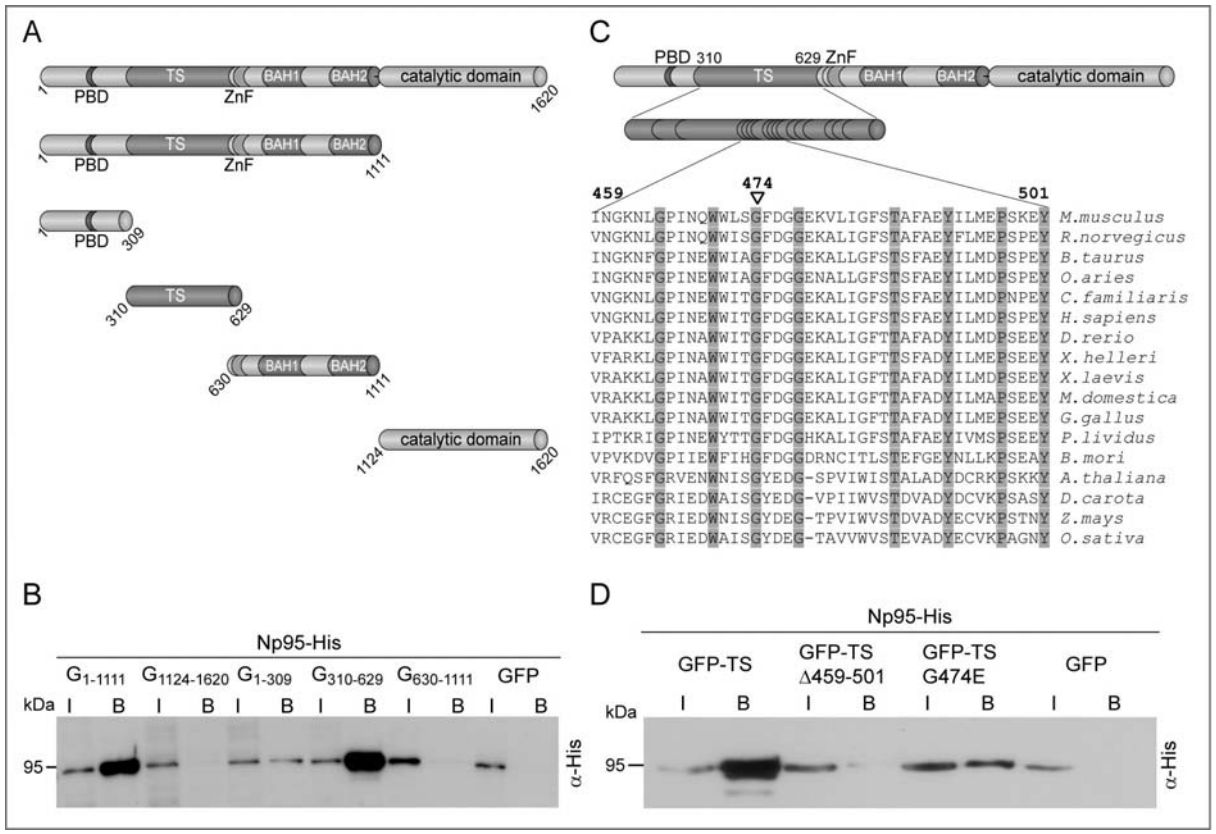

Figure 2.5 Np95 interacts with the TS domain of Dnmt1. (A) Schematic representation of GFP-Dnmt1 fusion constructs used for mapping the interaction site with Np95 (N-terminal GFP tag is not shown). PBD, PCNA binding domain; TS, targeting sequence; ZnF, CXXC-type zinc finger; BAH, bromo adjacent homology domain. (B) Co-immunoprecipitation of Np95-His with the GFP-Dnmt1 constructs shown in A from extracts of transiently transfected HEK293T cells. G indicates the GFP fusion and numbers in subscript indicate amino acid positions in Dnmt1. 1% of input (I) and 70% of bound (B) fractions were subjected to SDS-PAGE and immunoblot analysis and proteins detected with an antibody against His; molecular size markers are indicated. (C) Domain structure of Dnmt1 and alignment of the conserved core of the TS domain from higher eukaryotes. Invariant amino acids are indicated as black lines in the blown up drawing of the TS domain and shaded in grey in the alignment. The arrowhead points to the conserved glycine 474, which was mutated to glutamate to generate the GFP-Dnmt1G474E construct. Accession numbers: *M. musculus*: P13864; *R. norvegicus*: Q9Z330; *B. taurus*: O44952; *O. aries*: O39704; *C. familiaris*: P848593; *H. sapiens*: P26358; *D. rerio*: Q8QGB8; *X. helleri*: F73200; *X. laevis*: P79922; *M. domestica*: Q8MJ28; *G. gallus*: Q92072; *P. lividus*: Q27746; *B. mori*: Q5W7N6; *A. thaliana*: Q9T0I1; *D. carota*: O48867; *Z. mays*: Q8LPU6 ; *O. sativa*: Q8S4C3. (D) Fine mapping of the Np95 interaction site within the TS domain. The co-immunoprecipitation scheme and loading of input (I) and bound (B) fractions are as in B.

Np95 co-precipitated efficiently with the Dnmt1 N-terminus but not with the C-terminus. Within the N-terminal region we found robust co-immunoprecipitation of His-tagged Np95 with the targeting sequence (TS) of Dnmt1, while the fragments upstream and downstream to the TS domain showed only very weak and no binding to Np95, respectively. We then examined whether the interaction with Np95 is mediated by the highly conserved core of the TS domain (Figure 2.5C). The conservative substitution of the invariant glycine 474 with glutamate (G474E) drastically diminished binding to Np95 and deletion of the entire conserved core from the isolated TS domain (Δ459-501) essentially abolished the interaction with Np95 (Figure 2.5D). These data indicate that the highly conserved core of the TS domain in Dnmt1 is the major binding site for Np95.

We confirmed the biochemical interaction data using the F2H assay that allows the analysis of protein interactions in living cells (outlined in chapter 1, page 9; (Zolghadr et al., 2008)).

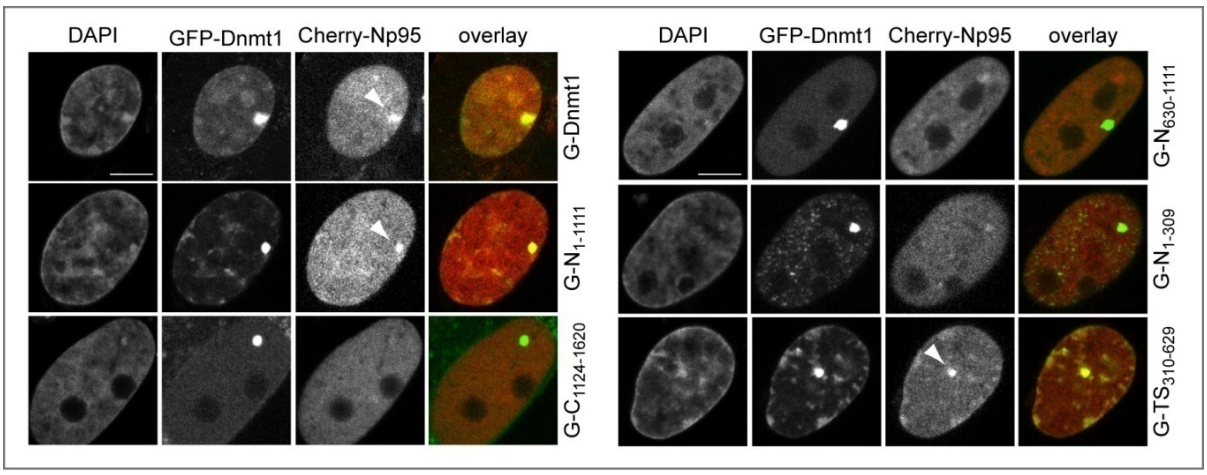

Figure 2.6 Np95 interacts with Dnmt1 TS domain. F2H assay shows clear recruitment of Cherry-Np95 (prey) at the *lac* operator array when GFP-Dnmt1 full-length, the N-terminal domain (G-N_{1-1111}) or the TS domain (G-$TS_{310-629}$) are used as baits (marked by white arrowheads), a very weak recruitment to G-N_{1-309} but no recruitment to the last third of the N-termins G-$N_{630-1111}$ or the catalytic domain (G-$C_{1124-1620}$). Scale bars represent 5 µm.

GFP-Dnmt1 fusion constructs were used as baits by tethering them to the *lac* operator array present in BHK cells. Thereby the array was visible as distinct nuclear spot of high GFP fluorescence (Figure 2.6). We observed recruitment of Cherry-Np95 (prey) only to the GFP-Dnmt1 full-length or N-terminus but not to the C-terminus. More specifically, Np95 strongly interacted with the Dnmt1 TS domain but only weakly or not with the N- or C-terminal parts of the N-terminal domain, respectively.

Taken together, from biochemical and cell biological experiments we can conclude that the TS domain of Dnmt1 is the major Np95 interacting domain.

Furthermore, we asked which part of Np95 is involved in this contact. Interestingly, the N-terminal region of Np95 containing the ubiquitin-like domain (aa 1-81) and the tandem tudor domain (aa 126-285) was pulled down with GFP-Dnmt1 whereas all other domains (PHD, SRA, RING) did not interact with GFP-Dnmt1 (Figure 2.7A/B). To test the involvement of the ubiquitin-like domain of Np95 we compared interactions between GFP-Dnmt1 and Np95 deletion constructs in co-immunoprecipitation experiments as described above. Deletion of

only the ubiquitin-like domain (Ubl, aa 1-81) almost abolished the interaction with Dnmt1 (Figure 2.7D). In summary, these results point to an interaction between the ubiquitin-like domain of Np95 and the TS domain of Dnmt1.

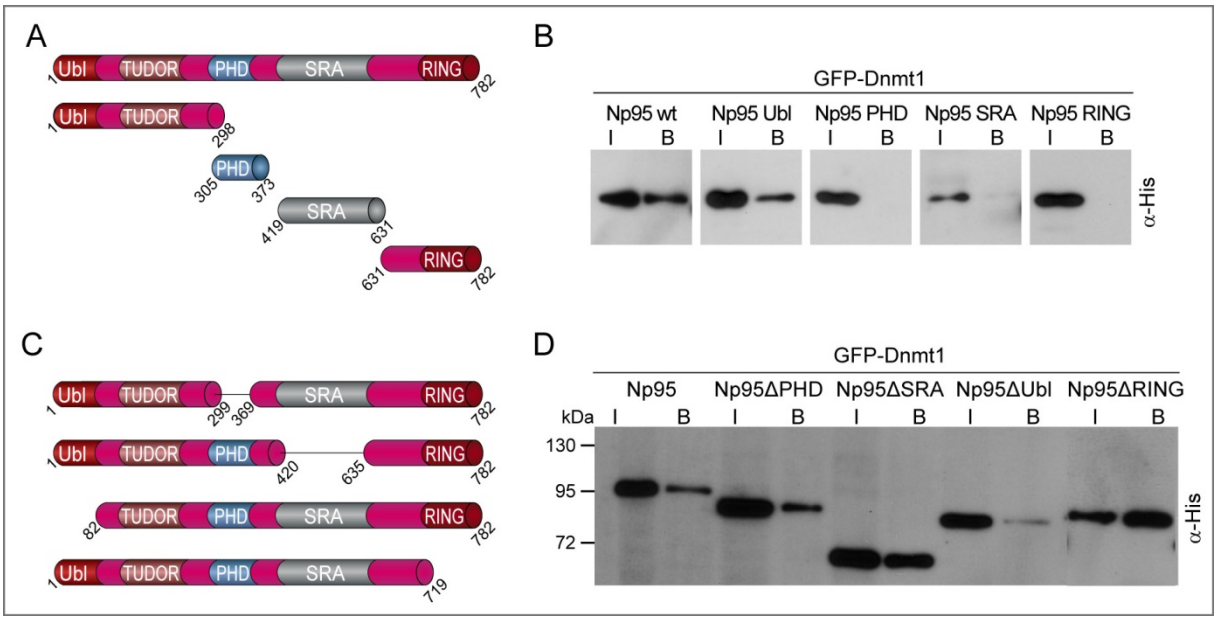

Figure 2.7 Mapping the Dnmt1-Np95 interaction within Np95. (A+C) Overview of Np95 constructs used for co-immunoprecipiations presented in (B+D), respectively, C-terminal His tag is not shown. Ubl, ubiquitin-like domain, PHD, plant homeo domain; SRA, SET and Ring associated domain; RING, really interesting new gene, containing ubiquitin E3 ligase activity. (B+D) 1% of input (I) and 80% of bound (B) fractions were loaded and proteins detected with an antibody against His. Quantitative precipitation of GFP-Dnmt1 was confirmed by immunoblotting against GFP (not shown).

As Np95 was described to play a major role in maintenance of DNA methylation, we wanted to elucidate how it regulates Dnmt1. The mutant GFP-Dnmt1Δ459-501 does not interact with Np95. Therefore, we asked whether this Dnmt1 mutant first shows a normal cell cycle dependent distribution and second whether it is catalytically active. Furthermore, if GFP-Dnmt1Δ459-501 is active, has it the capacity to rescue methylation patterns in *dnmt1*$^{-/-}$ ESCs as GFP-Dnmt1 wt?

GFP-Dnmt1 wt or GFP-Dnmt1Δ459-501 was co-expressed with the replication marker PCNA (RFP-PCNA) in C2C12 mouse fibroblast cells and live-cell fluorescence microscopy was performed. Both constructs localized normally at replication foci in early and mid-S phase but GFP-Dnmt1Δ459-501 showed a higher diffuse fraction in late S phase compared to GFP-Dnmt1 wt (Figure 2.8). However, TS mediated enrichment at PH temporally overlaps with PH replication (late S phase) and thus could be masked by the interaction of Dnmt1 with the replication machinery. To differentiate between these two phenomena we combined the TS mutation with the PBD (Q162E) that abolishes the interaction with PCNA (Schermelleh et al., 2007). The double mutant displayed a completely diffuse distribution in all cell-cycle stages,

clearly indicating that the TS mutation abolishes the accumulation of Dnmt1 at PH (Figure 2.8C).

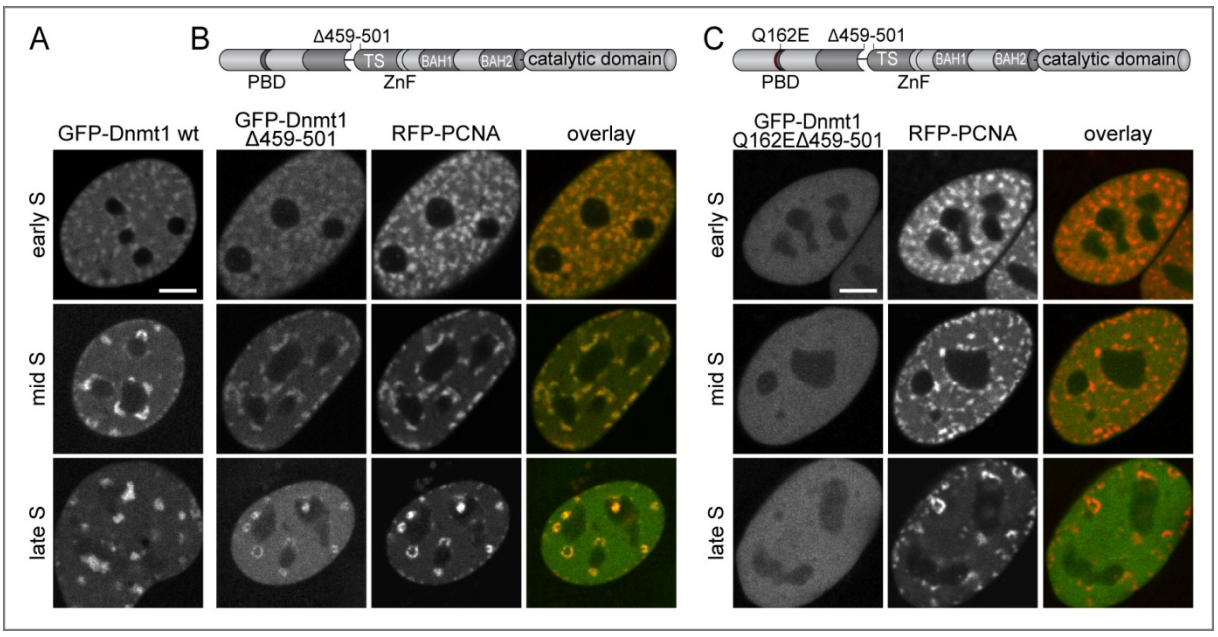

Figure 2.8 Localization of GFP-Dnmt1Δ459-501 mutants during S phase. Top: Schematic overview of Dnmt1Δ459-501 and Dnmt1Q162E Δ459-501; N-terminal GFP-tag is not shown. PBD, PCNA binding domain; TS, targeting sequence; BAH1+2, bromo adjacent homology domains 1+2. (A) Distribution of GFP-Dnmt1 wt and (B) GFP-Dnmt1Δ459-501 during S phase; RFP-PCNA serves as S phase marker. Co-localization of GFP-Dnmt1Δ459-501 and RFP-PCNA during early and mid S phase but only weak in late S phase. Scale bar represents 5 µm. (C) GFP-Dnmt1Q162E Δ459-501 shows a completely diffuse distribution throughout S phase.

GFP-Dnmt1Q162EΔ459-501 - that interacts neither with PCNA nor with Np95 – is not recruited to PH. These results indicate that Np95 is responsible for targeting Dnmt1 to PH and the question emerged whether this GFP-Dnmt1Δ459-501 is catalytically active and involved in DNA methylation of genomic targets. To test this, we used the trapping assay (Schermelleh et al., 2005). The method is based on the incorporation of a 2′-deoxycytidine (dC) analogue 5′-aza-2′-deoxycytidine (5-aza-dC) into the DNA during DNA replication in cells co-expressing GFP-Dnmt1 and the S phase marker protein PCNA fused to mRFP (RFP-PCNA). During the catalytic mechanism of methylation, Dnmt1 forms a transient covalent complex with dC and is released after transfer of the methyl group by a β-elimination process. However, if 5-aza-dC is incorporated in the DNA instead of dC, the release of Dnmt1 from the covalent complex with DNA cannot take place and Dnmt1 is captured at the site of action. The replication machinery proceeds to new replicons while Dnmt1 is trapped. Therefore, a time-dependent separation of the replication foci (monitored by RFP-PCNA) and GFP-Dnmt1 can be observed. In other words, only if Dnmt1 is catalytically active, a separation of red (RFP-PCNA) and green (GFP-Dnmt1) foci takes place. It was previously published by our group that loss of the interaction with PCNA by the Q162E mutation prevents

accumulation of GFP-Dnmt1Q162E at replication foci (Schermelleh et al., 2007). Nonetheless, incorporation of 5-aza-dC caused accumulation of GFP-Dnmt1Q162E at replication foci and kinetic analysis showed that covalent complex formation of GFP-Dnmt1Q162E was reduced only by twofold compared to GFP-Dnmt1 wt. Accordingly, we tested the catalytic activity of Dnmt1 double mutants that bind neither PCNA nor Np95. Incorporation of 5-aza-dC resulted in accumulation of Dnmt1 double mutants at RF throughout S-phase, but kinetic studies (FRAP analysis) showed that the formation of distinct foci was 2-3 fold times delayed compared to GFP-Dnmt1 wt (Figure 2.9).

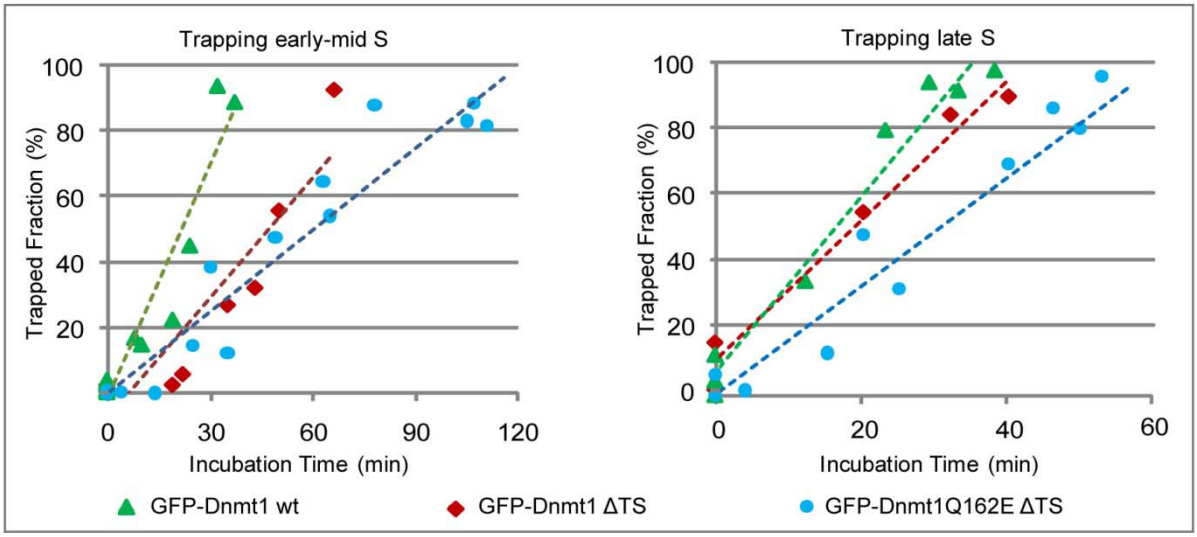

Figure 2.9 Trapping assay of GFP-Dnmt1 wt and mutants to analyze the property to form covalent complexes with substrate DNA. C2C12 mouse myoblast cells were co-transfected with RFP-PCNA and GFP-Dnmt1 wt or mutants and quantitative ROI FRAP analysis (3µm x 3µm) was performed at selected time points after incubation with 5-aza-dC in early-mid (left) and late S phase (right). Time dependent increase of immobile fractions of GFP-Dnmt1 wt (green triangles), GFP-Dnmt1Δ459-501 (red diamonds) and Dnmt1Q162E Δ459-501 (blue dots) is plotted and shows that both mutants accumulate at the DNA after 5-aza-dC incorporation but with a delayed kinetic compared to GFP-Dnmt1 wt.

Hence, disruption of both PCNA and Np95 interaction reduced the rate of postreplicative Dnmt1-DNA complex formation during S-phase. Moreover, results of a radioactive DNA methyltransferase assay showed normal Dnmt1 activity of the Np95 interaction mutant *in vitro* (not shown). These results suggest that the interaction of Dnmt1 with Np95 may not be essential but *np95*$^{-/-}$ ES cells display a strong hypomethylation of both repetitive sequences and single copy genes (Sharif et al., 2007). These reduced methylation levels are highly similar to the hypomethylation status in *dnmt1*$^{-/-}$ ESCs. The genome-wide loss of methylation without sequence preference in *np95*$^{-/-}$ ESCs is surprising since the interaction of Np95 with the TS domain of Dnmt1 would suggest a preferential reduction of methylation at pericentric satellite sequences.

Therefore, we tested the ability of the Dnmt1 mutant deficient in Np95 interaction to restore methylation patterns in hypomethylated *dnmt1*$^{-/-}$ ESCs. We stably expressed GFP-

Dnmt1Δ459-501 or GFP-Dnmt1 wt in *dnmt1*$^{-/-}$ ESCs and quantitatively analyzed methylation patterns of different types of sequences such as major and minor satellite DNA, retroviral elements intracisternal A-type particle (IAP) and single copy genes by pyrosequencing (unpublished data from W. Qin). GFP-Dnmt1 wt was able to restore methylation patterns of all types of sequences up to almost wildtype methylation levels. However, GFP-Dnmt1Δ459-501 failed to restore methylation patterns of any sequence type.

These results clearly indicate that the interaction of Dnmt1 with Np95 is essential for maintenance of methylation patterns in ESCs in vivo. The interaction with Np95 seems to target und to permit Dnmt1 to access DNA target sites in chromatin.

2.5 Np95 Interacts with *de novo* DNA Methyltransferases Dnmt3a and 3b and Mediates Epigenetic Silencing

Np95 Interacts with *de novo* DNA Methyltransferases Dnmt3a and 3b and Mediates Epigenetic Silencing

Karin Fellinger[1,4], Daniela Meilinger[1,4], Sebastian Bultmann[1], Ian Marc Bonapace[2], Wolfgang E. F. Klinkert[3], Fabio Spada[1,*] and Heinrich Leonhardt[1,*]

[1]Ludwig Maximilians University Munich, Department of Biology II and Center for Integrated Protein Science Munich (CIPS[M]), Großhaderner Str. 2, 82152 Planegg-Martinsried, Germany.

[2]University of Insubria, Department of Structural and Functional Biology, Via da Giussano 12, 21052 Busto Arsizio (VA), Italy.

[3]Max Planck Institute of Neurobiology, Am Klopferspitz 18, 82152 Martinsried

[4]These authors contributed equally to this work.

[*]Corresponding authors: f.spada@lmu.de; tel: +49-89-218074230, fax: +49-89-218074236;

H.Leonhardt@lmu.de; tel: +49-89-218074232

Running Title: Np95 interacts with Dnmt3a and 3b

Key Words: DNA methylation, DNA methyltransferase, epigenetics, Uhrf1, silencing.

ABSTRACT

Recent studies indicated that Np95 is essential for maintaining genomic methylation by recruiting Dnmt1 to hemi-methylated sites. Here we show that Np95 interacts even stronger with the regulatory domains of the *de novo* DNA methyltransferases Dnmt3a and 3b. To investigate possible functions we developed an epigenetic silencing assay with fluorescent reporters. We found that genetic inactivation of Np95 in ESCs results in a loss of promoter *de novo* methylation and silencing activity just like the simultaneous inactivation of *dnmt1*, *dnmt3a* and *3b*. These results assign Np95 a previously unrecognised role in epigenetic silencing mediated by *de novo* methyltransferases Dnmt3a and 3b.

INTRODUCTION

In mammals DNA methylation contributes to the establishment and maintenance of cell type-specific gene expression programs, imprinting, X chromosome inactivation and genome stability (Bird, 2002). The vast majority of genomic methylation occurs at cytosine residues within CpG dinucleotides and is catalyzed by the DNA methyltransferases (Dnmt) 1, 3a and 3b. Dnmt1 is responsible for maintaining genomic methylation, while Dnmt3a and 3b are mainly involved in *de novo* establishment of methylation patterns during cellular differentiation (Lei et al., 1996; Leonhardt et al., 1992; Li et al., 1992; Okano et al., 1999). Np95 (also known as Uhrf1) has recently emerged as an essential cofactor for maintaining genomic methylation (Achour et al., 2008; Bostick et al., 2007; Sharif et al., 2007). *dnmt1*$^{-/-}$ and *np95*$^{-/-}$ embryonic stem cells (ESCs) and embryos have very similarly reduced levels of DNA methylation. In addition, Np95 interacts with Dnmt1, binds hemi-methylated CpG sites through its SRA (Set and Ring associated) domain and both Np95 and Dnmt1 accumulate at replication sites (Arita et al., 2008; Avvakumov et al., 2008; Bostick et al., 2007; Hashimoto et al., 2008; Papait et al., 2007; Uemura et al., 2000). Thus, it has been proposed that Np95 mediates maintenance of genomic methylation by recruiting Dnmt1 to hemi-methylated CpG sites generated during replication.

Here we investigated a possible involvement of Np95 in epigenetic regulation beyond its role in Dnmt1 mediated maintenance of DNA methylation. We found that Np95 interacts with the *de novo* methyltransferases Dnmt3a and 3b and mediates promoter *de novo* methylation and epigenetic silencing.

RESULTS AND DISCUSSION

Np95 Interacts with Dnmt3a and 3b

Immunoprecipitation experiments revealed that different isoforms of both *de novo* methyltransferases Dnmt3a and 3b interact with Np95 in wild type ESCs, including the more abundant Dnmt3a2 and Dnmt3b1 (Fig. 1A). Using a GFP nanotrap (Rothbauer et al., 2008), we also co-immunoprecipitated endogenous Dnmt3a and Dnmt3b isoforms with a GFP-Np95 fusion construct transiently expressed in *np95*$^{-/-}$ ESCs and, vice versa, endogenous Np95 co-immunoprecipitated with GFP-Dnmt3a or GFP-Dnmt3b1 fusions in *dnmt3a* and *3b* double knockout (*dnmt3* DKO) ESCs (Supplementary Fig. S1A and B). In addition, we observed co-immunoprecipitation of endogenous DNMT3b and ICBP90 (the human homolog of Np95) from HEK293T cell extracts (Supplementary Fig. S1C). We confirmed the interaction of Np95 with Dnmt3a/b using a recently developed fluorescent two-hybrid (F2H) assay (Rothbauer et al., 2008). GFP-Dnmt3 fusion constructs were used as baits by tethering them to a *lac* operator array present in BHK cells, so that the array was visible as a distinct nuclear spot of enriched GFP fluorescence (Fig. 1B). A Cherry-Np95 fusion (prey) accumulated at this spot only when GFP fusions of full length Dnmt3a and 3b1 or their N-terminal regions were used as baits and not with their isolated C-terminal catalytic domains. We further mapped the interaction of Np95 with Dnmt3a/b by co-immunoprecipitation of deletion constructs and isolated domains transiently expressed in HEK293T cells (Supplementary Fig. S2). Consistent with the results obtained with the F2H assay, the N-terminal regions of Dnmt3a and 3b1, but not their C-terminal catalytic domains, interacted with Np95. Deletion of the PHD or the PWWP domain of Dnmt3a and 3b did not eliminate the interaction with Np95. We then determined which Np95 domains are involved in this interaction. We found that the SRA domain and the N-terminal 298 aa of Np95, that include the Ubiquitin-like domain, interacted with Dnmt3a and 3b1, while the PHD and the C-terminal 132 aa, including the Ring domain, did not.

To compare the stability of Np95 interactions with different Dnmts we transiently co-expressed Np95-His with either GFP-Dnmt1, GFP-Dnmt3a or GFP-Dnmt3b1 in HEK293T cells and performed immunoprecipitations in the presence of different salt concentrations (Fig. 1C and Supplementary Fig. S3). Interestingly, under high salt conditions the interaction between Np95-His and GFP-Dnmt1 was lost, while co-immunoprecipitation of GFP-Dnmt3a and

GFP-Dnmt3b1 remained relatively unaffected. These data clearly indicate that Np95 interacts with the *de novo* methyltransferases Dnmt3a and 3b even stronger than with Dnmt1.

Np95 Mediates Epigenetic Silencing and Promoter de novo Methylation

As DNA methylation plays a central role in epigenetic silencing we investigated the requirement of DNA methyltransferases and Np95 for promoter silencing in ESCs. To this aim we established an epigenetic silencing assay based on the observation that in ESCs the immediate-early CMV promoter is prone to silencing, while the chimeric CAG promoter is relatively refractory. ESCs were cotransfected with two distinct plasmids, one expressing monomeric red fluorescent protein (mRFP) under the CMV promoter, the other expressing GFP driven by the CAG promoter. mRFP and GFP expression was monitored for up to ten days after transfection by automated image acquisition and quantification of fluorescent signals (Supplementary Fig. S4A). The ratio between mRFP and GFP expression declined steadily in wild type ESCs, reflecting preferential silencing of the CMV promoter (Fig. 2). In contrast, *dnmt3* DKO and *dnmt1*, *3a* and *3b* triple knockout (TKO) ESCs showed no preferential silencing of the CMV promoter. Surprisingly, *np95*$^{-/-}$ ESCs were also unable to silence the CMV promoter, while *dnmt1*$^{-/-}$ ESCs showed slower silencing kinetics than wild type cells, which is consistent with only partially reduced *de novo* methyltransferase activity in these cells (Lei et al., 1996). We could rule out potential artefacts arising from differences in GFP and mRFP stability or their coding sequences since the exchange of these reporters gave very similar results (Supplementary Fig. S4B). Thus, despite expressing a full complement of DNA methyltransferases, ESCs lacking Np95 are as deficient in promoter silencing activity as ESCs lacking all three major Dnmts. We next investigated whether silencing is accompanied by CpG methylation and detected substantial methylation in the CMV promoter ten days after transfection of wt, but not *np95*$^{-/-}$ ESCs (Fig. 3).

These results show that not only DNA methyltransferases but also Np95 are required for de novo methylation and gene silencing. The interaction of Np95 with the regulatory domains of Dnmt3a and 3b described here suggests that Np95 may recruit and/or activate these *de novo* methyltransferases at target sites and thus mediate epigenetic silencing. Recent studies showed that the histone H3 lysine 9 methyltransferase (H3K9 MTase) G9a interacts with Dnmt3a and 3b and is also required for *de novo* methylation and stable silencing of promoters upon differentiation of ESCs (Dong et al., 2008; Epsztejn-Litman et al., 2008;

Feldman et al., 2006; Kim et al., 2008; Tachibana et al., 2008). This raises the question whether Np95 and G9a operate along the same pathway and how they both contribute in a non-redundant fashion to *de novo* methylation and stable promoter silencing. Notably, the reporter gene expression in our assay steadily declined even before *de novo* methylation of the promoter was detected, arguing for an essential role of Np95 as well as the *de novo* Dnmts in early and late events of gene silencing (Fig. 2A, 3 and data not shown). Interestingly, Np95, Dnmt3a and 3b were all shown to interact with histone deacetylases (Fuks et al., 2001; Geiman et al., 2004; Unoki et al., 2004). In addition, an interaction between Np95 and G9a has been recently described and association of the *de novo* Dnmts with other H3K9 MTases had been previously reported (Fuks et al., 2003; Kim et al., 2008; Lehnertz et al., 2003; Li et al., 2006). Thus, Np95 and *de novo* Dnmts may be required for histone deacetylation and/or H3K9 methylation at the onset of silencing.

In summary, we show that Np95 interacts with the *de novo* DNA methyltransferases Dnmt3a and 3b and that Np95 and the *de novo* DNA methyltransferases are required for promoter silencing in ESCs. These data clearly support a role for Np95 in epigenetic silencing mediated by Dnmt3a and 3b and make Np95 an interesting target for epigenetic reprogramming.

METHODS

Cell Culture and Transfection

HEK293T cells, BHK cells and ESCs were cultured and transfected as described (Schermelleh et al., 2007), except FuGENE HD (Roche) was used for transfection of ESCs. The *dnmt1*$^{-/-}$ J1 ESCs used in this study are homozygous for the c allele (Lei et al., 1996). BHK cells were co-transfected on glass coverslips with GFP-Dnmt3 and Cherry-Np95 constructs using Transfectin (Bio-Rad) according to the manufacturer's instructions. Cell fixation and microscopy were carried out as described (Rothbauer et al., 2008).

Co-Immunoprecipitation

ESCs and HEK293T cell extracts were harvested in lysis buffer (20 mM Tris/HCl pH 7.5, 0.5 mM EDTA, 2 mM PMSF, 0.5% NP40) containing 150 or 300 mM NaCl (high salt condition) and diluted with lysis buffer without NP40. GFP nanotrap (Rothbauer et al., 2008) and a specific rabbit antiserum (Citterio et al., 2004) were used for immunoprecipitation of GFP fusions and endogenous Np95, respectively. GFP nanotrap and protein G beads (Sigma) were washed with dilution buffer containing increasing salt concentrations (150 and 300 mM or 300 and 500 mM NaCl for the high salt condition) and resuspended in SDS-PAGE sample buffer. The following mouse monoclonal antibodies were used for immunoblotting: anti-His (C-term., Invitrogen), anti-Dnmt3a (clone 64B1446, Imgenex) and anti-Dnmt3b (clone 52A1018, Abcam). Np95 was detected with the same antiserum used for immunoprecipitation. HRP conjugated rabbit anti-mouse or goat anti-rabbit secondary antibodies (Sigma) and ECL Plus reagent (GE Healthcare) were used for detection.

Silencing Assay

ESCs were cotransfected with pCAG-eGFP-IB and pCMV-mRFP as described above and images from living cells were acquired at the indicated time points with an InCell Analyser 1000 (GE Healthcare) using a 20x air-objective (NA = 0.45) and standard filter settings for GFP and RFP. 90-150 images were acquired for each channel using the same exposure time throughout the time course. Cells were passaged every second day and images were taken 4-5 h after seeding. Images were analysed with ImageJ v1.42a software. To calculate fluorescent reporter expression pictures were processed using a Gaussian blur algorithm (radius (sigma) = 2) and a threshold for maximal signal and minimal background coverage was adjusted and

applied to each channel (Supplementary Fig. S4A). The threshold was converted into area selection and the total size of the selected area was measured.

Bisulfite Sequencing of the CMV Promoter

ESCs were transfected as for the silencing assay with pCAG-eGFP-IB and pCMV-mRFP and GFP positive cells were sequentially sorted with a FACS Vantage (Becton Dikinson) at day 6 and 10 after transfection. After the last sorting genomic DNA was isolated with the QIAmp DNA Mini kit (Qiagen), bisulfite treated with the EZ DNA Methylation-Gold kit (Zymo research) and amplified with primers CMV-forward TGGGATTTTTTTATTTGGTAGT and CMV-reverse ATGGGAGTTTGTTTTGGTATTA primers, PCR fragments were cloned with StrataClone PCR cloning (Stratagene). Individual clones were sequenced at Eurofins MWG Operon.

ACKNOWLEDGEMENTS

We are grateful to Masahiro Muto and Haruhiko Koseki (RIKEN Research Center for Allergy and Immunology, Yokohama, Japan) for providing wild type and *np95*$^{-/-}$ E14 ESCs, to En Li (Novartis Institutes for Biomedical Research, Boston, MA) for *dnmt1*$^{-/-}$ and *dnmt3a*$^{-/-}$*; 3b*$^{-/-}$ J1 ESCs and to Masaki Okano (RIKEN Center for Developmental Biology, Kobe, Japan) for the TKO ESCs. We thank Lothar Schermelleh for help with image processing and Kourosh Zolghadr for assistance with the InCell Analyzer. This work was supported by the Nanosystems Initiative Munich (NIM) and BioImaging Network Munich (BIN) and by grants from the Deutsche Forschungsgemeinschaft (DFG) to HL.

REFERENCES

Achour M, Jacq X, Ronde P, Alhosin M, Charlot C, Chataigneau T, Jeanblanc M, Macaluso M, Giordano A, Hughes AD, Schini-Kerth VB, Bronner C (2008) The interaction of the SRA domain of ICBP90 with a novel domain of DNMT1 is involved in the regulation of VEGF gene expression. *Oncogene* **27**(15)**:** 2187-2197

Arita K, Ariyoshi M, Tochio H, Nakamura Y, Shirakawa M (2008) Recognition of hemi-methylated DNA by the SRA protein UHRF1 by a base-flipping mechanism. *Nature* **455**(7214)**:** 818-821

Avvakumov GV, Walker JR, Xue S, Li Y, Duan S, Bronner C, Arrowsmith CH, Dhe-Paganon S (2008) Structural basis for recognition of hemi-methylated DNA by the SRA domain of human UHRF1. *Nature* **455**(7214)**:** 822-825

Bird A (2002) DNA methylation patterns and epigenetic memory. *Genes Dev* **16**(1)**:** 6-21

Bostick M, Kim JK, Esteve P-O, Clark A, Pradhan S, Jacobsen SE (2007) UHRF1 Plays a Role in Maintaining DNA Methylation in Mammalian Cells. *Science* **317**(5845)**:** 1760-1764

Citterio E, Papait R, Nicassio F, Vecchi M, Gomiero P, Mantovani R, Di Fiore PP, Bonapace IM (2004) Np95 is a histone-binding protein endowed with ubiquitin ligase activity. *Mol Cell Biol* **24**(6)**:** 2526-2535

Dong KB, Maksakova IA, Mohn F, Leung D, Appanah R, Lee S, Yang HW, Lam LL, Mager DL, Schubeler D, Tachibana M, Shinkai Y, Lorincz MC (2008) DNA methylation in ES cells requires the lysine methyltransferase G9a but not its catalytic activity. *EMBO J* **27**(20)**:** 2691-2701

Epsztejn-Litman S, Feldman N, Abu-Remaileh M, Shufaro Y, Gerson A, Ueda J, Deplus R, Fuks F, Shinkai Y, Cedar H, Bergman Y (2008) De novo DNA methylation promoted by G9a prevents reprogramming of embryonically silenced genes. *Nat Struct Mol Biol* **15**(11)**:** 1176-1183

Feldman N, Gerson A, Fang J, Li E, Zhang Y, Shinkai Y, Cedar H, Bergman Y (2006) G9a-mediated irreversible epigenetic inactivation of Oct-3/4 during early embryogenesis. *Nat Cell Biol* **8**(2)**:** 188-194

Fuks F, Burgers WA, Godin N, Kasai M, Kouzarides T (2001) Dnmt3a binds deacetylases and is recruited by a sequence-specific repressor to silence transcription. *Embo J* **20**(10)**:** 2536-2544

Fuks F, Hurd PJ, Deplus R, Kouzarides T (2003) The DNA methyltransferases associate with HP1 and the SUV39H1 histone methyltransferase. *Nucleic Acids Res* **31**(9)**:** 2305-2312

Geiman TM, Sankpal UT, Robertson AK, Zhao Y, Robertson KD (2004) DNMT3B interacts with hSNF2H chromatin remodeling enzyme, HDACs 1 and 2, and components of the histone methylation system. *Biochem Biophys Res Commun* **318**(2)**:** 544-555

Hashimoto H, Horton JR, Zhang X, Bostick M, Jacobsen SE, Cheng X (2008) The SRA domain of UHRF1 flips 5-methylcytosine out of the DNA helix. *Nature* **455**(7214)**:** 826-829

Kim JK, Esteve PO, Jacobsen SE, Pradhan S (2008) UHRF1 binds G9a and participates in p21 transcriptional regulation in mammalian cells. *Nucleic Acids Res*

Lehnertz B, Ueda Y, Derijck AA, Braunschweig U, Perez-Burgos L, Kubicek S, Chen T, Li E, Jenuwein T, Peters AH (2003) Suv39h-mediated histone H3 lysine 9 methylation directs DNA methylation to major satellite repeats at pericentric heterochromatin. *Curr Biol* **13**(14)**:** 1192-1200

Lei H, Oh S, Okano M, Juttermann R, Goss K, Jaenisch R, Li E (1996) De novo DNA cytosine methyltransferase activities in mouse embryonic stem cells. *Development* **122**(10)**:** 3195-3205

Leonhardt H, Page AW, Weier HU, Bestor TH (1992) A targeting sequence directs DNA methyltransferase to sites of DNA replication in mammalian nuclei. *Cell* **71**(5)**:** 865-873

Li E, Bestor TH, Jaenisch R (1992) Targeted mutation of the DNA methyltransferase gene results in embryonic lethality. *Cell* **69**(6)**:** 915-926

Li H, Rauch T, Chen Z-X, Szabo PE, Riggs AD, Pfeifer GP (2006) The Histone Methyltransferase SETDB1 and the DNA Methyltransferase DNMT3A Interact Directly and Localize to Promoters Silenced in Cancer Cells. *J Biol Chem* **281**(28)**:** 19489-19500

Okano M, Bell DW, Haber DA, Li E (1999) DNA methyltransferases Dnmt3a and Dnmt3b are essential for de novo methylation and mammalian development. *Cell* **99**(3)**:** 247-257

Papait R, Pistore C, Negri D, Pecoraro D, Cantarini L, Bonapace IM (2007) Np95 Is Implicated in Pericentromeric Heterochromatin Replication and in Major Satellite Silencing. *Mol Biol Cell* **18**(3)**:** 1098-1106

Rothbauer U, Zolghadr K, Muyldermans S, Schepers A, Cardoso MC, Leonhardt H (2008) A versatile nanotrap for biochemical and functional studies with fluorescent fusion proteins. *Mol Cell Proteomics* **7**(2)**:** 282-289

Schermelleh L, Haemmer A, Spada F, Rosing N, Meilinger D, Rothbauer U, Cristina Cardoso M, Leonhardt H (2007) Dynamics of Dnmt1 interaction with the replication machinery and its role in postreplicative maintenance of DNA methylation. *Nucl Acids Res* **35**(13)**:** 4301-4312

Sharif J, Muto M, Takebayashi S, Suetake I, Iwamatsu A, Endo TA, Shinga J, Mizutani-Koseki Y, Toyoda T, Okamura K, Tajima S, Mitsuya K, Okano M, Koseki H (2007) The SRA protein Np95 mediates epigenetic inheritance by recruiting Dnmt1 to methylated DNA. *Nature* **450**(7171)**:** 908-912

Tachibana M, Matsumura Y, Fukuda M, Kimura H, Shinkai Y (2008) G9a/GLP complexes independently mediate H3K9 and DNA methylation to silence transcription. *EMBO J* **27**(20)**:** 2681-2690

Uemura T, Kubo E, Kanari Y, Ikemura T, Tatsumi K, Muto M (2000) Temporal and spatial localization of novel nuclear protein NP95 in mitotic and meiotic cells. *Cell Struct Funct* **25**(3)**:** 149-159

Unoki M, Nishidate T, Nakamura Y (2004) ICBP90, an E2F-1 target, recruits HDAC1 and binds to methyl-CpG through its SRA domain. *Oncogene* **23**(46)**:** 7601-7610

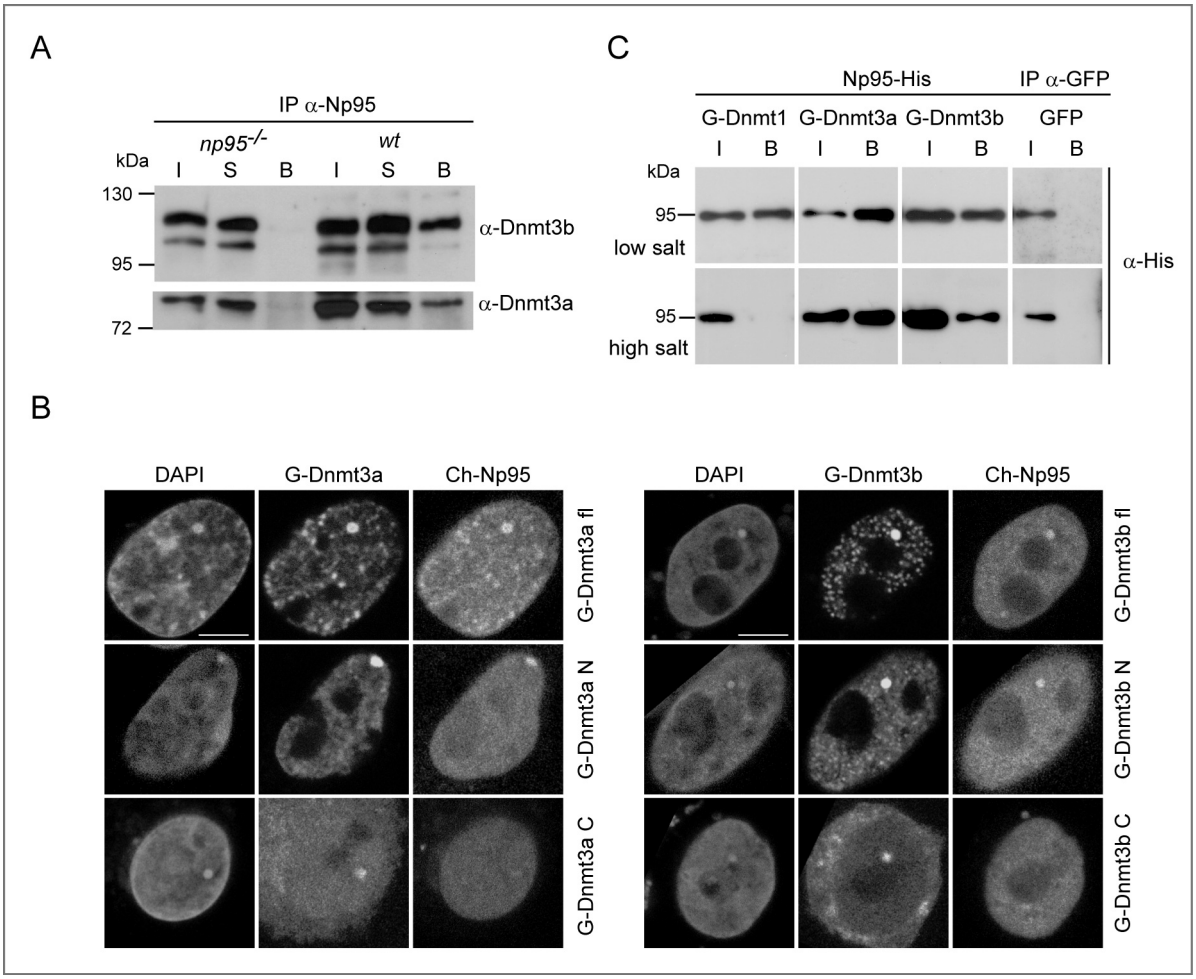

Figure 1

Np95 interacts with *de novo* methyltransferases Dnmt3a and 3b. **(A)** Co-immunoprecipitation of Dnmt3a and Dnmt3b isoforms with Np95 in wild type and *np95* $^{-/-}$ E14 ESCs. **(B)** Fluorescent two-hybrid assay (F2H) shows recruitment of Cherry-Np95 (prey) at the *lac* operator array when GFP fusions of full length Dnmt3a and 3b1 (G-Dnmt3a/b fl) or their N-terminal regions (G-Dnmt3a/b N) are used as baits and not with their isolated C-terminal catalytic domains (G-Dnmt3a/b C). Scale bars represent 5 µm. **(C)** Co-immunoprecipitation of Np95-His with GFP tagged Dnmt1, 3a and 3b1 (G-Dnmt) transiently co-expressed in HEK293T cells. Co-expression of GFP was used as control. In the upper row immunoprecipitations in the presence of 150 mM NaCl throughout the procedure are shown, while in the lower row immunoprecipitation and wash buffers contained 300 mM and the 500 mM NaCl, respectively. 2% of input (I) and supernatant (S) relative to bound (B) fractions were loaded in a and c.

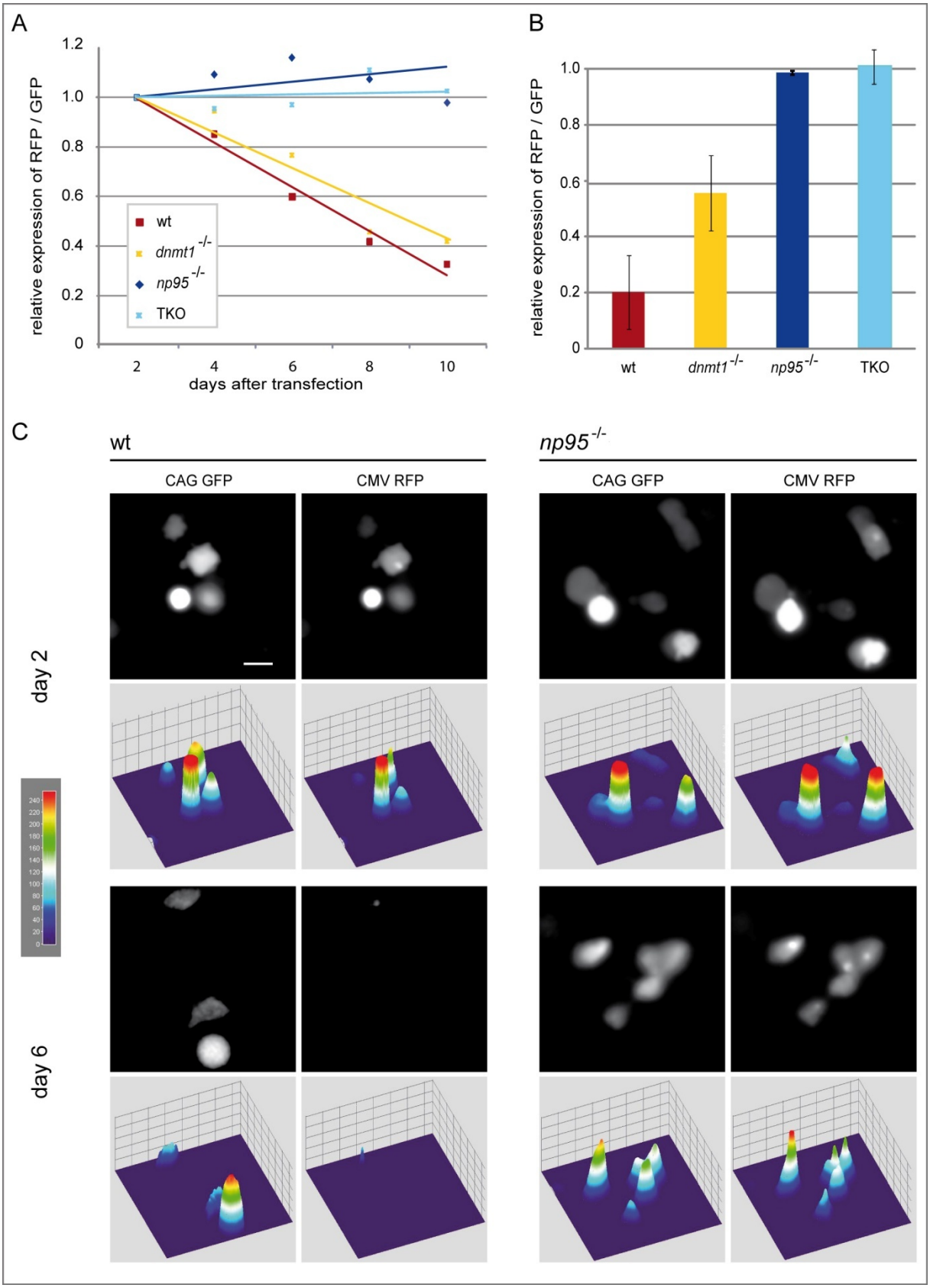
A
relative expression of RFP / GFP
1.2
1.0
0.8
0.6
0.4
0.2
0
wt
dnmt1 -/-
np95 -/-
TKO
2
4
6
8
10
days after transfection
B
relative expression of RFP / GFP
1.0
0.8
0.6
0.4
0.2
0
wt
dnmt1 -/-
np95 -/-
TKO
C
wt
np95 -/-
CAG GFP
CMV RFP
CAG GFP
CMV RFP
day 2
day 6

Figure 2

Figure 2

Promoter silencing activity in wild type, *np95*$^{-/-}$, *dnmt1*$^{-/-}$ and TKO ESCs. Indicated ESC lines were transiently cotransfected with CMV promoter-driven mRFP and CAG promoter-driven GFP reporter constructs. Between 90 and 150 images per sample were acquired either every second day after transfection from a single experiment **(A)** or only at day 2 and 7-10 after transfection from 3-5 independent experiments. **(B)** Relative levels of red vs. green fluorescence are shown with values for day 2 (first day of imaging) set to 1. Wild type (wt) and *dnmt3a*$^{-/-}$*;3b*$^{-/-}$ J1 cells (not shown) gave very similar results to wt E14 and TKO cells, respectively. **(C)** Representative images of wt and *np95*$^{-/-}$ E14 ESCs co-transfected as in A and B (upper panels) and respective heat map intensity plots (lower panels). The scale bar represents 15 µm.

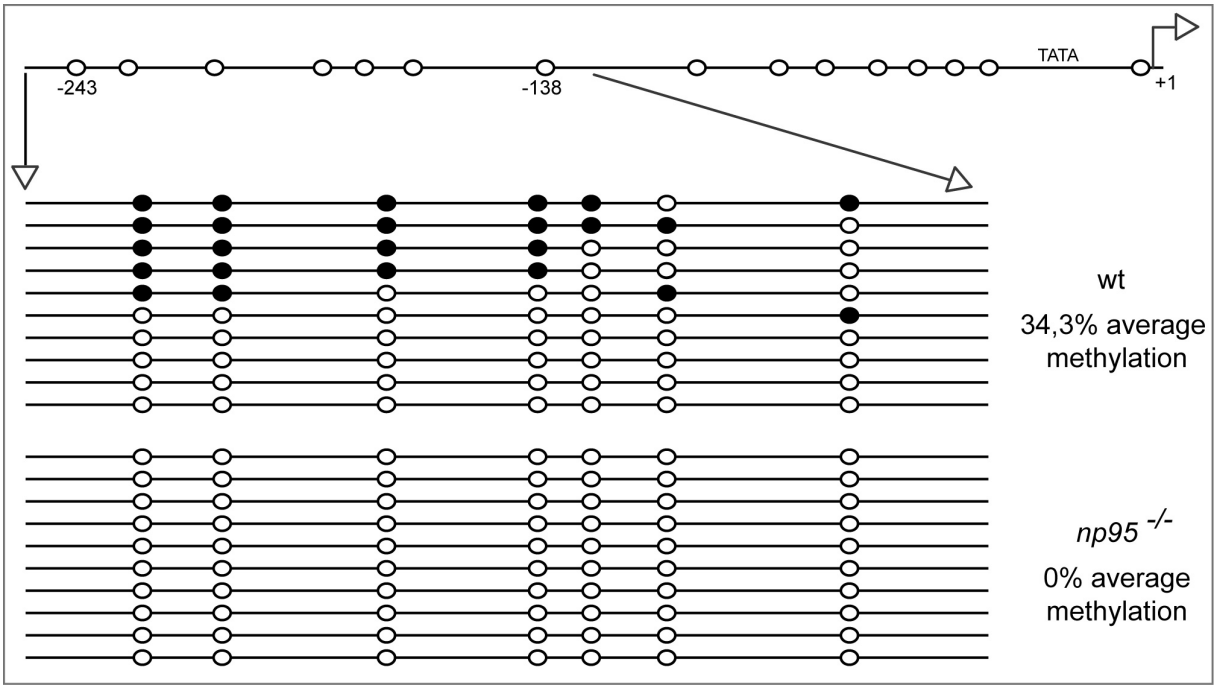

Figure 3

Methylation analysis of the CMV promoter 10 days after transfection of wt and *np95* $^{-/-}$ ESCs. Total isolated DNA was subjected to bisulfite sequencing for the proximal part of the promoter. Sequences from individual clones are shown as lines with unmethylated and methylated CpG sites represented by open and solid circles, respectively.

SUPPLEMENTARY INFORMATION

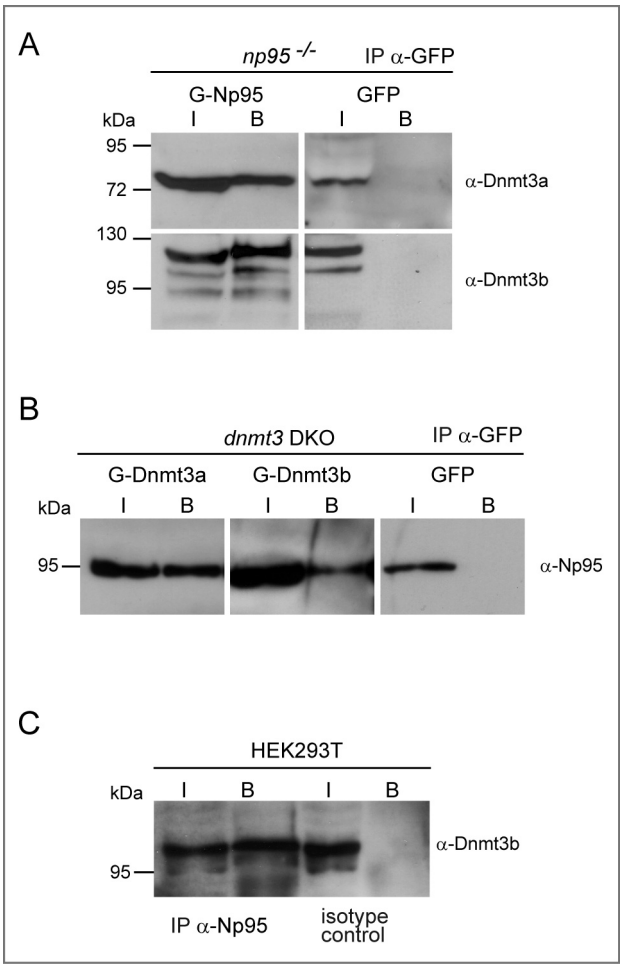

Supplementary Figure 1

Np95 interacts with *de novo* methyltransferases Dnmt3a and 3b. **(A)** Co-immunoprecipitation of endogenous Dnmt3a and Dnmt3b isoforms with GFP-Np95 transiently expressed in *np95*$^{-/-}$ ESCs. **(B)** Co-immunoprecipitation of endogenous Np95 with either GFP-Dnmt3a (upper panel) or GFP-Dnmt3b1 (lower panel) transiently expressed in *dnmt3a*$^{-/-}$*;3b*$^{-/-}$ ESCs. Transient expression of GFP was used as control. GFP and GFP fusions were immunoprecipitated with GFP nanotrap as in experiments shown in Fig. 1B. 2% of input (I) relative to bound (B) fractions was loaded in A and B. **(C)** Co-immunoprecipitation of endogenous ICBP90/UHRF1 and DNMT3b in HEK293T cells. Antibodies to mouse proteins cross-react with the respective human homologues. 4% of input (I) relative to bound (B) fractions was loaded.

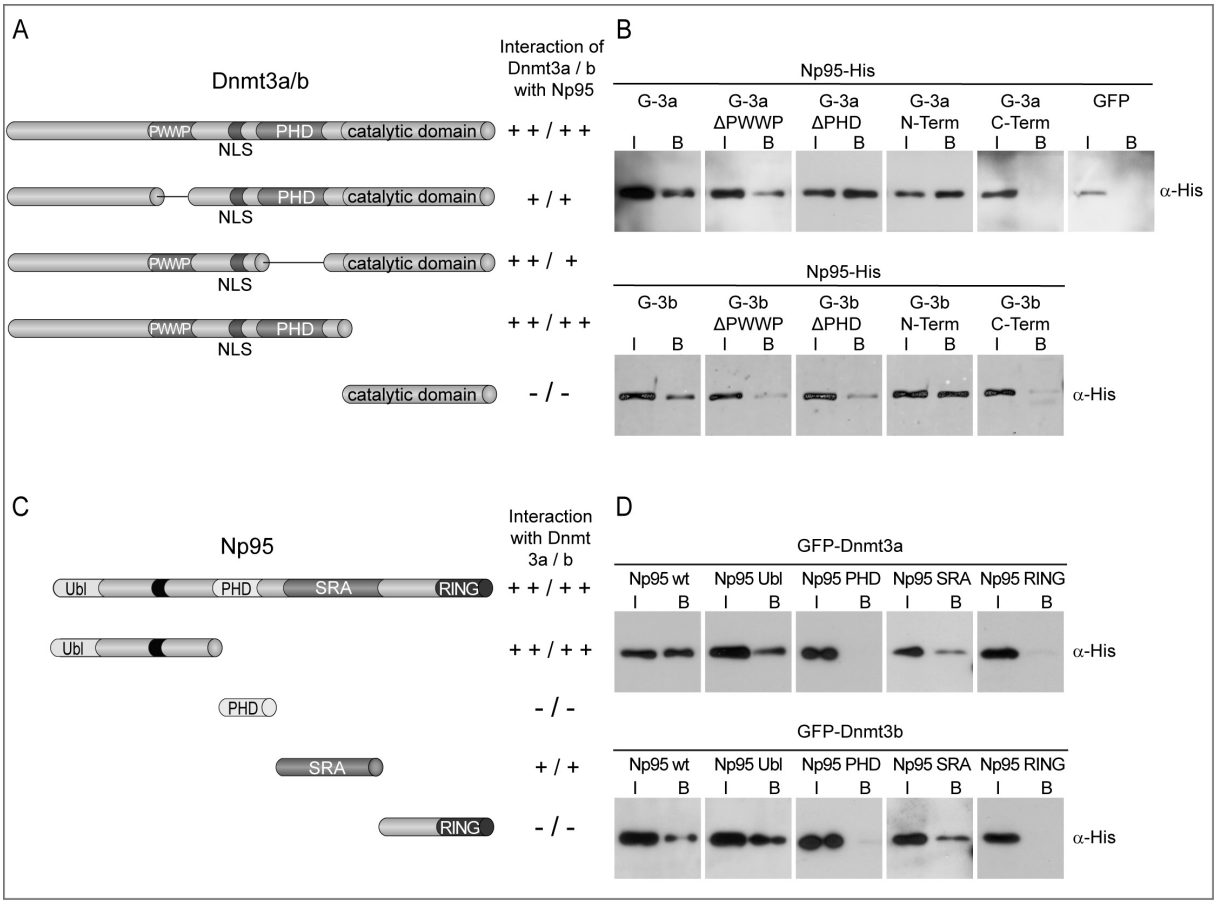

Supplementary Figure 2

Mapping the interaction domains of Dnmt3a/b and Np95. **(A)** Schematic representation of GFP-Dnmt3a/b fusion constructs used for mapping the interaction site with Np95 (N-terminal GFP tag is not shown). **(B)** Co-immunoprecipitation of Np95-His with GFP-Dnmt3 constructs (G-3a/b) from extracts of transiently transfected HEK293T cells. **(C)** Schematic representation of Np95-His constructs used for mapping the interaction site with Dnmt3a/b. **(D)** Co-immunoprecipitation of Np95-His domains shown in c with GFP-Dnmt3a/b constructs from extracts of transiently transfected HEK293T cells. G indicates the GFP fusion. 0,5% of input (I) and 40% of bound (B) fractions were loaded. PWWP, domain with conserved pro-trp-trp-pro motif; NLS, nuclear localization signal; PHD, plant homeo domain; Ubl, ubiquitin-like domain; SRA, set and ring associated domain; RING, really interesting new gene domain. Results of mapping are scored by + or -.

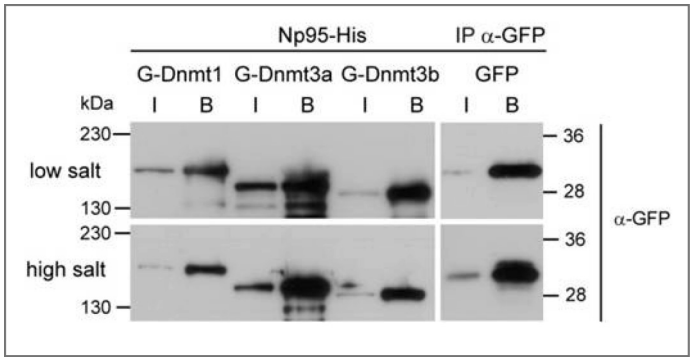

Supplementary Figure 3

Relative stability of Np95 interactions with Dnmt1, 3a and 3b. The same blot as in Fig. 1b is shown here probed with an anti-GFP antibody to reveal that similar amounts of each GFP construct were immunoprecipitated in low and high salt conditions, indicating that binding of Np95 to Dnmt3a or 3b is more stable than that to Dnmt1.

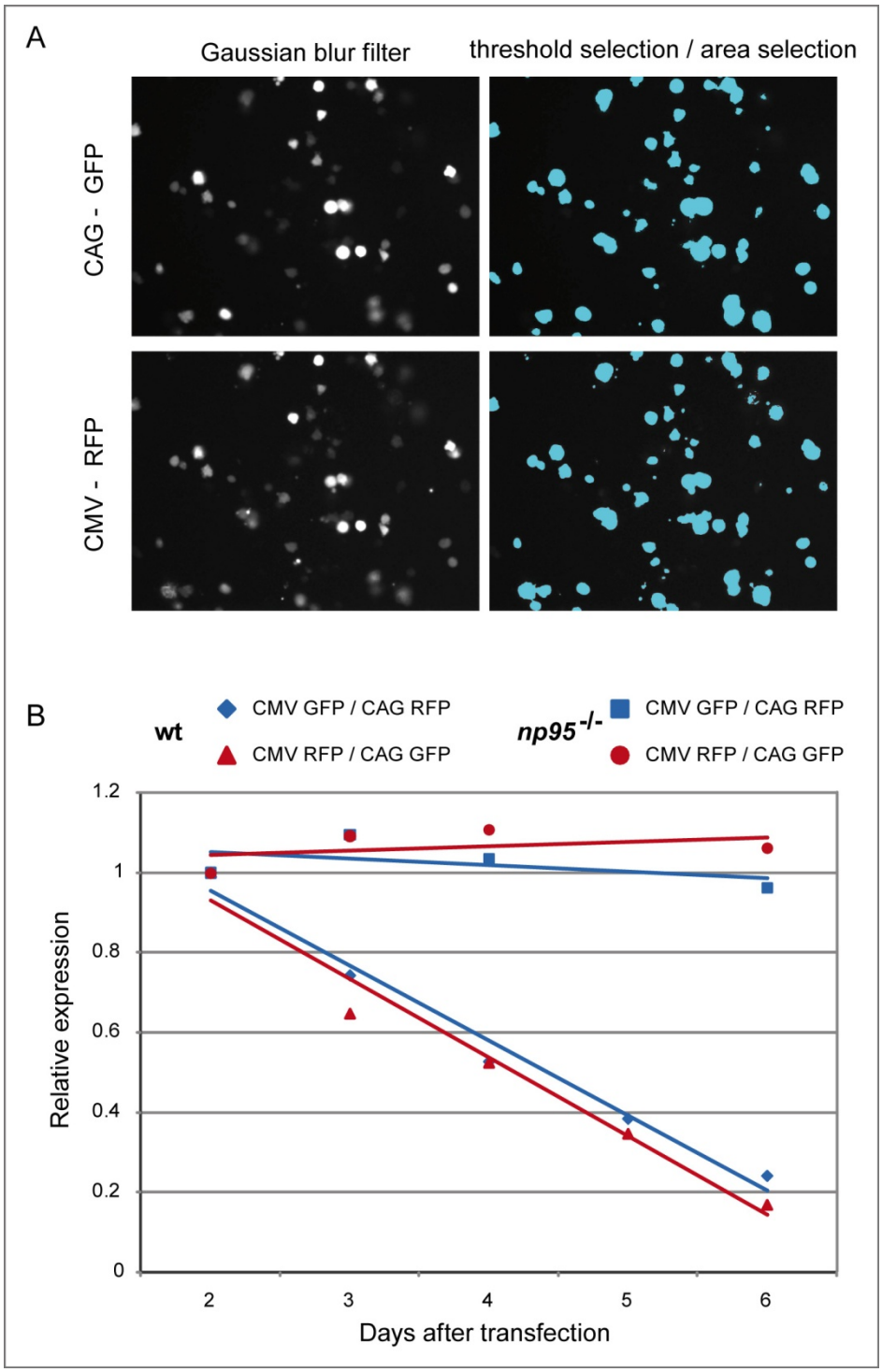

Supplementary Figure 4

(A) Automated procedure for quantification of fluorescent signals from digital micrographs for the promoter silencing assay. A macro was written for the ImageJ software that applies a Gaussian blur filter (left panel) and signal thresholding (right panel) to raw images (data not shown) and then calculates the total signal area. **(B)** Silencing assay results are not affected by the choice of fluorescent reporter. wt and *np95*$^{-/-}$ ESC were cotransfected with either CMV-

driven mRFP and CAG-driven GFP (red) or CAG-driven mRFP and CMV-driven GFP (blue) expression constructs and the ratio of CMV- over CAG-driven fluorescence was quantified at the indicated time points after transfection as for Figure 2A.

SUPPLEMENTARY METHODS

Plasmid construction

The CMV-driven enhanced GFP construct was from Clontech (pEGFP-C1). To generate the CMV-driven mRFP construct (pCMV-mRFP) the coding sequence for eGFP in pEGFP-C1 was replaced with that for mRFP from pRSETB-mRFP(Campbell et al., 2002) (provided by Roger Tsien). To create CAG-driven eGFP, mRFP and mCherry expression constructs (pCAG-eGFP-IB, pCAG-mRFP-IB and pCAG-mCherry-IB, respectively) sequences coding for the respective fluorescent proteins from pEGFP, pRSETB-mRFP and pRSETB-mCherry(Shaner et al., 2004) (also provided by R. Tsien) were inserted downstream to the CAG promoter in the pCAG-IRESblast vector(Chen et al., 2003). The expression construct for Np95-His was described previously(Citterio et al., 2004). To generate expression constructs for GFP-Np95, Ch-Np95, GFP-Dnmt3a and GFP-Dnmt3b1 the sequences coding for Np95, Dnmt3a or Dnmt3b1 were then transferred from the respective CMV promoter-driven constructs(Chen et al., 2003; Citterio et al., 2004) to either pCAG-eGFP-IB or pCAG-mCherry-IB downstream to sequences coding for the fluorescent protein. GFP-Dnmt3a and GFP-Dnmt3b1 deletion constructs were generated by overlap extension mutagenesis(Ho et al., 1989) to remove the following amino acids from Dnmt3a and 3b1, respectively: 278-343 and 223-287 ΔPWWP); 485-582 and 435-532 (ΔPHD). GFP fusion constructs of N-terminal regions (aa 1-629 and 1-580) and C-terminal domains (aa 630-908 and 581-859) of Dnmt3a and 3b, respectively, were generated by PCR cloning using full length constructs as templates. All constructs were characterised by sequencing and immunoblotting.

SUPPLEMENTARY REFERENCES

Campbell RE, Tour O, Palmer AE, Steinbach PA, Baird GS, Zacharias DA, Tsien RY (2002) A monomeric red fluorescent protein. Proc Natl Acad Sci U S A 99(12): 7877-7882

Chen T, Ueda Y, Dodge JE, Wang Z, Li E (2003) Establishment and maintenance of genomic methylation patterns in mouse embryonic stem cells by Dnmt3a and Dnmt3b. Mol Cell Biol 23(16): 5594-5605

Citterio E, Papait R, Nicassio F, Vecchi M, Gomiero P, Mantovani R, Di Fiore PP, Bonapace IM (2004) Np95 is a histone-binding protein endowed with ubiquitin ligase activity. Mol Cell Biol 24(6): 2526-2535

Ho SN, Hunt HD, Horton RM, Pullen JK, Pease LR (1989) Site-directed mutagenesis by overlap extension using the polymerase chain reaction. Gene 77(1): 51-59

Shaner NC, Campbell RE, Steinbach PA, Giepmans BNG, Palmer AE, Tsien RY (2004) Improved monomeric red, orange and yellow fluorescent proteins derived from Discosoma sp. red fluorescent protein. Nat Biotechnol 22(12): 1567-1572

3. Discussion

3.1 Mutagenesis Strategies to Study Protein-Protein Interactions

Mutagenesis is used to engineer proteins for an improved function and to investigate the contribution of single domains or amino acids to protein function. In general, there are two different approaches to address this issue, random and site-directed mutagenesis. Random mutagenesis can be applied for directed protein evolution by generating a library of protein variants using error-prone PCR and selecting candidates by screening for the improved function. We use site-directed mutagenesis to determine protein regions and amino acids that are crucial for protein-protein interactions. Recently, a Y2H based strategy to map interacting protein domains of Dnmt3a and Dnmt3L has been described. Protein variants of Dnmt3a were generated by random mutagenesis, 76 interacting variants were sequenced and aligned. The region that had no mutations acquired was taken as the interacting domain and therefore this approach was called "absence of interference". The findings were confirmed by site-directed mutagenesis and structural analysis (Dhayalan et al., 2008). We are studying DNA methyltransferases in their native environment, in mammalian cells to account for posttranslational modifications that might be absent in yeast. In addition, our mutagenesis strategy (chapter 2.1) consists only of three simple steps and does not require cost-intensive sequencing of multiple clones for evaluation.

As no structural information of Dnmt1 was available at that time to decide about target amino acids for mutagenesis, we headed for hydrophilic regions that are in general exposed at the surface of globular proteins and hence might be involved in protein-protein interactions. To determine such hydrophilic regions we generated a hydrophilicity plot of Dnmt1 using the Hopp and Woods algorithm (Hopp and Woods, 1981). A hydrophilicity value is assigned to every amino acid and average values are calculated for windows with selected size along the protein sequence. The hydrophilicity plot (Figure 3.1A) depicts the C-terminal region of the TS domain, the peaks indicate hydrophilic regions. Based on this plot, we generated a deletion between the two hydrophilic peaks EDS and DDE (Δ553-578). Recently, the structure of the human TS domain was solved (aa 351-600, PDB 3epz; (Walker, 2008b)). Interestingly, the hydrophilic region that was deleted based on the hydrophilicity plot, forms a distinct α-helix as highlighted in the crystal structure (Figure 3.1B) and its deletion did not affect catalytic activity of Dnmt1 as determined with the trapping assay

((Schermelleh et al., 2005); chapter 2.1). In summary, based on secondary structure analysis we generated a deletion mutant where a distinct structural element was deleted and the overall protein folding was not disturbed. Comparison of the structure and the previously generated mutations provides new insights on potential binding surfaces and allows specifically targeted mutagenesis design in the future.

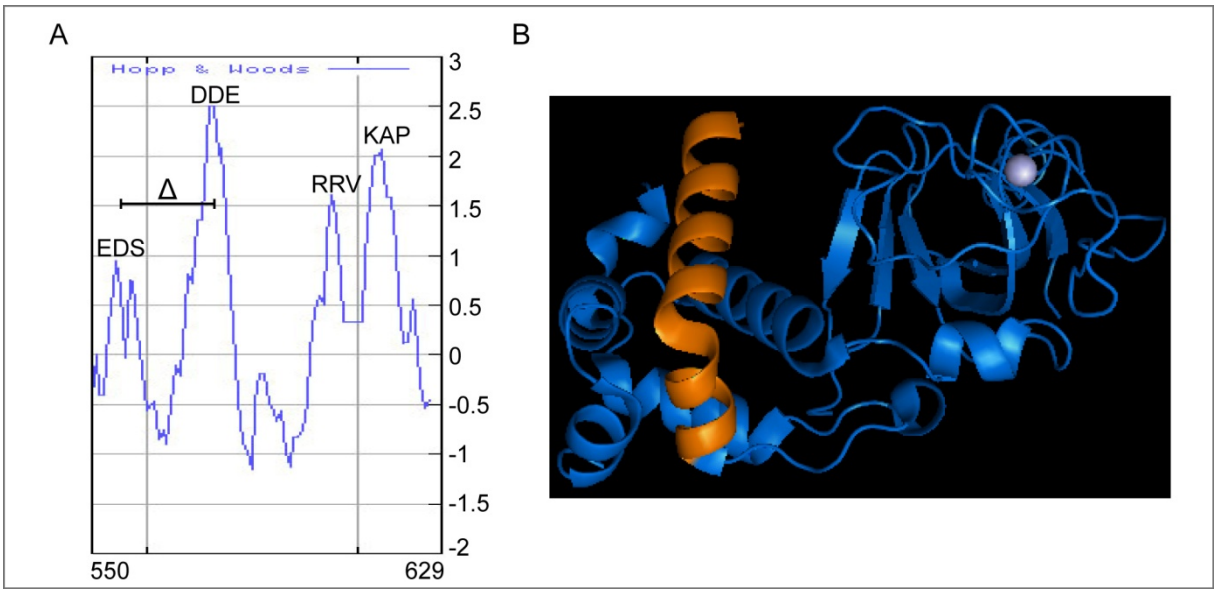

Figure 3.1 Structural analysis of Dnmt TS domain. (A) Hydrophilicity plot (Hopp and Woods, 1981) of the C-terminal part of the TS domain (aa 550-629); a window size of six was applied using the linear weight variation model; peaks designate hydrophilic regions and respective amino acids are indicated; deletion (Δ) is marked between two hydrophilic peaks: EDS-DDE (553-578). (B) Crystal structure of TS domain (PDB 3epz, (Walker, 2008b)). The deleted hydrophilic region is highlighted in orange and forms a distinct α-helix, a zinc-ion (gray ball) is complexed. The image was generated using the PyMOL software (DeLano, 2002).

Various site-directed mutagenesis strategies and kits are available presenting different advantages and disadvantages. Our requirements were not only to develop a fast and robust strategy that allows inexpensive screening of clones but also a streamlined generation of point, deletion and insertion mutants that can be easily expanded. As none of the kits fulfilled all these requirements, we designed a novel alanine-scanning mutagenesis strategy that allows first, the generation of alanine substitution, deletion and insertion mutants of one protein in parallel, and second, introduces a restriction site (SacII or NotI) as marker for fast and inexpensive screening of mutant clones. Third, fast generation of a large toolbox of protein variants allows easy extension by swapping domains or different combination of insert fragments by cut and paste with the restriction sites introduced by the initial mutagenesis. Fourth, we are not limited to vectors with a maximal size of 8 kb as some commercial kits (Invitrogen, Genetailor) and successfully applied the strategy to larger vectors (about 10 kb). As we are extensively studying the protein family of DNA methyltransferases,

rapid enlargement of our set of mutants allows us to efficiently address new emerging questions with a tailored set of protein variants.

The newly developed mutagenesis strategy offers a long term advantage for our analysis of Dnmts, without depending on expensive commercial kits and new mutagenesis design for each new question.

3.2 Biochemical Analysis of N-C Terminal Dnmt1 Interactions

Dnmt1 is a large enzyme comprising 1620 amino acids and a molecular mass of 183 kDa. The regulatory N-terminal domain contains 1111 amino acids and several functional and only partially characterized subdomains. A glycine-lysine repeat linker $(GK)_7$ connects the N-terminal domain to the C-terminal catalytic domain. This linker provides conformational flexibility and allows dynamic interactions between catalytic C-terminal domain and the regulatory N-terminal domain that was reported to play a role in sequence specific DNA recognition by Dnmt1 (Bestor, 1992). The C-terminal catalytic domain contains all characteristic motifs known from bacterial methyltransferases. Bacterial methyltransferases do not have any separate regulatory domains but show sequence specific DNA recognition and methylation patterns. In contrast, the catalytic domain of Dnmt1 is not catalytically active per se (Fatemi et al., 2001; Margot et al., 2003; Zimmermann et al., 1997) but requires allosteric activation through the N-terminal regulatory domain (Bacolla et al., 1999). This complex regulatory domain and the linker connecting the two domains might account for various active and nonactive conformations of Dnmt1. So far, structural information of Dnmt1 is only available of a 250 aa region of the N-terminal domain corresponding to the TS domain (PDB: 3epz (Walker, 2008b)), while structural information of other Dnmts that all contain smaller N-terminal domains is already available: Dnmt2, 3a, 3b, 3L (Dong et al., 2001; Jia et al., 2007; Ooi et al., 2007; Qiu et al., 2002). To understand the N-C-terminal regulation of Dnmt1 we determined the minimal region of the N-terminus that is required for interaction with the catalytic domain. Only the N-terminal 309 amino acids were not necessary for the N-C terminal interaction. Neither the TS domain nor the BAH regions were dispensable for the interaction, nor were the individual domains sufficient to interact with the catalytic domain. These results indicate that the proper overall folding of the N-terminus is crucial for this interaction. Moreover, analysis of the Dnmt1 sequence and the intron-exon distribution revealed that Dnmt1 has evolved from the fusion of at least three genes (Margot et al., 2000). Dnmt1 N-terminus seems to be composed of originally two genes while the C-terminus corresponds to a third distinct gene and is very similar to the bacterial methyltransferases. Interestingly, the N-terminal region of 309 aa that are dispensable for the N-C terminal interaction and methyltransferase activity correspond well to one of the proposed ancestral genes.

3.2.1 Role of the Dnmt1 CXXC Zinc Finger for Catalytic Activity

In addition, we assessed the role of the N-terminal CXXC zinc finger for the N-C-terminal interaction. Our results showed that the zinc finger (ZnF, aa 655-696) was dispensable for N-C-terminal interaction of Dnmt1. Previously published data indicated that the zinc finger domain (aa 613-748) is even sufficient for interaction and allosteric activation of the catalytic domain and preferential recognition of methylated CpG DNA (Fatemi et al., 2001). The authors performed *in vitro* affinity purification to test Dnmt1 domain interactions using individual Dnmt1 domains recombinantly produced in *E.coli*. We addressed this question with a different strategy: Based on structural information of a very similar zinc finger from MLL (Allen et al., 2006) and by applying our versatile mutagenesis strategy, we concisely deleted the zinc finger without affecting surrounding protein regions (ΔZnF, Δ655-696). To test the interactions, N- and C-terminal domains of Dnmt1 were expressed in human cells (HEK293T) and co-immunoprecipitation experiments and immunoblotting were performed. Deletion of the ZnF from the N-terminus did not affect the N-C-terminal interaction. Moreover, GFP-Dnmt1ΔZnF was tested for localization and catalytic activity *in vivo* and behaved like GFP-Dnmt1 wt (unpublished data from A. Rottach). The differences between the results described by Fatemi et al. and our data might originate from major differences in the experimental setups: First, Fatemi et al. used a single zinc-binding domain (aa 613-748) that is larger than our deletion mutant lacking precisely the zinc-finger motif (aa 655-696). Second, they produced Dnmt1 domains in bacteria, where correct folding might be hampered due to a lack of distinct chaperone proteins or posttranslational modifications while we used a mammalian expression system. Third, the authors applied the domains to affinity purification to test interactions while we performed co-immunoprecipitation with cell extracts from human cells expressing N- and C-terminal Dnmt1 domains.

A second, recent publication dealing with the Dnmt1 CXXC zinc finger indicated an essential role of the zinc finger domain for catalytic activity of Dnmt1 (Pradhan et al., 2008). Using gel-shift assays of the recombinantly produced CXXC zinc finger domain (aa 645-737) from *E.coli*, binding to unmethylated CpG DNA was observed. In addition, mutation of cysteines in the zinc finger abolished DNA binding and Dnmt1 point and deletion mutants of the zinc finger (Δ647-690) displayed reduced catalytic activity in a radioactive methyltransferase activity assay. Moreover, a stable conditional knock-in COS-7 cell line was generated, where the expression of Dnmt1Δ647-690 was induced for 10 days and the methylation status of rDNA

repeat sequences, that are normally methylated, was assessed by bisulfate sequencing. As the authors observed a partial loss of rDNA methylation (25%) they proposed a dominant negative effect of Dnmt1Δ647-690.

Our data clearly indicate that the zinc finger does not play a role in N-C interaction, normal Dnmt1 activity was measured *in vivo* and *in vitro* (Frauer and Leonhardt, 2009; Schermelleh et al., 2005); unpublished data from A. Rottach and C. Frauer). In addition, the *in vitro* methyltransferase activity assay showed that GFP-Dnmt1Δ655-696 had the same activity and preference for hemi-methylated DNA substrate as GFP-Dnmt1 wt. An *in vitro* DNA binding assay showed a preferential binding to unmethylated CpG sites for the ZnF domain (GFP-ZnF 643-700, enriched from a HEK293T cell lysate). This is in line with the results from Pradhan et al. whereas as Fatemi et al. found the zinc finger domain preferential binding to methylated CpGs. Expression of human DNMT1Δ647-690 in COS-7 cells (Pradhan et al., 2008) on top of the endogenous enzyme is artificial, causes elevated Dnmt1 levels and the endogenous protein might mask or influence the effect of the deletion mutant. As described in this work, Dnmt1 can form stable dimers, so that in case of this stable COS-7 cell lines chimeric Dnmt1 dimers could be present. A better experiment to assess the function of the Dnmt1 zinc finger *in vivo* would be a rescue of *dnmt1*$^{-/-}$ ESCs with Dnmt1ΔZnF – and a characterization of that rescued cell line. Especially a quantitative methylation analysis of major and minor satellite sequences, retroviral elements such as IAPs and single copy genes should be performed by pyrosequencing.

3.2.2 Role of Dnmt1 S515 Phosphorylation for Dnmt1 Activity

Initially, Glickman et al identified serine 515 (S515) as major phosphorylation site of Dnmt1 by performing metabolic labeling and mass spectrometry (Glickman et al., 1997). A polymorphism in Dnmt1 aa F147 or aa SV 146-147 leads to serine numeration as S514 or S515. We work with the latter variant and therefore refer to the serine as S515. S515 is located in the center of the regulatory N-terminal domain of Dnmt1, within the TS domain that is indispensable for N-C-terminal interaction of Dnmt1. Therefore, we analyzed whether phosphorylation of S515 plays a role in the N-C terminal interaction and influences catalytic activity of Dnmt1. We used the phosphorylation mutants GFP-Dnmt1 and GFP-N-terminus S515A, where the phosphorylation site is eliminated ("P off") and S515D mutants where aspartic acid mimics the phosphate group sterically and in charge distribution ("P on") to study N-C-terminal interactions by co-immunprecipitation experiments. GFP-N-S515A

showed a comparable interaction with the catalytic domain as GFP-N wt while the S515D mutation weakened the N-C-terminal interaction. In addition, cell-cycle dependent localization of the mutants and catalytic activity *in vivo* and *in vitro* were tested and showed the same cellular distribution and catalytic activity as GFP-Dnmt1 wt (unpublished data from A. Rottach and C. Frauer). In summary, elimination of the S515 phosphorylation site did not have an impact on N-C-terminal interaction, localization and enzymatic activity of Dnmt1.

However, using *in vitro* assays Goyal et al. found a role of serine 515 in activation of Dnmt1. Dnmt1 was purified from a baculovirus system and S515 phosphorylation was confirmed by mass spectrometry. Enzymatic activity of Dnmt1S515A and DnmtS515E (negatively charged glutamic acid to mimic phosphorylation) were compared to wildtype Dnmt1 by an *in vitro* activity assay using hemi-methylated DNA as substrate. In contrast to wildtype Dnmt1 (100% activity), Dnmt1S515E retained 73% activity but Dnmt1S515A showed only minimal activity (1.5%). As the N-C-terminal interaction is essential for Dnmt1 activity, the authors tested whether S515 phosphorylation influences catalytic activity. A phosphorylated peptide mimicking the region around S515 was tested as inhibitor of wildtype Dnmt1. Indeed, they observed a 10-fold stronger inhibition of Dnmt1 by the phosphorylated peptide as by the nonphosphorylated peptide (Goyal et al., 2007). Therefore the authors concluded that S515 phosphorylation is important for activity of Dnmt1.

The data presented in this work together with other data of our group clearly indicate that GFP-Dnmt1S515A is catalytically active and behaves like GFP-Dnmt1 wt with respect to normal N-C-terminal interaction, localization, activity *in vivo* and *in vitro*. The different results might be explained by the different experimental approaches. Goyal et al. performed exclusively *in vitro* studies with baculovirus expressed protein while our data where acquired by both, biochemical *in vitro* and cell-biological *in vivo* experiments analyzing Dnmt1 expressed in mammalian cells. We used constructs with an N-terminal GFP-tag that allowed us to conduct with one tag both, biochemical assays with the GFP Nanotrap (Rothbauer et al., 2008) and cell biological experiments. Normal enzymatic activity of GFP-tagged Dnmt1 has been shown previously (Spada et al., 2007).

To finally clarify the impact of S515 phosphorylation on Dnmt1 activity and methylation maintenance, a stable rescue of *dnmt1*$^{-/-}$ ESCs could be generated with Dnmt1S515A. A detailed characterization of the cell line, primarily of the methylation status of different types of sequences such as repetitive sequences, major and minor-satellite DNA, IAPs and single copy genes would answer the question whether deletion of the S515 phosphorylation site has an effect on Dnmt1 maintenance function. Moreover, a specific antibody against phosphorylated S515 could help to elucidate whether Dnmt1 phosphorylation is regulated in a cell-cycle dependent manner, as described for Dnmt1 localization.

3.3 The N-Terminal TS Domain Mediates Dnmt1 Dimerization

Dimerization of C5 DNA methyltransferases has been described for bacterial and mammalian enzymes including HhaI, Dnmt3a and Dnmt3L (Dong et al., 2004; Jia et al., 2007). In this work, dimerization of Dnmt1 was shown (see chapter 2.3). In gelfiltration analyses of recombinant DNMT1, the enzyme presented the molecular weight of a dimer. Further investigations confirmed these observations and the Dnmt1 dimerization domain could be mapped by co-immunoprecipitation experiments and the F2H assay to the N-terminal TS domain (aa 310-629). Fine-mapping within the TS domain revealed a bipartite interaction surface between the two TS domains that is responsible for Dnmt1 dimerization (aa 310-410 and aa 476-502). The N-terminal domain allosterically activates the catalytic domain of Dnmt1 (Fatemi et al., 2001; Margot et al., 2003). Deletions within the TS domain most likely disrupt the structural integrity of the N-terminus and thus the required conformations for allosteric activation of the catalytic domain cannot be accomplished. Careful alanine scanning mutagenesis (Fellinger et al, 2008), substituting three adjacent amino acids to alanine in that region did not disrupt dimerization. Deletion of the dimerization region would require eliminating almost 200 amino acids (310-502) from the center of the N-terminal domain. Previous experiments have shown that deletions within the N-terminal domain abolished enzymatic activity of Dnmt1 (Fatemi et al., 2001; Margot et al., 2000; Zimmermann et al., 1997). Thus, with deletion mutagenesis it is not possible to pinpoint the functional consequences of the dimerization as deletions in the TS domain affect the enzyme folding and disrupt catalytic activity.

In summary, the TS domain is a multifunctional key domain in Dnmt1 regulation: First, it is required for N-C-terminal interaction and allosteric activation of the Dnmt1 catalytic domain and second, it recruits Dnmt1 to PH by interaction with Np95 (chapter 2.4). Third, the TS domain is responsible for Dnmt1 dimerization (chapter 2.3).

Interestingly, Dnmt3a dimerization is mediated by interactions between the catalytic domains and the interface (aa 806-880) is located very close to the catalytic center of the enzyme. Moreover, substitution of the key residues for dimerization R881 and D872 abolished catalytic activity of Dnmt3a, indicating that either the dimer conformation of Dnmt3a might be crucial for enzymatic activity or that disruption of the dimer interface that is close to the catalytic center affects proper folding of that region and therefore abolishes Dnmt3a activity. In contrast to Dnmt1 where the N-terminal multifunctional TS domain mediates dimerization, the N-terminal regulatory domains of Dnmt3a or 3L are not involved in dimer formation (Jia et al., 2007). Recently, first structural insights into the N-terminal region corresponding to the TS domain were gained (aa 351-600; PDB: 3epz; (Walker, 2008b)). Despite some flexible, unstructured regions the crystal structure shows that the conserved core region (aa 465-500) forms three consecutive beta sheets and builds a potential binding pocket in the center of the domain. Where this region is situated in the context of the full-length enzyme remains unclear. However, these first structural insights facilitate future mutagenesis approaches.

Dnmt1 is a very complex enzyme, a large N-terminal regulatory domain is connected by a $(GK)_7$ linker to the catalytic domain. This unique composition likely yields a variety of different conformations and could be one explanation for the limited success of Dnmt1 crystallization attempts so far, compared to other Dnmt members (Dong et al., 2001; Jia et al., 2007; Ooi et al., 2007; Qiu et al., 2002). Hence, a variety of intra- and intermolecular interactions of Dnmt1 are responsible for the complex regulation of Dnmt1. In addition to dimerization, the TS domain contributes to allosteric activation of the catalytic domain (Fatemi et al., 2001; Margot et al., 2000; Zimmermann et al., 1997) and mediates association with pericentric heterochromatin by interaction with Np95 (Easwaran et al., 2004).

Further studies are necessary to elucidate the temporal and spatial coordination of these multiple functions of the TS domain and to analyze whether Dnmt1 dimer formation facilitates the discrimination of hemi-methylated CpG sites.

3.4 Np95 is a Key Regulator of DNA Methyltransferases

Np95 was described to play a role in maintenance of DNA methylation patterns and to interact with Dnmt1 (Bostick et al., 2007; Sharif et al., 2007). Moreover, we found Np95 to be essential for gene silencing through *de novo* methylation by Dnmt3a and3b. We showed interaction of Np95 with the three major Dnmts Dnmt1, 3a and 3b by biochemical and cell biological experiments and mapped the interaction to the regulatory N-terminal domains of Dnmts (Figure 3.2).

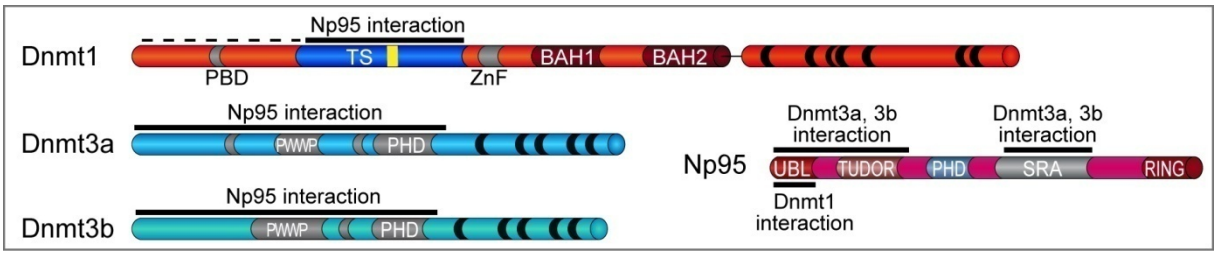

Figure 3.2 Summary of Dnmt-Np95 interacting domains. Schematic overview of Dnmts and Np95; PBD, PCNA binding domain; TS, targeting sequence; ZnF, zinc finger; BAH1+2, bromo adjacent homology domains 1+2, PWWP, pro-trp-trp-pro motif, PHD, plant homeo domain; UBL, ubiquitin-like domain; TUDOR, tandem tudor domain; SRA, SET and RING associated domain; RING, really interesting new gene, containing ubiquitin E3 ligase activity. Black lines indicate the respective interacting domains between Dnmts and Np95, yellow box within the Dnmt1 TS domain highlights the major interaction site.

While in Dnmt1 mainly the TS domain mediates the interaction, in Dnmt3a and 3b no distinct N-terminal subdomain such as PWWP or PHD was exclusively responsible for the interaction with Np95. Within Np95 we found the N-terminal domain containing the ubiquitin like-domain and the tandem tudor domain to interact with Dnmt3a and 3b and the SRA domain as second binding interface. The Np95 interaction with Dnmt1 is exclusively mediated by the ubiquitin-like domain. Two recent publications describe Np95 as an essential factor for methylation maintenance by recruiting Dnmt1 to replication sites (Bostick et al., 2007; Sharif et al., 2007). By performing GST-pulldowns of purified protein domains from *E. coli* Bostick et al. found the PHD domain (aa 220-416) of human NP95 responsible for interaction with DNMT1 and the N-terminal region 1-446 and C-terminal region 1081-1408 of DNMT1 interacting with NP95. Achour et al. identified in an Y2H screen an N-terminal region corresponding to the TS domain (406-615) to interact with the SRA domain (357-635) of NP95 (Achour et al., 2008) which corresponds to our data of the TS domain as major interaction site of Dnmt1. In addition, our data showed that even a single point mutation within the TS domain (G474E) strongly impaired the interaction with Np95, while deletion of a highly conserved stretch of amino acids (459-501) completely abolished the interaction.

The Np95 interaction mutant GFP-Dnmt1Δ459-501 localized at replication sites during early- and mid-S phase and showed a higher diffuse fraction in late S-phase. These results indicated

that Dnmt1 can normally interact with the replication platform PCNA while the interaction with Np95 that is essential for directing Dnmt1 to pericentric heterochromatin (PH) in late S-phase was abolished. The cell-cycle dependent localization of Dnmt1 is summarized in Figure 3.3.

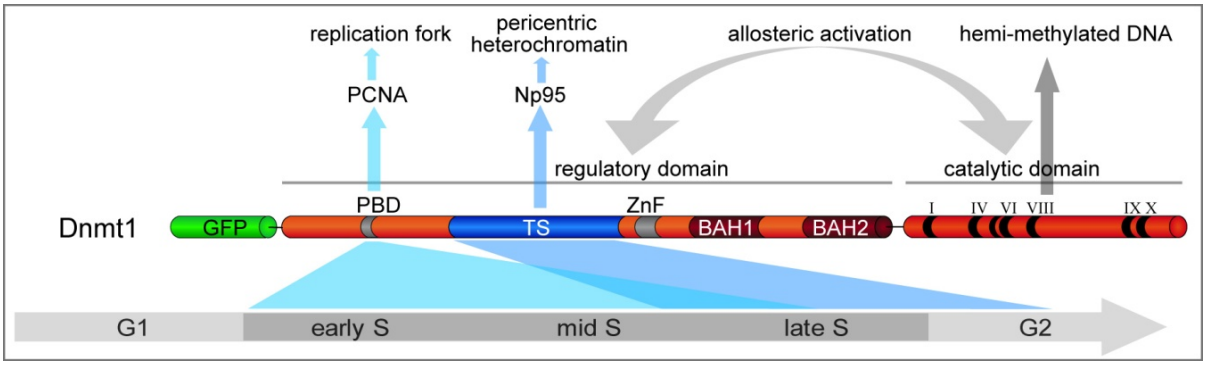

Figure 3.3 Overview of GFP-Dnmt1 domain structure. Depicted in green is a N-terminal GFP that was used to visualize Dnmt1 by fluorescence microscopy. PBD, PCNA binding domain; TS, targeting sequence; ZnF, zinc finger; BAH1+2, bromo adjacent homology domains 1+2, methyltransferase motifs I-X. Cell cycle stages are indicated at the bottom. Interaction with PCNA directs Dnmt1 to the replication machinery from early to late S phase; from late S phase into M/G2 Np95 interaction targets Dnmt1 to pericentric heterochromatin, indicated by the blue arrows. Dnmt1 has several DNA binding sites but DNA binding through the catalytic domain is specific for hemi-methylated DNA. A grey arrow points out the interaction between the regulatory N-terminal and the catalytic C-terminal domain that is necessary for allosteric activation of Dnmt1.

We found the Np95 interaction mutant GFP-Dnmt1Δ459-501 to behave with an approximately two-fold slower kinetics than GFP-Dnmt1 wt in the *in vivo* trapping assay in C2C12 mouse myoblast cells (Schermelleh et al., 2005). The trapping assay is based on the incorporation of the cytosine analogue 5-aza-dC into the DNA. Dnmt1 molecules that are capable to form a covalent complex with this base analogue are trapped at their target sites as this complex cannot be resolved. This accumulation can be visualized by fluorescence microscopy and FRAP analysis. Moreover, GFP-Dnmt1Δ459-501 showed normal activity in a radioactive methyltransferase activity assay using hemi-methylated oligonucleotide DNA as substrate.

This result indicates that the deletion did not disrupt the overall protein structure and that GFP-Dnmt1Δ459-501 was able to methylate "naked" DNA.

Interestingly, stable expression of GFP-Dnmt1Δ459-501 in *dnmt1*$^{-/-}$ ESCs failed to restore DNA methylation at different types of sequences, major and minor satellite DNA, IAPs and single copy genes (unpublished pyrosequencing data from W. Qin). The differing results of the trapping assay and ESC methylation rescue experiment might be due to the different experimental setups: First, the trapping assay was performed by measuring the covalent complex formation of GFP-Dnmt1Δ459-501 in somatic cells that contain normal levels of endogenous Dnmt1. Upon the formation of Dnmt1 dimers – a mutant and an endogenous wt molecule could form a chimeric complex, interact with Np95, thereby access its target sites in DNA and hence account for the accumulation of GFP-Dnmt1Δ459-501 at RF. Second, we analyzed the cells only during S phase in the presence of elevated levels of GFP-Dnmt1 and the interactor RFP-PCNA that were both over-expressed. In addition, the cells contained a high concentration of the trapping substrate 5-aza-dC (30 µM). Third, the trapping assay was performed in somatic cells while the rescue experiments were carried out in ESCs. In *dnmt1*$^{-/-}$ ESCs is no background level of endogenous Dnmt1 as in the somatic myoblast cells used for the trapping assay. Moreover, there might be different pathways active that change from undifferentiated ESCs during differentiation to somatic cells.

In contrast, rescue of *dnmt1*$^{-/-}$ ESCs analyzed and compared the behavior of the Dnmt1 mutant and wt *in vivo*, the only difference to wt ESCs is a lower DNA methylation level in this cell line. Moreover, stably expressing GFP-Dnmt1Δ459-501 ESCs with Dnmt1 protein levels corresponding to endogenous Dnmt1 levels were selected. However, GFP-Dnmt1Δ459-501 failed to re-methylate the DNA while GFP-Dnmt1 wt succeeded. This loss of function suggests that the interaction with Np95 might be necessary *in vivo* to direct Dnmt1 to its target sites and / or facilitate its access.

Taken together, deletion of the 42 amino acids within the TS domain that are crucial for interaction with Np95, lead to normal Dnmt1 activity in vitro but not in vivo. In line with previously published data, our results lead to the conclusion that the interaction with Np95 is indispensable for proper methylation maintenance function of Dnmt1 as it is also reflected by the low methylation levels in np95$^{-/-}$ *ESCs that phenocopy the dnmt1*$^{-/-}$ *ESCs. Further investigations are necessary to find out whether Np95 opens the chromatin for Dnmt1 accessibility.*

As the PHD domain of Np95 was described to open chromatin in chromocenters (Papait et al., 2008) one could rescue *np95*$^{-/-}$ ESCs with Np95 mutants (ΔPHD) and analyze the effect of potentially missing chromatin remodeling activity of Np95 on DNA methylation. Moreover, an *in vitro* Dnmt1 methyltransferase activity test could be performed using nucleosomal hemi-methylated DNA as substrate in the presence and absence of Np95. This experiment could show whether a potential remodeling activity of Np95 enables Dnmt1 to access a target CpG site in chromatin.

Structural analyses of the SRA domain indicated that binding of Np95 to hemi-methylated DNA would block the target strand for methylation (Arita et al., 2008; Avvakumov et al., 2008; Hashimoto et al., 2008). Therefore, Np95 might target Dnmt1 to a hemi-methylated DNA region where the enzyme could then find other hemi-methylated sites by linear diffusion on DNA. Further dissociation of Np95 from the DNA could then make the site accessible for Dnmt1 (Jeltsch, 2008). Such a mechanism could account for the high accuracy of Dnmt1 mediated methylation as the Np95 mark on DNA could be recognized by Dnmt1 more efficiently than a hemi-methylated cytosine in the DNA helix that might be masked by chromatin and chromatin binding proteins. In addition, Np95 might open up the chromatin for accessibility of DNA methyltransferases. As both, Np95 and Dnmt1 have a preference for hemi-methylated DNA this could be a synergistic targeting mechanism to ensure proper maintenance of methylation *in vivo*.

We also found, that Np95 interacts with *de novo* methyltransferases Dnmt3a and 3b and that these interactions are even stronger than with Dnmt1. Moreover, we observed that Np95 is essential in epigenetic silencing. The role of Np95 in epigenetic transgene silencing was investigated in wt and *np95*$^{-/-}$ ESCs using a CMV driven fluorescent reporter gene (Fellinger et al, under review at EMBO Reports, silencing assay data from D. Meilinger and S. Bultmann). The decrease of the CMV promoter driven reporter gene expression was normalized to a chicken β-actin (CAG) promoter driven reporter gene. As the latter originates from a house keeping gene and contains a CpG-island, it is protected from silencing. The CMV reporter gene expression was epigenetically silenced by *de novo* DNA methylation after 10 days in wt ESCs and with a slower silencing kinetics in *dnmt1*$^{-/-}$ ESCs whereas in *np95*$^{-/-}$ and TKO ESCs (that are deficient in Dnmt1, 3a and 3b) no silencing was observed. Despite the presence of

all Dnmts transgene expression was not silenced in *np95*$^{-/-}$ ESCs and no methylation was detected.

These results indicate that Np95 also plays a major role in epigenetic gene silencing mediated by de novo methylation through Dnmt3a and 3b. The interaction of Np95 with the regulatory N-terminal domains of Dnmt3a and 3b described in this work suggests that Np95 might recruit de novo methyltransferases to target sites, possibly activates them and hence controls epigenetic silencing by de novo DNA methylation.

Besides binding to hemi-methylated DNA, Np95 was shown to interact with chromatin proteins (Citterio et al., 2004; Hashimoto et al., 2009; Karagianni et al., 2008; Papait et al., 2007), and specifically with trimethylated H3K9 through its tandem tudor domain (PDB: 3db3; (Walker, 2008a)) and to posses some sort of remodeling activity through its PHD domain (Papait et al., 2008). The H3K9 methyltransferase G9a was reported to be required for *de novo* methylation independent of its histone methyltransferase activity and to recruit Dnmt3a and 3b to promoter sequences in differentiating ESCs (Epsztejn-Litman et al., 2008). In addition, an interaction between Np95 and G9a was published recently, indicating that Np95 might recruit G9a to promoter regions to regulate transcription (Kim et al., 2008) or vice versa.

Future investigations to elucidate the order of events in endogenous gene silencing should be undertaken. One possibility would be to differentiate various ESC lines (*dnmt1*$^{-/-}$, *np95* $^{-/-}$, *dnmt3a*$^{-/-}$ *3b*$^{-/-}$, *TKO, g9a*$^{-/-}$,wt*)* and to perform chromatin immunoprecipitations (e.g. anti Np95, anti G9a or anti 5mC) from different time points during differentiation. The protein complexes bound to chromatin should be analyzed by mass spectrometry and in addition promoter methylation should be checked by bisulfate sequencing of genes that are down regulated during ESC differentiation such as Oct4 or Nanog.

In summary, with Np95 we found a key regulatory factor that controls de novo and maintenance DNA methylation in embryonic stem cells by interaction with the de novo DNA methyltransferases Dnmt3a and 3b and the maintenance methyltransferase Dnmt1. We showed that both, Np95 and the de novo DNA methyltransferases are required for transgene promoter silencing in ESCs. These data clearly support a role for Np95 in epigenetic silencing and make it an interesting target for epigenetic reprogramming.

4. Annex

4.1 References

Aapola, U., I. Liiv, and P. Peterson. 2002. Imprinting regulator DNMT3L is a transcriptional repressor associated with histone deacetylase activity. *Nucleic Acids Res*. 30:3602-8.

Achour, M., X. Jacq, P. Ronde, M. Alhosin, C. Charlot, T. Chataigneau, M. Jeanblanc, M. Macaluso, A. Giordano, A.D. Hughes, V.B. Schini-Kerth, and C. Bronner. 2008. The interaction of the SRA domain of ICBP90 with a novel domain of DNMT1 is involved in the regulation of VEGF gene expression. *Oncogene*. 27:2187-97.

Aebersold, R., and M. Mann. 2003. Mass spectrometry-based proteomics. *Nature*. 422:198-207.

Ai, H.W., K.L. Hazelwood, M.W. Davidson, and R.E. Campbell. 2008. Fluorescent protein FRET pairs for ratiometric imaging of dual biosensors. *Nat Methods*. 5:401-3.

Allen, M.D., C.G. Grummitt, C. Hilcenko, S.Y. Min, L.M. Tonkin, C.M. Johnson, S.M. Freund, M. Bycroft, and A.J. Warren. 2006. Solution structure of the nonmethyl-CpG-binding CXXC domain of the leukaemia-associated MLL histone methyltransferase. *EMBO J*. 25:4503-12.

Andrews, C.A., and S.A. Lesley. 1998. Selection strategy for site-directed mutagenesis based on altered beta-lactamase specificity. *Biotechniques*. 24:972-4, 976, 978 passim.

Anker, J.N., W.P. Hall, O. Lyandres, N.C. Shah, J. Zhao, and R.P. Van Duyne. 2008. Biosensing with plasmonic nanosensors. *Nat Mater*. 7:442-53.

Aoki, A., I. Suetake, J. Miyagawa, T. Fujio, T. Chijiwa, H. Sasaki, and S. Tajima. 2001. Enzymatic properties of de novo-type mouse DNA (cytosine-5) methyltransferases. *Nucleic Acids Res*. 29:3506-12.

Aravin, A.A., R. Sachidanandam, D. Bourc'his, C. Schaefer, D. Pezic, K.F. Toth, T. Bestor, and G.J. Hannon. 2008. A piRNA pathway primed by individual transposons is linked to de novo DNA methylation in mice. *Mol Cell*. 31:785-99.

Arita, K., M. Ariyoshi, H. Tochio, Y. Nakamura, and M. Shirakawa. 2008. Recognition of hemi-methylated DNA by the SRA protein UHRF1 by a base-flipping mechanism. *Nature*. 455:818-21.

Ashkenazi, A., L.G. Presta, S.A. Marsters, T.R. Camerato, K.A. Rosenthal, B.M. Fendly, and D.J. Capon. 1990. Mapping the CD4 binding site for human immunodeficiency virus by alanine-scanning mutagenesis. *Proc Natl Acad Sci U S A*. 87:7150-7154.

Avvakumov, G.V., J.R. Walker, S. Xue, Y. Li, S. Duan, C. Bronner, C.H. Arrowsmith, and S. Dhe-Paganon. 2008. Structural basis for recognition of hemi-methylated DNA by the SRA domain of human UHRF1. *Nature*. 455:822-5.

Bachman, K.E., B.H. Park, I. Rhee, H. Rajagopalan, J.G. Herman, S.B. Baylin, K.W. Kinzler, and B. Vogelstein. 2003. Histone modifications and silencing prior to DNA methylation of a tumor suppressor gene. *Cancer Cell*. 3:89-95.

Bachman, K.E., M.R. Rountree, and S.B. Baylin. 2001. Dnmt3a and Dnmt3b are transcriptional repressors that exhibit unique localization properties to heterochromatin. *J Biol Chem*. 276:32282-7.

Bacolla, A., S. Pradhan, R.J. Roberts, and R.D. Wells. 1999. Recombinant human DNA (cytosine-5) methyltransferase. II. Steady-state kinetics reveal allosteric activation by methylated dna. *J Biol Chem*. 274:33011-9.

Becker, P.B., and W. Horz. 2002. ATP-dependent nucleosome remodeling. *Annu Rev Biochem*. 71:247-73.

Bestor, T.H. 1992. Activation of mammalian DNA methyltransferase by cleavage of a Zn binding regulatory domain. *Embo J*. 11:2611-7.

Bestor, T.H., G. Gundersen, A.B. Kolsto, and H. Prydz. 1992. CpG islands in mammalian gene promoters are inherently resistant to de novo methylation. *Genet Anal Tech Appl*. 9:48-53.

Bird, A. 2002. DNA methylation patterns and epigenetic memory. *Genes Dev*. 16:6-21.

Bird, A.P. 1986. CpG-rich islands and the function of DNA methylation. *Nature*. 321:209-13.

Birke, M., S. Schreiner, M.P. Garcia-Cuellar, K. Mahr, F. Titgemeyer, and R.K. Slany. 2002. The MT domain of the proto-oncoprotein MLL binds to CpG-containing DNA and discriminates against methylation. *Nucleic Acids Res*. 30:958-65.

Bonapace, I.M., L. Latella, R. Papait, F. Nicassio, A. Sacco, M. Muto, M. Crescenzi, and P.P. Di Fiore. 2002. Np95 is regulated by E1A during mitotic reactivation of terminally differentiated cells and is essential for S phase entry. *J Cell Biol*. 157:909-14.

Bostick, M., J.K. Kim, P.O. Esteve, A. Clark, S. Pradhan, and S.E. Jacobsen. 2007. UHRF1 plays a role in maintaining DNA methylation in mammalian cells. *Science*. 317:1760-4.

Boxem, M., Z. Maliga, N. Klitgord, N. Li, I. Lemmens, M. Mana, L. de Lichtervelde, J.D. Mul, D. van de Peut, M. Devos, N. Simonis, M.A. Yildirim, M. Cokol, H.L. Kao, A.S. de Smet, H. Wang, A.L. Schlaitz, T. Hao, S. Milstein, C. Fan, M. Tipsword, K. Drew, M. Galli, K. Rhrissorrakrai, D. Drechsel, D. Koller, F.P. Roth, L.M. Iakoucheva, A.K. Dunker, R. Bonneau, K.C. Gunsalus, D.E. Hill, F. Piano, J. Tavernier, S. van den Heuvel, A.A. Hyman, and M. Vidal. 2008. A protein domain-based interactome network for C. elegans early embryogenesis. *Cell*. 134:534-45.

Boyer, L.A., T.I. Lee, M.F. Cole, S.E. Johnstone, S.S. Levine, J.P. Zucker, M.G. Guenther, R.M. Kumar, H.L. Murray, R.G. Jenner, D.K. Gifford, D.A. Melton, R. Jaenisch, and R.A. Young. 2005. Core transcriptional regulatory circuitry in human embryonic stem cells. *Cell*. 122:947-56.

Brooks, A.R., R.N. Harkins, P. Wang, H.S. Qian, P. Liu, and G.M. Rubanyi. 2004. Transcriptional silencing is associated with extensive methylation of the CMV promoter following adenoviral gene delivery to muscle. *J Gene Med*. 6:395-404.

Butler, J.S., J.H. Lee, and D.G. Skalnik. 2008. CFP1 interacts with DNMT1 independently of association with the Setd1 Histone H3K4 methyltransferase complexes. *DNA Cell Biol*. 27:533-43.

Caiafa, P., and M. Zampieri. 2005. DNA methylation and chromatin structure: the puzzling CpG islands. *J Cell Biochem*. 94:257-65.

Callebaut, I., J.C. Courvalin, and J.P. Mornon. 1999. The BAH (bromo-adjacent homology) domain: a link between DNA methylation, replication and transcriptional regulation. *FEBS Lett*. 446:189-93.

Chedin, F., M.R. Lieber, and C.L. Hsieh. 2002. The DNA methyltransferase-like protein DNMT3L stimulates de novo methylation by Dnmt3a. *Proc Natl Acad Sci U S A*. 99:16916-21.

Chen, T., N. Tsujimoto, and E. Li. 2004. The PWWP domain of Dnmt3a and Dnmt3b is required for directing DNA methylation to the major satellite repeats at pericentric heterochromatin. *Mol Cell Biol*. 24:9048-58.

Chen, T., Y. Ueda, J.E. Dodge, Z. Wang, and E. Li. 2003. Establishment and maintenance of genomic methylation patterns in mouse embryonic stem cells by Dnmt3a and Dnmt3b. *Mol Cell Biol*. 23:5594-605.

Cheng, X., and R.J. Roberts. 2001. AdoMet-dependent methylation, DNA methyltransferases and base flipping. *Nucleic Acids Res*. 29:3784-95.

Cho, S., S.G. Park, D.H. Lee, and B.C. Park. 2004. Protein-protein interaction networks: from interactions to networks. *J Biochem Mol Biol*. 37:45-52.

Choi, K.H., H. Basma, J. Singh, and P.W. Cheng. 2005. Activation of CMV promoter-controlled glycosyltransferase and beta -galactosidase glycogenes by butyrate, tricostatin A, and 5-aza-2'-deoxycytidine. *Glycoconj J*. 22:63-9.

Chuang, L.S., H.I. Ian, T.W. Koh, H.H. Ng, G. Xu, and B.F. Li. 1997. Human DNA-(cytosine-5) methyltransferase-PCNA complex as a target for p21WAF1. *Science*. 277:1996-2000.

Chuang, L.S., H.H. Ng, J.N. Chia, and B.F. Li. 1996. Characterisation of independent DNA and multiple Zn-binding domains at the N terminus of human DNA-(cytosine-5) methyltransferase: modulating the property of a DNA-binding domain by contiguous Zn-binding motifs. *J Mol Biol*. 257:935-48.

Citterio, E., R. Papait, F. Nicassio, M. Vecchi, P. Gomiero, R. Mantovani, P.P. Di Fiore, and I.M. Bonapace. 2004. Np95 is a histone-binding protein endowed with ubiquitin ligase activity. *Mol Cell Biol*. 24:2526-35.

Cokus, S.J., S. Feng, X. Zhang, Z. Chen, B. Merriman, C.D. Haudenschild, S. Pradhan, S.F. Nelson, M. Pellegrini, and S.E. Jacobsen. 2008. Shotgun bisulphite sequencing of the Arabidopsis genome reveals DNA methylation patterning. *Nature*. 452:215-9.

Cunningham, B.C., and J.A. Wells. 1989. High-resolution epitope mapping of hGH-receptor interactions by alanine-scanning mutagenesis. *Science*. 244:1081-1085.

De La Fuente, R., C. Baumann, T. Fan, A. Schmidtmann, I. Dobrinski, and K. Muegge. 2006. Lsh is required for meiotic chromosome synapsis and retrotransposon silencing in female germ cells. *Nat Cell Biol*. 8:1448-54.

Deane, C.M., L. Salwinski, I. Xenarios, and D. Eisenberg. 2002. Protein interactions: two methods for assessment of the reliability of high throughput observations. *Mol Cell Proteomics*. 1:349-56.

DeLano, W. 2002. The PyMOL User's Manual.

Deng, W.P., and J.A. Nickoloff. 1992. Site-directed mutagenesis of virtually any plasmid by eliminating a unique site. *Anal Biochem*. 200:81-8.

Dennis, K., T. Fan, T. Geiman, Q. Yan, and K. Muegge. 2001. Lsh, a member of the SNF2 family, is required for genome-wide methylation. *Genes Dev*. 15:2940-4.

Deplus, R., C. Brenner, W.A. Burgers, P. Putmans, T. Kouzarides, Y. de Launoit, and F. Fuks. 2002. Dnmt3L is a transcriptional repressor that recruits histone deacetylase. *Nucleic Acids Res*. 30:3831-8.

Dhayalan, A., T.P. Jurkowski, H. Laser, R. Reinhardt, D. Jia, X. Cheng, and A. Jeltsch. 2008. Mapping of protein-protein interaction sites by the 'absence of interference' approach. *J Mol Biol*. 376:1091-9.

Di Croce, L., V.A. Raker, M. Corsaro, F. Fazi, M. Fanelli, M. Faretta, F. Fuks, F. Lo Coco, T. Kouzarides, C. Nervi, S. Minucci, and P.G. Pelicci. 2002. Methyltransferase recruitment and DNA hypermethylation of target promoters by an oncogenic transcription factor. *Science*. 295:1079-82.

Dodge, J.E., B.H. Ramsahoye, Z.G. Wo, M. Okano, and E. Li. 2002. De novo methylation of MMLV provirus in embryonic stem cells: CpG versus non-CpG methylation. *Gene*. 289:41-8.

Domon, B., and R. Aebersold. 2006. Mass spectrometry and protein analysis. *Science*. 312:212-7.

Dong, A., J.A. Yoder, X. Zhang, L. Zhou, T.H. Bestor, and X. Cheng. 2001. Structure of human DNMT2, an enigmatic DNA methyltransferase homolog that displays denaturant-resistant binding to DNA. *Nucleic Acids Res*. 29:439-48.

Dong, A., L. Zhou, X. Zhang, S. Stickel, R.J. Roberts, and X. Cheng. 2004. Structure of the Q237W mutant of HhaI DNA methyltransferase: an insight into protein-protein interactions. *Biol Chem*. 385:373-9.

Durfee, T., K. Becherer, P.L. Chen, S.H. Yeh, Y. Yang, A.E. Kilburn, W.H. Lee, and S.J. Elledge. 1993. The retinoblastoma protein associates with the protein phosphatase type 1 catalytic subunit. *Genes Dev*. 7:555-69.

Easwaran, H.P., L. Schermelleh, H. Leonhardt, and M.C. Cardoso. 2004. Replication-independent chromatin loading of Dnmt1 during G2 and M phases. *EMBO Rep*. 5:1181-6.

Ekins, R., and F. Chu. 1992. Multianalyte microspot immunoassay. The microanalytical 'compact disk' of the future. *Ann Biol Clin (Paris)*. 50:337-53.

Epsztejn-Litman, S., N. Feldman, M. Abu-Remaileh, Y. Shufaro, A. Gerson, J. Ueda, R. Deplus, F. Fuks, Y. Shinkai, H. Cedar, and Y. Bergman. 2008. De novo DNA methylation promoted by G9a prevents reprogramming of embryonically silenced genes. *Nat Struct Mol Biol*. 15:1176-83.

Esteve, P.O., H.G. Chin, A. Smallwood, G.R. Feehery, O. Gangisetty, A.R. Karpf, M.F. Carey, and S. Pradhan. 2006. Direct interaction between DNMT1 and G9a coordinates DNA and histone methylation during replication. *Genes Dev*. 20:3089-103.

Fatemi, M., A. Hermann, S. Pradhan, and A. Jeltsch. 2001. The activity of the murine DNA methyltransferase Dnmt1 is controlled by interaction of the catalytic domain with the N-terminal part of the enzyme leading to an allosteric activation of the enzyme after binding to methylated DNA. *J Mol Biol*. 309:1189-99.

Feinberg, A.P., and B. Tycko. 2004. The history of cancer epigenetics. *Nat Rev Cancer*. 4:143-53.

Fellinger, K., H. Leonhardt, and F. Spada. 2008. A mutagenesis strategy combining systematic alanine scanning with larger mutations to study protein interactions. *Anal Biochem*. 373:176-8.

Ferguson-Smith, A.C., and J.M. Greally. 2007. Epigenetics: perceptive enzymes. *Nature*. 449:148-9.

Fields, S., and O. Song. 1989. A novel genetic system to detect protein-protein interactions. *Nature*. 340:245-6.

Fitzsimons, H.L., R.J. Bland, and M.J. During. 2002. Promoters and regulatory elements that improve adeno-associated virus transgene expression in the brain. *Methods*. 28:227-36.

Frauer, C., and H. Leonhardt. 2009. A versatile non-radioactive assay for DNA methyltransferase activity and DNA binding. *Nucleic Acids Res*.

Fuks, F., W.A. Burgers, N. Godin, M. Kasai, and T. Kouzarides. 2001. Dnmt3a binds deacetylases and is recruited by a sequence-specific repressor to silence transcription. *EMBO J*. 20:2536-44.

Fuks, F., P.J. Hurd, R. Deplus, and T. Kouzarides. 2003. The DNA methyltransferases associate with HP1 and the SUV39H1 histone methyltransferase. *Nucleic Acids Res*. 31:2305-12.

Gaudet, F., J.G. Hodgson, A. Eden, L. Jackson-Grusby, J. Dausman, J.W. Gray, H. Leonhardt, and R. Jaenisch. 2003. Induction of tumors in mice by genomic hypomethylation. *Science*. 300:489-92.

Gaudet, F., W.M. Rideout, 3rd, A. Meissner, J. Dausman, H. Leonhardt, and R. Jaenisch. 2004. Dnmt1 expression in pre- and postimplantation embryogenesis and the maintenance of IAP silencing. *Mol Cell Biol*. 24:1640-8.

Ge, Y.Z., M.T. Pu, H. Gowher, H.P. Wu, J.P. Ding, A. Jeltsch, and G.L. Xu. 2004. Chromatin targeting of de novo DNA methyltransferases by the PWWP domain. *J Biol Chem*. 279:25447-54.

Geiman, T.M., U.T. Sankpal, A.K. Robertson, Y. Zhao, and K.D. Robertson. 2004. DNMT3B interacts with hSNF2H chromatin remodeling enzyme, HDACs 1 and 2, and components of the histone methylation system. *Biochem Biophys Res Commun*. 318:544-55.

Glickman, J.F., J.G. Pavlovich, and N.O. Reich. 1997. Peptide mapping of the murine DNA methyltransferase reveals a major phosphorylation site and the start of translation. *J Biol Chem*. 272:17851-7.

Goll, M.G., F. Kirpekar, K.A. Maggert, J.A. Yoder, C.L. Hsieh, X. Zhang, K.G. Golic, S.E. Jacobsen, and T.H. Bestor. 2006. Methylation of tRNAAsp by the DNA methyltransferase homolog Dnmt2. *Science*. 311:395-8.

Gowher, H., K. Liebert, A. Hermann, G. Xu, and A. Jeltsch. 2005. Mechanism of stimulation of catalytic activity of Dnmt3A and Dnmt3B DNA-(cytosine-C5)-methyltransferases by Dnmt3L. *J Biol Chem*. 280:13341-8.

Goyal, R., P. Rathert, H. Laser, H. Gowher, and A. Jeltsch. 2007. Phosphorylation of serine-515 activates the Mammalian maintenance methyltransferase Dnmt1. *Epigenetics*. 2:155-60.

Grassi, G., P. Maccaroni, R. Meyer, H. Kaiser, E. D'Ambrosio, E. Pascale, M. Grassi, A. Kuhn, P. Di Nardo, R. Kandolf, and J.H. Kupper. 2003. Inhibitors of DNA methylation and histone deacetylation activate cytomegalovirus promoter-controlled reporter gene expression in human glioblastoma cell line U87. *Carcinogenesis*. 24:1625-35.

Hamers-Casterman, C., T. Atarhouch, S. Muyldermans, G. Robinson, C. Hamers, E.B. Songa, N. Bendahman, and R. Hamers. 1993. Naturally occurring antibodies devoid of light chains. *Nature*. 363:446-8.

Hashimoto, H., J.R. Horton, X. Zhang, M. Bostick, S.E. Jacobsen, and X. Cheng. 2008. The SRA domain of UHRF1 flips 5-methylcytosine out of the DNA helix. *Nature*. 455:826-9.

Hashimoto, H., J.R. Horton, X. Zhang, and X. Cheng. 2009. UHRF1, a modular multi-domain protein, regulates replication-coupled crosstalk between DNA methylation and histone modifications. *Epigenetics*. 4.

Hata, K., M. Okano, H. Lei, and E. Li. 2002. Dnmt3L cooperates with the Dnmt3 family of de novo DNA methyltransferases to establish maternal imprints in mice. *Development*. 129:1983-93.

Hejnar, J., P. Hajkova, J. Plachy, D. Elleder, V. Stepanets, and J. Svoboda. 2001. CpG island protects Rous sarcoma virus-derived vectors integrated into nonpermissive cells from DNA methylation and transcriptional suppression. *Proc Natl Acad Sci U S A*. 98:565-9.

Herman, J.G., A. Umar, K. Polyak, J.R. Graff, N. Ahuja, J.P. Issa, S. Markowitz, J.K. Willson, S.R. Hamilton, K.W. Kinzler, M.F. Kane, R.D. Kolodner, B. Vogelstein, T.A. Kunkel, and S.B. Baylin. 1998. Incidence and functional consequences of hMLH1 promoter hypermethylation in colorectal carcinoma. *Proc Natl Acad Sci U S A*. 95:6870-5.

Hogrefe, H.H., J. Cline, G.L. Youngblood, and R.M. Allen. 2002. Creating randomized amino acid libraries with the QuikChange Multi Site-Directed Mutagenesis Kit. *Biotechniques*. 33:1158-60, 1162, 1164-5.

Hopp, T.P., and K.R. Woods. 1981. Prediction of protein antigenic determinants from amino acid sequences. *Proc Natl Acad Sci U S A*. 78:3824-8.

Howlett, S.K., and W. Reik. 1991. Methylation levels of maternal and paternal genomes during preimplantation development. *Development*. 113:119-27.

Hu, C.D., Y. Chinenov, and T.K. Kerppola. 2002. Visualization of interactions among bZIP and Rel family proteins in living cells using bimolecular fluorescence complementation. *Mol Cell*. 9:789-98.

Hu, J.C., M.G. Kornacker, and A. Hochschild. 2000. Escherichia coli one- and two-hybrid systems for the analysis and identification of protein-protein interactions. *Methods*. 20:80-94.

Hu, Y.G., R. Hirasawa, J.L. Hu, K. Hata, C.L. Li, Y. Jin, T. Chen, E. Li, M. Rigolet, E. Viegas-Pequignot, H. Sasaki, and G.L. Xu. 2008. Regulation of DNA methylation activity through Dnmt3L promoter methylation by Dnmt3 enzymes in embryonic development. *Hum Mol Genet*. 17:2654-64.

Huang, J., T. Fan, Q. Yan, H. Zhu, S. Fox, H.J. Issaq, L. Best, L. Gangi, D. Munroe, and K. Muegge. 2004. Lsh, an epigenetic guardian of repetitive elements. *Nucleic Acids Res*. 32:5019-28.

Hyde, S.C., I.A. Pringle, S. Abdullah, A.E. Lawton, L.A. Davies, A. Varathalingam, G. Nunez-Alonso, A.M. Green, R.P. Bazzani, S.G. Sumner-Jones, M. Chan, H. Li, N.S. Yew, S.H. Cheng, A.C. Boyd, J.C. Davies, U. Griesenbach, D.J. Porteous, D.N. Sheppard, F.M. Munkonge, E.W. Alton, and D.R. Gill. 2008. CpG-free plasmids confer reduced inflammation and sustained pulmonary gene expression. *Nat Biotechnol*. 26:549-51.

Jach, G., M. Pesch, K. Richter, S. Frings, and J.F. Uhrig. 2006. An improved mRFP1 adds red to bimolecular fluorescence complementation. *Nat Methods*. 3:597-600.

Jeltsch, A. 2008. Reading and writing DNA methylation. *Nat Struct Mol Biol*. 15:1003-4.

Jenkins, Y., V. Markovtsov, W. Lang, P. Sharma, D. Pearsall, J. Warner, C. Franci, B. Huang, J. Huang, G.C. Yam, J.P. Vistan, E. Pali, J. Vialard, M. Janicot, J.B. Lorens, D.G. Payan, and Y. Hitoshi. 2005. Critical role of the ubiquitin ligase activity of UHRF1, a nuclear RING finger protein, in tumor cell growth. *Mol Biol Cell*. 16:5621-9.

Jia, D., R.Z. Jurkowska, X. Zhang, A. Jeltsch, and X. Cheng. 2007. Structure of Dnmt3a bound to Dnmt3L suggests a model for de novo DNA methylation. *Nature*. 449:248-51.

Jin, F., L. Avramova, J. Huang, and T. Hazbun. 2007. A yeast two-hybrid smart-pool-array system for protein-interaction mapping. *Nat Methods*. 4:405-7.

Jones, R.B., A. Gordus, J.A. Krall, and G. MacBeath. 2006. A quantitative protein interaction network for the ErbB receptors using protein microarrays. *Nature*. 439:168-74.

Jorgensen, H.F., I. Ben-Porath, and A.P. Bird. 2004. Mbd1 is recruited to both methylated and nonmethylated CpGs via distinct DNA binding domains. *Mol Cell Biol*. 24:3387-95.

Joung, J.K., E.I. Ramm, and C.O. Pabo. 2000. A bacterial two-hybrid selection system for studying protein-DNA and protein-protein interactions. *Proc Natl Acad Sci U S A*. 97:7382-7.

Jurkowska, R.Z., N. Anspach, C. Urbanke, D. Jia, R. Reinhardt, W. Nellen, X. Cheng, and A. Jeltsch. 2008. Formation of nucleoprotein filaments by mammalian DNA methyltransferase Dnmt3a in complex with regulator Dnmt3L. *Nucleic Acids Res*. 36:6656-63.

Jurkowski, T.P., M. Meusburger, S. Phalke, M. Helm, W. Nellen, G. Reuter, and A. Jeltsch. 2008. Human DNMT2 methylates tRNA(Asp) molecules using a DNA methyltransferase-like catalytic mechanism. *RNA*. 14:1663-70.

Kaneda, M., M. Okano, K. Hata, T. Sado, N. Tsujimoto, E. Li, and H. Sasaki. 2004. Essential role for de novo DNA methyltransferase Dnmt3a in paternal and maternal imprinting. *Nature*. 429:900-3.

Kanno, T., E. Bucher, L. Daxinger, B. Huettel, G. Bohmdorfer, W. Gregor, D.P. Kreil, M. Matzke, and A.J. Matzke. 2008. A structural-maintenance-of-chromosomes hinge domain-containing protein is required for RNA-directed DNA methylation. *Nat Genet*. 40:670-5.

Karagianni, P., L. Amazit, J. Qin, and J. Wong. 2008. ICBP90, a novel methyl K9 H3 binding protein linking protein ubiquitination with heterochromatin formation. *Mol Cell Biol*. 28:705-17.

Kareta, M.S., Z.M. Botello, J.J. Ennis, C. Chou, and F. Chedin. 2006. Reconstitution and mechanism of the stimulation of de novo methylation by human DNMT3L. *J Biol Chem*. 281:25893-902.

Kerppola, T.K. 2006. Visualization of molecular interactions by fluorescence complementation. *Nat Rev Mol Cell Biol*. 7:449-56.

Kim, G.D., J. Ni, N. Kelesoglu, R.J. Roberts, and S. Pradhan. 2002. Co-operation and communication between the human maintenance and de novo DNA (cytosine-5) methyltransferases. *Embo J*. 21:4183-95.

Kim, J.K., P.O. Esteve, S.E. Jacobsen, and S. Pradhan. 2008. UHRF1 binds G9a and participates in p21 transcriptional regulation in mammalian cells. *Nucleic Acids Res*.

Kimura, H., and K. Shiota. 2003. Methyl-CpG-binding protein, MeCP2, is a target molecule for maintenance DNA methyltransferase, Dnmt1. *J Biol Chem*. 278:4806-12.

Kirber, M.T., K. Chen, and J.F. Keaney, Jr. 2007. YFP photoconversion revisited: confirmation of the CFP-like species. *Nat Methods*. 4:767-8.

Kiskinis, E., M. Hallberg, M. Christian, M. Olofsson, S.M. Dilworth, R. White, and M.G. Parker. 2007. RIP140 directs histone and DNA methylation to silence Ucp1 expression in white adipocytes. *EMBO J*. 26:4831-40.

Klimasauskas, S., S. Kumar, R.J. Roberts, and X. Cheng. 1994. HhaI methyltransferase flips its target base out of the DNA helix. *Cell*. 76:357-69.

Kung, L.A., and M. Snyder. 2006. Proteome chips for whole-organism assays. *Nat Rev Mol Cell Biol*. 7:617-22.

Kuramochi-Miyagawa, S., T. Watanabe, K. Gotoh, Y. Totoki, A. Toyoda, M. Ikawa, N. Asada, K. Kojima, Y. Yamaguchi, T.W. Ijiri, K. Hata, E. Li, Y. Matsuda, T. Kimura, M. Okabe, Y. Sakaki, H. Sasaki, and T. Nakano. 2008. DNA methylation of retrotransposon genes is regulated by Piwi family members MILI and MIWI2 in murine fetal testes. *Genes Dev*. 22:908-17.

Lebowitz, J., M.S. Lewis, and P. Schuck. 2002. Modern analytical ultracentrifugation in protein science: a tutorial review. *Protein Sci*. 11:2067-79.

Lee, J.H., K.S. Voo, and D.G. Skalnik. 2001. Identification and characterization of the DNA binding domain of CpG-binding protein. *J Biol Chem*. 276:44669-76.

Lee, T.T., S. Agarwalla, and R.M. Stroud. 2005. A unique RNA Fold in the RumA-RNA-cofactor ternary complex contributes to substrate selectivity and enzymatic function. *Cell*. 120:599-611.

Lehnertz, B., Y. Ueda, A.A. Derijck, U. Braunschweig, L. Perez-Burgos, S. Kubicek, T. Chen, E. Li, T. Jenuwein, and A.H. Peters. 2003. Suv39h-mediated histone H3 lysine 9 methylation directs DNA methylation to major satellite repeats at pericentric heterochromatin. *Curr Biol*. 13:1192-200.

Lei, H., S.P. Oh, M. Okano, R. Juttermann, K.A. Goss, R. Jaenisch, and E. Li. 1996. De novo DNA cytosine methyltransferase activities in mouse embryonic stem cells. *Development*. 122:3195-205.

Leonhardt, H., and M.C. Cardoso. 2000. DNA methylation, nuclear structure, gene expression and cancer. *J Cell Biochem Suppl*. Suppl:78-83.

Leonhardt, H., A.W. Page, H.U. Weier, and T.H. Bestor. 1992. A targeting sequence directs DNA methyltransferase to sites of DNA replication in mammalian nuclei. *Cell*. 71:865-73.

Li, E. 2002. Chromatin modification and epigenetic reprogramming in mammalian development. *Nat Rev Genet*. 3:662-73.

Li, E., T.H. Bestor, and R. Jaenisch. 1992. Targeted mutation of the DNA methyltransferase gene results in embryonic lethality. *Cell*. 69:915-26.

Li, H., T. Rauch, Z.X. Chen, P.E. Szabo, A.D. Riggs, and G.P. Pfeifer. 2006. The histone methyltransferase SETDB1 and the DNA methyltransferase DNMT3A interact directly and localize to promoters silenced in cancer cells. *J Biol Chem*. 281:19489-500.

Li, J.Y., M.T. Pu, R. Hirasawa, B.Z. Li, Y.N. Huang, R. Zeng, N.H. Jing, T. Chen, E. Li, H. Sasaki, and G.L. Xu. 2007. Synergistic function of DNA methyltransferases Dnmt3a and Dnmt3b in the methylation of Oct4 and Nanog. *Mol Cell Biol*. 27:8748-59.

Liang, G., M.F. Chan, Y. Tomigahara, Y.C. Tsai, F.A. Gonzales, E. Li, P.W. Laird, and P.A. Jones. 2002. Cooperativity between DNA methyltransferases in the maintenance methylation of repetitive elements. *Mol Cell Biol*. 22:480-91.

Liu, Y., E.J. Oakeley, L. Sun, and J.P. Jost. 1998. Multiple domains are involved in the targeting of the mouse DNA methyltransferase to the DNA replication foci. *Nucleic Acids Res*. 26:1038-45.

Liu, Z., and R.A. Fisher. 2004. RGS6 interacts with DMAP1 and DNMT1 and inhibits DMAP1 transcriptional repressor activity. *J Biol Chem*. 279:14120-8.

MacBeath, G., and S.L. Schreiber. 2000. Printing proteins as microarrays for high-throughput function determination. *Science*. 289:1760-3.

Magliery, T.J., C.G. Wilson, W. Pan, D. Mishler, I. Ghosh, A.D. Hamilton, and L. Regan. 2005. Detecting protein-protein interactions with a green fluorescent protein fragment reassembly trap: scope and mechanism. *J Am Chem Soc*. 127:146-57.

Maherali, N., R. Sridharan, W. Xie, J. Utikal, S. Eminli, K. Arnold, M. Stadtfeld, R. Yachechko, J. Tchieu, R. Jaenisch, K. Plath, and K. Hochedlinger. 2007. Directly reprogrammed fibroblasts show global epigenetic remodeling and widespread tissue contribution. *Cell Stem Cell*. 1:55-70.

Margot, J.B., A.M. Aguirre-Arteta, B.V. Di Giacco, S. Pradhan, R.J. Roberts, M.C. Cardoso, and H. Leonhardt. 2000. Structure and function of the mouse DNA methyltransferase gene: Dnmt1 shows a tripartite structure. *J Mol Biol*. 297:293-300.

Margot, J.B., A.E. Ehrenhofer-Murray, and H. Leonhardt. 2003. Interactions within the mammalian DNA methyltransferase family. *BMC Mol Biol*. 4:7.

Matthews, B.W. 1996. Structural and genetic analysis of the folding and function of T4 lysozyme. *Faseb J*. 10:35-41.

Mehta, A.K., S.S. Majumdar, P. Alam, N. Gulati, and V. Brahmachari. 2009. Epigenetic regulation of cytomegalovirus major immediate-early promoter activity in transgenic mice. *Gene*. 428:20-4.

Meier, J.L. 2001. Reactivation of the human cytomegalovirus major immediate-early regulatory region and viral replication in embryonal NTera2 cells: role of trichostatin A, retinoic acid, and deletion of the 21-base-pair repeats and modulator. *J Virol*. 75:1581-93.

Min, J.H., and N.P. Pavletich. 2007. Recognition of DNA damage by the Rad4 nucleotide excision repair protein. *Nature*. 449:570-5.

Minc, E., J.C. Courvalin, and B. Buendia. 2000. HP1gamma associates with euchromatin and heterochromatin in mammalian nuclei and chromosomes. *Cytogenet Cell Genet*. 90:279-84.

Mortusewicz, O., L. Schermelleh, J. Walter, M.C. Cardoso, and H. Leonhardt. 2005. Recruitment of DNA methyltransferase I to DNA repair sites. *Proc Natl Acad Sci U S A*. 102:8905-9.

Murphy, J.C., W. Fischle, E. Verdin, and J.H. Sinclair. 2002. Control of cytomegalovirus lytic gene expression by histone acetylation. *EMBO J*. 21:1112-20.

Muto, M., Y. Kanari, E. Kubo, T. Takabe, T. Kurihara, A. Fujimori, and K. Tatsumi. 2002. Targeted disruption of Np95 gene renders murine embryonic stem cells hypersensitive to DNA damaging agents and DNA replication blocks. *J Biol Chem*. 277:34549-55.

Muyldermans, S., T. Atarhouch, J. Saldanha, J.A. Barbosa, and R. Hamers. 1994. Sequence and structure of VH domain from naturally occurring camel heavy chain immunoglobulins lacking light chains. *Protein Eng*. 7:1129-35.

Muyldermans, S., and M. Lauwereys. 1999. Unique single-domain antigen binding fragments derived from naturally occurring camel heavy-chain antibodies. *J Mol Recognit*. 12:131-40.

Muyldermans, S., and A.A. Travers. 1994. DNA sequence organization in chromatosomes. *J Mol Biol*. 235:855-70.

Myant, K., and I. Stancheva. 2008. LSH cooperates with DNA methyltransferases to repress transcription. *Mol Cell Biol*. 28:215-26.

Nagano, T., J.A. Mitchell, L.A. Sanz, F.M. Pauler, A.C. Ferguson-Smith, R. Feil, and P. Fraser. 2008. The Air noncoding RNA epigenetically silences transcription by targeting G9a to chromatin. *Science*. 322:1717-20.

Nakagawa, M., M. Koyanagi, K. Tanabe, K. Takahashi, T. Ichisaka, T. Aoi, K. Okita, Y. Mochiduki, N. Takizawa, and S. Yamanaka. 2008. Generation of induced pluripotent stem cells without Myc from mouse and human fibroblasts. *Nat Biotechnol*. 26:101-6.

Ohsawa, K., Y. Imai, D. Ito, and S. Kohsaka. 1996. Molecular cloning and characterization of annexin V-binding proteins with highly hydrophilic peptide structure. *J Neurochem*. 67:89-97.

Okano, M., D.W. Bell, D.A. Haber, and E. Li. 1999. DNA methyltransferases Dnmt3a and Dnmt3b are essential for de novo methylation and mammalian development. *Cell*. 99:247-57.

Okano, M., S. Xie, and E. Li. 1998. Cloning and characterization of a family of novel mammalian DNA (cytosine-5) methyltransferases. *Nat Genet*. 19:219-20.

Okita, K., T. Ichisaka, and S. Yamanaka. 2007. Generation of germline-competent induced pluripotent stem cells. *Nature*. 448:313-7.

Ong, S.E., and M. Mann. 2005. Mass spectrometry-based proteomics turns quantitative. *Nat Chem Biol*. 1:252-62.

Ooi, S.K., C. Qiu, E. Bernstein, K. Li, D. Jia, Z. Yang, H. Erdjument-Bromage, P. Tempst, S.P. Lin, C.D. Allis, X. Cheng, and T.H. Bestor. 2007. DNMT3L connects unmethylated lysine 4 of histone H3 to de novo methylation of DNA. *Nature*. 448:714-7.

Palii, S.S., and K.D. Robertson. 2007. Epigenetic control of tumor suppression. *Crit Rev Eukaryot Gene Expr*. 17:295-316.

Papait, R., C. Pistore, U. Grazini, F. Babbio, S. Cogliati, D. Pecoraro, L. Brino, A.L. Morand, A.M. Dechampesme, F. Spada, H. Leonhardt, F. McBlane, P. Oudet, and I.M. Bonapace. 2008. The PHD domain of Np95 (mUHRF1) is involved in large-scale reorganization of pericentromeric heterochromatin. *Mol Biol Cell*. 19:3554-63.

Papait, R., C. Pistore, D. Negri, D. Pecoraro, L. Cantarini, and I.M. Bonapace. 2007. Np95 is implicated in pericentromeric heterochromatin replication and in major satellite silencing. *Mol Biol Cell*. 18:1098-106.

Parker, J.B., M.A. Bianchet, D.J. Krosky, J.I. Friedman, L.M. Amzel, and J.T. Stivers. 2007. Enzymatic capture of an extrahelical thymine in the search for uracil in DNA. *Nature*. 449:433-7.

Periasamy, A. 2001. Fluorescence resonance energy transfer microscopy: a mini review. *J Biomed Opt*. 6:287-91.

Phair, R.D., and T. Misteli. 2001. Kinetic modelling approaches to in vivo imaging. *Nat Rev Mol Cell Biol*. 2:898-907.

Phillips, K.S., and Q. Cheng. 2007. Recent advances in surface plasmon resonance based techniques for bioanalysis. *Anal Bioanal Chem*. 387:1831-40.

Pradhan, M., P.O. Esteve, H.G. Chin, M. Samaranayke, G.D. Kim, and S. Pradhan. 2008. CXXC domain of human DNMT1 is essential for enzymatic activity. *Biochemistry*. 47:10000-9.

Qiu, C., K. Sawada, X. Zhang, and X. Cheng. 2002. The PWWP domain of mammalian DNA methyltransferase Dnmt3b defines a new family of DNA-binding folds. *Nat Struct Biol*. 9:217-24.

Reale, A., G.D. Matteis, G. Galleazzi, M. Zampieri, and P. Caiafa. 2005. Modulation of DNMT1 activity by ADP-ribose polymers. *Oncogene*. 24:13-9.

Robertson, K.D., S. Ait-Si-Ali, T. Yokochi, P.A. Wade, P.L. Jones, and A.P. Wolffe. 2000. DNMT1 forms a complex with Rb, E2F1 and HDAC1 and represses transcription from E2F-responsive promoters. *Nat Genet*. 25:338-42.

Rothbauer, U., K. Zolghadr, S. Muyldermans, A. Schepers, M.C. Cardoso, and H. Leonhardt. 2008. A versatile nanotrap for biochemical and functional studies with fluorescent fusion proteins. *Mol Cell Proteomics*. 7:282-9.

Rottach, A., E. Kremmer, D. Nowak, H. Leonhardt, and M.C. Cardoso. 2008. Generation and characterization of a rat monoclonal antibody specific for multiple red fluorescent proteins. *Hybridoma (Larchmt)*. 27:337-43.

Rountree, M.R., K.E. Bachman, and S.B. Baylin. 2000. DNMT1 binds HDAC2 and a new co-repressor, DMAP1, to form a complex at replication foci. *Nat Genet*. 25:269-77.

Santos, F., B. Hendrich, W. Reik, and W. Dean. 2002. Dynamic reprogramming of DNA methylation in the early mouse embryo. *Dev Biol*. 241:172-82.

Sawamura, D., R. Abe, M. Goto, M. Akiyama, H. Hemmi, S. Akira, and H. Shimizu. 2005. Direct injection of plasmid DNA into the skin induces dermatitis by activation of monocytes through toll-like receptor 9. *J Gene Med*. 7:664-71.

Schermelleh, L., A. Haemmer, F. Spada, N. Rosing, D. Meilinger, U. Rothbauer, M.C. Cardoso, and H. Leonhardt. 2007. Dynamics of Dnmt1 interaction with the replication machinery and its role in postreplicative maintenance of DNA methylation. *Nucleic Acids Res*. 35:4301-12.

Schermelleh, L., F. Spada, H.P. Easwaran, K. Zolghadr, J.B. Margot, M.C. Cardoso, and H. Leonhardt. 2005. Trapped in action: direct visualization of DNA methyltransferase activity in living cells. *Nat Methods*. 2:751-6.

Schmidt, E.V., G. Christoph, R. Zeller, and P. Leder. 1990. The cytomegalovirus enhancer: a pan-active control element in transgenic mice. *Mol Cell Biol*. 10:4406-11.

Schultz, D.C., K. Ayyanathan, D. Negorev, G.G. Maul, and F.J. Rauscher, 3rd. 2002. SETDB1: a novel KAP-1-associated histone H3, lysine 9-specific methyltransferase that contributes to HP1-mediated silencing of euchromatic genes by KRAB zinc-finger proteins. *Genes Dev*. 16:919-32.

Sharif, J., M. Muto, S. Takebayashi, I. Suetake, A. Iwamatsu, T.A. Endo, J. Shinga, Y. Mizutani-Koseki, T. Toyoda, K. Okamura, S. Tajima, K. Mitsuya, M. Okano, and H. Koseki. 2007. The SRA protein Np95 mediates epigenetic inheritance by recruiting Dnmt1 to methylated DNA. *Nature*. 450:908-12.

Spada, F., A. Haemmer, D. Kuch, U. Rothbauer, L. Schermelleh, E. Kremmer, T. Carell, G. Langst, and H. Leonhardt. 2007. DNMT1 but not its interaction with the replication machinery is required for maintenance of DNA methylation in human cells. *J Cell Biol*. 176:565-71.

Stec, I., S.B. Nagl, G.J. van Ommen, and J.T. den Dunnen. 2000. The PWWP domain: a potential protein-protein interaction domain in nuclear proteins influencing differentiation? *FEBS Lett*. 473:1-5.

Stein, R., Y. Gruenbaum, Y. Pollack, A. Razin, and H. Cedar. 1982. Clonal inheritance of the pattern of DNA methylation in mouse cells. *Proc Natl Acad Sci U S A*. 79:61-5.

Suetake, I., F. Shinozaki, J. Miyagawa, H. Takeshima, and S. Tajima. 2004. DNMT3L stimulates the DNA methylation activity of Dnmt3a and Dnmt3b through a direct interaction. *J Biol Chem*. 279:27816-23.

Suzuki, H., D.N. Watkins, K.W. Jair, K.E. Schuebel, S.D. Markowitz, W.D. Chen, T.P. Pretlow, B. Yang, Y. Akiyama, M. Van Engeland, M. Toyota, T. Tokino, Y. Hinoda, K. Imai, J.G. Herman, and S.B. Baylin. 2004. Epigenetic inactivation of SFRP genes allows constitutive WNT signaling in colorectal cancer. *Nat Genet*. 36:417-22.

Takahashi, K., and S. Yamanaka. 2006. Induction of pluripotent stem cells from mouse embryonic and adult fibroblast cultures by defined factors. *Cell*. 126:663-76.

Taketo, M.M. 2004. Shutting down Wnt signal-activated cancer. *Nat Genet*. 36:320-2.

Tam, O.H., A.A. Aravin, P. Stein, A. Girard, E.P. Murchison, S. Cheloufi, E. Hodges, M. Anger, R. Sachidanandam, R.M. Schultz, and G.J. Hannon. 2008. Pseudogene-derived small interfering RNAs regulate gene expression in mouse oocytes. *Nature*. 453:534-8.

Tatematsu, K.I., T. Yamazaki, and F. Ishikawa. 2000. MBD2-MBD3 complex binds to hemi-methylated DNA and forms a complex containing DNMT1 at the replication foci in late S phase. *Genes Cells*. 5:677-88.

Templin, M.F., D. Stoll, J.M. Schwenk, O. Potz, S. Kramer, and T.O. Joos. 2003. Protein microarrays: promising tools for proteomic research. *Proteomics*. 3:2155-66.

Uemura, T., E. Kubo, Y. Kanari, T. Ikemura, K. Tatsumi, and M. Muto. 2000. Temporal and spatial localization of novel nuclear protein NP95 in mitotic and meiotic cells. *Cell Struct Funct*. 25:149-59.

Unoki, M., T. Nishidate, and Y. Nakamura. 2004. ICBP90, an E2F-1 target, recruits HDAC1 and binds to methyl-CpG through its SRA domain. *Oncogene*. 23:7601-10.

Valentin, G., C. Verheggen, T. Piolot, H. Neel, M. Coppey-Moisan, and E. Bertrand. 2005. Photoconversion of YFP into a CFP-like species during acceptor photobleaching FRET experiments. *Nat Methods*. 2:801.

Varga-Weisz, P.D., and P.B. Becker. 2006. Regulation of higher-order chromatin structures by nucleosome-remodelling factors. *Curr Opin Genet Dev*. 16:151-6.

Vidal, M. 2005. Interactome modeling. *FEBS Lett*. 579:1834-8.

Vidal, M., R.K. Brachmann, A. Fattaey, E. Harlow, and J.D. Boeke. 1996a. Reverse two-hybrid and one-hybrid systems to detect dissociation of protein-protein and DNA-protein interactions. *Proc Natl Acad Sci U S A*. 93:10315-20.

Vidal, M., P. Braun, E. Chen, J.D. Boeke, and E. Harlow. 1996b. Genetic characterization of a mammalian protein-protein interaction domain by using a yeast reverse two-hybrid system. *Proc Natl Acad Sci U S A*. 93:10321-6.

Vidal, M., and P. Legrain. 1999. Yeast forward and reverse 'n'-hybrid systems. *Nucleic Acids Res*. 27:919-29.

Villuendas, G., A. Gutierrez-Adan, A. Jimenez, C. Rojo, E.R. Roldan, and B. Pintado. 2001. CMV-driven expression of green fluorescent protein (GFP) in male germ cells of transgenic mice and its effect on fertility. *Int J Androl*. 24:300-5.

Vire, E., C. Brenner, R. Deplus, L. Blanchon, M. Fraga, C. Didelot, L. Morey, A. Van Eynde, D. Bernard, J.M. Vanderwinden, M. Bollen, M. Esteller, L. Di Croce, Y. de Launoit, and F. Fuks. 2006. The Polycomb group protein EZH2 directly controls DNA methylation. *Nature*. 439:871-4.

Vojtek, A.B., S.M. Hollenberg, and J.A. Cooper. 1993. Mammalian Ras interacts directly with the serine/threonine kinase Raf. *Cell*. 74:205-14.

Walker, J.R., Avvakumov, G.V., Xue, S., Dong, A., Li, Y., Bountra, C., Weigelt, J., Arrowsmith, C.H., Edwards, A.M., Bochkarev, A., Dhe-Paganon, S. 2008a. Crystal structure of the tandem tudor domains of the E3 ubiquitin-protein ligase UHRF1 in complex with trimethylated histone H3-K9 peptide *Structural Genomics Consortium (SGC)*

Walker, J.R., Avvakumov, G.V., Xue, S., Li, Y., Bountra, C., Weigelt, J., Arrowsmith, C.H., Edwards, A.M., Bochkarev, A., Dhe-Paganon, S. . 2008b. Structure of the replication foci-targeting sequence of human DNA cytosine methyltransferase DNMT1. *Structural Genomics Consortium (SGC)*

Watanabe, T., Y. Totoki, A. Toyoda, M. Kaneda, S. Kuramochi-Miyagawa, Y. Obata, H. Chiba, Y. Kohara, T. Kono, T. Nakano, M.A. Surani, Y. Sakaki, and H. Sasaki. 2008. Endogenous siRNAs from naturally formed dsRNAs regulate transcripts in mouse oocytes. *Nature*. 453:539-43.

Wernig, M., A. Meissner, J.P. Cassady, and R. Jaenisch. 2008. c-Myc is dispensable for direct reprogramming of mouse fibroblasts. *Cell Stem Cell*. 2:10-2.

Wernig, M., A. Meissner, R. Foreman, T. Brambrink, M. Ku, K. Hochedlinger, B.E. Bernstein, and R. Jaenisch. 2007. In vitro reprogramming of fibroblasts into a pluripotent ES-cell-like state. *Nature*. 448:318-24.

Wilson, G.G., and N.E. Murray. 1991. Restriction and modification systems. *Annu Rev Genet*. 25:585-627.

Wu, J.C., and D.V. Santi. 1987. Kinetic and catalytic mechanism of HhaI methyltransferase. *J Biol Chem*. 262:4778-86.

Xie, S., Z. Wang, M. Okano, M. Nogami, Y. Li, W.W. He, K. Okumura, and E. Li. 1999. Cloning, expression and chromosome locations of the human DNMT3 gene family. *Gene*. 236:87-95.

Xu, G.L., T.H. Bestor, D. Bourc'his, C.L. Hsieh, N. Tommerup, M. Bugge, M. Hulten, X. Qu, J.J. Russo, and E. Viegas-Pequignot. 1999. Chromosome instability and immunodeficiency syndrome caused by mutations in a DNA methyltransferase gene. *Nature*. 402:187-91.

Yamada, Y., L. Jackson-Grusby, H. Linhart, A. Meissner, A. Eden, H. Lin, and R. Jaenisch. 2005. Opposing effects of DNA hypomethylation on intestinal and liver carcinogenesis. *Proc Natl Acad Sci U S A*. 102:13580-5.

Yang, C.G., C. Yi, E.M. Duguid, C.T. Sullivan, X. Jian, P.A. Rice, and C. He. 2008. Crystal structures of DNA/RNA repair enzymes AlkB and ABH2 bound to dsDNA. *Nature*. 452:961-5.

Yang, L., Q. Mei, A. Zielinska-Kwiatkowska, Y. Matsui, M.L. Blackburn, D. Benedetti, A.A. Krumm, G.J. Taborsky, Jr., and H.A. Chansky. 2003. An ERG (ets-related gene)-associated histone methyltransferase interacts with histone deacetylases 1/2 and transcription co-repressors mSin3A/B. *Biochem J*. 369:651-7.

Yang, L., L. Xia, D.Y. Wu, H. Wang, H.A. Chansky, W.H. Schubach, D.D. Hickstein, and Y. Zhang. 2002. Molecular cloning of ESET, a novel histone H3-specific methyltransferase that interacts with ERG transcription factor. *Oncogene*. 21:148-52.

Yoder, J.A., N.S. Soman, G.L. Verdine, and T.H. Bestor. 1997. DNA (cytosine-5)-methyltransferases in mouse cells and tissues. Studies with a mechanism-based probe. *J Mol Biol*. 270:385-95.

Yu, J., M.A. Vodyanik, K. Smuga-Otto, J. Antosiewicz-Bourget, J.L. Frane, S. Tian, J. Nie, G.A. Jonsdottir, V. Ruotti, R. Stewart, Slukvin, II, and J.A. Thomson. 2007. Induced pluripotent stem cell lines derived from human somatic cells. *Science*. 318:1917-20.

Zhang, X., and G.L. Verdine. 1996. Mammalian DNA cytosine-5 methyltransferase interacts with p23 protein. *FEBS Lett*. 392:179-83.

Zhou, Q., A.T. Agoston, P. Atadja, W.G. Nelson, and N.E. Davidson. 2008. Inhibition of histone deacetylases promotes ubiquitin-dependent proteasomal degradation of DNA methyltransferase 1 in human breast cancer cells. *Mol Cancer Res*. 6:873-83.

Zhu, B., G. Cai, E.O. Hall, and G.J. Freeman. 2007. In-Fusion assemby: seamless engeneering of multidomain fusion proteins, modular vectors, and mutations. *BioTechniques*. 43:354-359.

Zimmermann, C., E. Guhl, and A. Graessmann. 1997. Mouse DNA methyltransferase (MTase) deletion mutants that retain the catalytic domain display neither de novo nor maintenance methylation activity in vivo. *Biol Chem*. 378:393-405.

Zolghadr, K., O. Mortusewicz, U. Rothbauer, R. Kleinhans, H. Goehler, E.E. Wanker, M.C. Cardoso, and H. Leonhardt. 2008. A fluorescent two-hybrid (F2H) assay for direct visualization of protein interactions in living cells. *Mol Cell Proteomics*. 7:2279-87.

4.2 Contributions

*Declaration of contributions to "*A mutagenesis strategy combining systematic alanine scanning with larger mutations to study protein interactions*."*

This project was conceived by Heinrich Leonhardt and me. I designed the mutagenesis strategy, performed all the experiments, prepared the figures and composed the first draft of the manuscript. The final version of the manuscript was written with Fabio Spada and Heinrich Leonhardt.

Declaration of contributions to "Dimerization of DNA methyltransferase 1 is mediated by its regulatory domain."

This project was initiated based on preliminary observations of Ulrich Rothbauer who contributed Figure 1A. I conceived the study together with Heinrich Leonhardt and Gernot Längst. Max Felle cloned the TS domain in a bacterial expression vector, performed protein purification and gelfiltration analysis (Figure 3A). I generated the majority of the expression constructs, confirmed the gelfiltration result, performed all the co-immunoprecipitation experiments and immunoblots. I prepared all the figures and wrote the manuscript with the help of Heinrich Leonhardt.

*Declaration of contributions to "*Np95 interacts with *de novo* DNA methyltransferases Dnmt3a and 3b and mediates epigenetic silencing."

This study was conceived by Heinrich Leonhardt and Fabio Spada. Daniela Meilinger developed the ESC silencing assay and performed the silencing experiments with the help of Sebastian Bultmann; cell sorting was done together with Wolfgang Klinkert.

I designed and performed all biochemical experiments and identified and mapped the interactions described. I cloned all the Dnmt3a/b mutant constructs, performed co-immunoprecipitation experiments and immunoblots. I contributed and prepared Figure 1, Supplementary Figures 1, 2, 3, wrote the corresponding figure legends and materials and methods sections. I wrote the manuscript with Daniela Meilinger, Fabio Spada and Heinrich Leonhardt.

4.3 Declaration According to the "Promotionsordnung der LMU München für die Fakultät Biologie"

Betreuung: Hiermit erkläre ich, dass die vorgelegte Arbeit an der LMU von Herrn Prof. Dr. Leonhardt betreut wurde.

Anfertigung: Hiermit versichere ich ehrenwörtlich, dass die Dissertation selbstständig und ohne unerlaubte Hilfsmittel angefertigt wurde. Über Beiträge, die im Rahmen der kumulativen Dissertation in Form von Manuskripten in der Dissertation enthalten sind, wurde im Kapitel 4.2 Rechenschaft abgelegt und die eigenen Leistungen wurden aufgelistet.

Prüfung: Hiermit erkläre ich, dass die Dissertation weder als ganzes noch in Teilen an einem anderen Ort einer Prüfungskommission vorgelegt wurde. Weiterhin habe ich weder an einem anderen Ort eine Promotion angestrebt oder angemeldet oder versucht eine Doktorprüfung abzulegen.

München, den 28. Januar 2009

_____

Karin Fellinger

4.4 Abbreviations

5-aza-dC	5-aza-2'-deoxycytidine
5mC	5 methyl-cytosine
aa	amino acids
amp	ampicilline
B2H	bacterial two-hybrid
BAH	bromo adjacent homology domain
BiFC	bimolecular flouresence complementation
blast	blasticidine
CAG	chicken beta actin
CFP	cyan fluorescent protein
CGBP	CpG binding protein
CMT	C-terminus of DNA methyltransferase
CMV	cytomegalie virus
CpG	cytosine-phosphatidyl-guanine
DAPI	4',6-diamidino-2'-phenylindole dihydrochloride
dC	deoxycytidine
DMR	differentially methylated region
Dnmt	DNA methyltransferase
DRM2	domains rearranged methylase 2
ESCs	ES cells
ESI	electrospray ionization
F2H	fluorescence two-hybrid
FRAP	fluorescence recovery after photo bleaching
FRET	fluorescence resonance energy transfer
GBP	GFP binding protein
genet	geneticine
GFP	green fluorescent protein
GST	gluthathione-S-transferase
HDACs	histone deacetylases
HP1	heterochromatin protein 1
IAP	intracisternal A-type particle
ICF	immunodeficiency, centromere instability and facial anomalies
IPS	induced pluripotent stem cell
kana	kanamycine
MBD	methyl CpG binding domain
MeCP2	Methyl CpG binding protein 2
MLL	mixed lineage leukemia
MT	methyltransferase
mRFP	monomeric red fluorescent protein
MS	mass spectrometer
neo	neomycine
NLS	nuclear localization signal
NMT	N-terminus of DNA methyltransferase
NMR	nuclear magnetic resonance
Np	nuclear protein

Orc1p	origin recognition complex 1
p	plasmid
PAGE	polyacrylamide gelelectrophoresis
PBD	PCNA binding domain
pc	plasmid collection
PCNA	proliferating cell nuclear antigen
PCR	polymerase chain reaction
PDB	Protein Data Bank
PH	pericentic heterochromatin
PHD	plant homeo domain
PWWP	proline-tryptophane-tryptophane-proline motif
RF	replication foci
RING	really interesting new gene
SAM	S-adenosyl-L-methionine
SDM	site-directed mutagenesis
SDS	sodium dodecylsulfate
SETDB1	suppressor of variegation, enhancer of zeste and trithorax domain bifurcated 1
Sirp1	silent information regulator 1
SPR	surface plasmon resonance
SRA	SET and RING associated domain
SUV39H1	suppressor of variegation 3-9 homolog 1
TKO	*dnmt1*$^{-/-}$*3a*$^{-/-}$*3b*$^{-/-}$ triple knockout ESCs
TLR 9	toll-like receptor 9
$tRNA_{Asp}$	transfer ribonucleic acid for aspartic acid
TS	targeting sequence
UAS	upstream activator sequence
UBL	ubiquitin-like domain
UHRF1	ubiquitin-like, containing PHD and RING finger domains 1
wt	wildtype
Y2H	yeast two-hybrid
YFP	yellow fluorescent protein
ZnF	zinc finger

4.5 List of Expression Constructs

Table 4.1 All expression constructs that were cloned during this work are listed. Nomenclature: pc, plasmid collection; p, plasmid, eG, eGFP; Ch, Cherry; CMT, C-terminus of Dnmt; NMT, N-terminus of Dnmt; numbers indicate amino acid positions; V, version; NLS, nuclear localization signal; CAG, chicken beta-actin promoter; PHD, plant homeo domain; PWWP, pro-trp-trp-pro motif containing domain; MT, methyltransferase; kana, kanamycine, neo, neomycine; genet; geneticine, amp, ampicilline, blast, blasticidine. Plasmids generated by PCR were confirmed by DNA sequencing. A detailed description of these plasmids was entered in the laboratory information database and is available upon request.

pc number	Dnmt1	Restriction sites used for cloning	Antibiotic resistances
1376	pChmCMT1his(1124-1620)	BsrGI, XbaI	kana, neo, genet
1377	peGNMT1(1-1111)	BsrGI, HindIII	kana, neo, genet
1431	peGNMT1(1-309)	BsrGI, HindIII	kana, neo, genet
1432	peGNMT1(630-1111)	BsrGI, HindIII	kana, neo, genet
1454	peGMT1L_V2	Oligo replaced linker	kana, neo, genet
1455	peGMT1L_V3	Oligo replaced SacII site	kana, neo, genet
1456	peGNMT1(1-1111)V2	Oligo replaced SacII site	kana, neo, genet
1481	peGMT1L_EDS553AAA	SalI, BglII	kana, neo, genet
1482	peGMT1L_VVS563AAA	SalI, BglII	kana, neo, genet
1489	peGMT1L_TTT622AAA	SalI, BglII	kana, neo, genet
1491	peGNMT1_EDS553AAA	SalI, BglII	kana, neo, genet
1492	peGNMT1_VVS563AAA	SalI, BglII	kana, neo, genet
1493	peGNMT1_DDE576AAA	SalI, BglII	kana, neo, genet
1494	peGNMT1_CMR586AAA	SalI, BglII	kana, neo, genet
1495	peGNMT1_GVS595AAA	SalI, BglII	kana, neo, genet
1496	peGNMT1_GQR599AAA	SalI, BglII	kana, neo, genet
1497	peGNMT1_RRV605AAA	SalI, BglII	kana, neo, genet
1498	peGNMT1_KAP616AAA	SalI, BglII	kana, neo, genet
1514	peGMT1L_dEDS-DDE	XhoI, SacII, XmaI	kana, neo, genet
1515	peGMT1L_dVVS-DDE	XhoI, SacII, XmaI	kana, neo, genet
1593	peGMT1L S515A	SalI, BglII	kana, neo, genet
1594	peGMT1L S515D	SalI, BglII	kana, neo, genet
1595	peGNMT1(1-1111) S515A	SalI, BglII	kana, neo, genet
1596	peGNMT1(1-1111) S515D	SalI, BglII	kana, neo, genet
1637	peGNMT1(1-1111)ENP451AAA	XhoI, SacII, XmaI	kana, neo, genet
1638	peGNMT1(1-1111)GEK478AAA	XhoI, SacII, XmaI	kana, neo, genet
1639	peGNMT1(1-1111)SKE498AAA	XhoI, SacII, XmaI	kana, neo, genet
1671	peGNMT1(1-1111)SKi515AAA	XhoI, SacII, XmaI	kana, neo, genet
1672	peGNMT1(1-1111)EDL531AAA	XhoI, SacII, XmaI	kana, neo, genet
1673	peGNMT1(1-1111)d478-498	XhoI, SacII, XmaI	kana, neo, genet

pc number	Dnmt1 TS domain	Restriction sites used for cloning	Antibiotic resistances
1375	pChmTShis(310-629)	BsrGI, XbaI	kana, neo, gene
1433	peGmTS(309-410)	BsrGI, HindIII	kana, neo, genet
1434	peGmTS(411-523)	BsrGI, HindIII	kana, neo, genet
1435	peGmTS(524-629)	BsrGI, HindIII	kana, neo, genet
1442	pNLSeGmTS_EDS553AAA	XhoI, SacII, XmaI	kana, neo, genet
1443	pNLSeGmTS_GQR599AAA	XhoI, SacII, XmaI	kana, neo, genet
1444	pNLSeGmTS_GVS595AAA	XhoI, SacII, XmaI	kana, neo, genet
1445	pNLSeGmTS_KAP616AAA	XhoI, SacII, XmaI	kana, neo, genet
1446	pNLSeGmTS_RRV605AAA	XhoI, SacII, XmaI	kana, neo, genet
1447	pNLSeGmTS_TTT622AAA	XhoI, SacII, XmaI	kana, neo, genet
1448	pNLSeGmTS_VVS563AAA	XhoI, SacII, XmaI	kana, neo, genet
1449	pNLSeGmTS_CMR586AAA	XhoI, SacII, XmaI	kana, neo, genet
1508	peGmTS dEDS-VVS(553-565)	XhoI, SacII, XmaI	kana, neo, genet
1509	peGmTS dEDS-DDE(553-578)	XhoI, SacII, XmaI	kana, neo, genet
1511	peGmTS dEDS-CMR(553-588)	XhoI, SacII, XmaI	kana, neo, genet
1512	peGmTS dVVS-CMRS(563-578)	XhoI, SacII, XmaI	kana, neo, genet
1513	peGmTS_DDE576AAA	XhoI, SacII, XmaI	kana, neo, genet
1531	pChmTS_EDS553AAA	XhoI, SacII, XmaI	kana, neo, genet
1532	pChmTS_VVS563AAA	XhoI, SacII, XmaI	kana, neo, genet
1533	pChmTS_DDE576AAA	XhoI, SacII, XmaI	kana, neo, genet
1534	pChmTS_CMR586AAA	XhoI, SacII, XmaI	kana, neo, genet
1541	peGmTS(310-629)	XhoI, XmaI	kana, neo, genet
1542	peGmTS(310-588)	XhoI, XmaI	kana, neo, genet
1543	peGmTS(310-550)	XhoI, XmaI	kana, neo, genet
1544	peGmTS(310-502)	XhoI, XmaI	kana, neo, genet
1545	peGmTS(361-629)	XhoI, XmaI	kana, neo, genet
1546	peGmTS(410-629)	XhoI, XmaI	kana, neo, genet
1547	peGmTS(475-629)	XhoI, XmaI	kana, neo, genet
1548	peGmTS(310-629)EDS553AAA	XhoI, SacII, XmaI	kana, neo, genet
1549	peGmTSdEDS-DDE(310-629)	XhoI, SacII, XmaI	kana, neo, genet
1581	peGmTSdVVS-CMR(310-629)	XhoI, SacII, XmaI	kana, neo, genet
1588	peGmTS(310-475)	XhoI, XmaI	kana, neo, genet
1589	peGmTS(310-409)	XhoI, XmaI	kana, neo, genet
1591	peGmTS(503-629)	XhoI, XmaI	kana, neo, genet
1592	peGmTS(551-629)	XhoI, XmaI	kana, neo, genet
1601	peChmTS(310-550)	XhoI, XmaI	kana, neo, genet

1602	peChmTS(310-502)	XhoI, XmaI	kana, neo, genet
1603	peChmTS(410-629)	XhoI, XmaI	kana, neo, genet
1604	peChmTS(476-629)	XhoI, XmaI	kana, neo, genet
1605	peChmTS(310-475)	XhoI, XmaI	kana, neo, genet
1606	peChmTS(310-409)	XhoI, XmaI	kana, neo, genet
1607	peChmTS(503-629)	XhoI, XmaI	kana, neo, genet
1608	peChmTS(551-629)	XhoI, XmaI	kana, neo, genet
1609	peGmTS(310-629) DER315AAA	XhoI, SacII, XmaI	kana, neo, genet
1611	peGmTS(310-629) SER340AAA	XhoI, SacII, XmaI	kana, neo, genet
1612	peGmTS(310-629) EDA378AAA	XhoI, SacII, XmaI	kana, neo, genet
1613	peGmTS(310-629) EDS406AAA	XhoI, SacII, XmaI	kana, neo, genet
1614	peGmTS(310-629) EKN435AAA	XhoI, SacII, XmaI	kana, neo, genet
1615	peGmTS(310-629)ENP451AAA	XhoI, SacII, XmaI	kana, neo, genet
1617	peGmTS(310-629)SKE498AAA	XhoI, SacII, XmaI	kana, neo, genet
1618	peGmTS(310-629)SKI515AAA	XhoI, SacII, XmaI	kana, neo, genet
1619	peGmTS(310-629)EDL531AAA	XhoI, SacII, XmaI	kana, neo, genet
1621	peGmTS(310-629)d478-498	XhoI, SacII, XmaI	kana, neo, genet
1675	pChmTS(310-629)d478-498	XhoI, SacII, XmaI	kana, neo, genet

pc number	Dnmt3a	Restriction sites used for cloning	Antibiotic resistances
1749	pCAG-eGMT3a2	AsiSI, NotI	amp, blast
1831	pCAG-eGMT3a dPWWP	AsiSI, NotI	amp, blast
1832	pCAG-eGMT3a dPHD	AsiSI, NotI	amp, blast
1833	pCAG-eGMT3a 1-629	AsiSI, NotI	amp, blast
1834	pCAG-eGMT3a 630-908	AsiSI, NotI	amp, blast

pc number	Dnmt3b	Restriction sites used for cloning	Antibiotic resistances
1751	pCAG-eGMT3b6	AsiSI, NotI	amp, blast
1752	pCAG-eGMT3b7	AsiSI, NotI	amp, blast
1753	pCAG-eGMT3b8	AsiSI, NotI	amp, blast
1835	pCAG-eGMT3b dPWWP	AsiSI, NotI	amp, blast
1836	pCAG-eGMT3b dPHD	AsiSI, NotI	amp, blast
1837	pCAG-eGMT3b 1-584	AsiSI, NotI	amp, blast
1838	pCAG-eGMT3b 585-863	AsiSI, NotI	amp, blast

4.6 Acknowledgements

I would like to thank Prof. Heinrich Leonhardt for giving me the unique opportunity to conduct my PhD research in his lab, for his support, ideas and fruitful discussions that contributed a lot to this work.

I am very grateful to Prof. Peter Becker and Dr. Friedrich Lottspeich for their participation in my thesis advisory committee, their interest and input for my work.

A very, very special thanks goes to Andrea Rottach who is a great colleague and friend – thank you for everything!

I thank our lab manager Anja Gahl who was always a great help and taking care that everything ran smoothly and Daniela Meilinger who also helped ordering and organizing things.

I would like to thank Kourosh Zolghadr and Oliver Mortusewicz for their help with computers, microscopes and the nice office atmosphere.

I thank Fabio Spada and Ulrich Rothbauer for valuable discussions and of course Uli for tons of GFP-Binder!

I would like to thank all labmembers for the open and friendly atmosphere which made it a pleasure to work with you all.

Also, I thank Hans-Joerg Schaeffer, coordinator of the IMPRS program for the organization of all the interesting workshops and seminars.

I am deeply grateful to my family for their lifelong support and motivation.
Most of all I would like to thank Peter, who always believed in me, encouraged me, made me happy and thereby supported fundamentally this work.

5. Curriculum Vitae

Personal Information:

Name	Karin Rosa Fellinger
Date of birth	05.05.1981
Place of Birth	Munich
Nationality	German
Current work address	Ludwig Maximilians University (LMU) Munich Department of Biology II, LMU Biocenter Großhadernerstr. 2, 82152 Martinsried-Planegg, Germany

Education:

09/2005 – present ***Munich***	PhD at the International Max Planck Research School for Molecular and Cellular Life Sciences (IMPRS - LS) Ludwig Maximilians University Munich, Prof. Leonhardt
10/2002 – 03/2005 ***Munich***	Studies of Biology: Diplom Advanced Study Period; Technical University (TU) Munich
10/2000–09/2002 ***Erlangen***	Basic Studies of Biology: Vordiplom Friedrich - Alexander University (FAU) Erlangen - Nürnberg
1991–2000	Secondary Education: Gymnasium Geretsried, Abitur
1987–1991	Primary Education: Grundschule am Isardamm, Geretsried

Scientific Experience:

05/2005 – 07/2005 ***Paris***	Laboratoire de Génétique Humaine des Maladies Infectieuses, INSERM U550, Prof. Casanova
04/2004 – 09/2004 ***Munich***	Institute for Medical Microbiology, Immunology and Hygiene of the Technical University of Munich; Prof. Wagner, Prof. Förster
11/2003 – 02/2004 ***Munich***	Molecular Oncology, Head and Neck Research Department, Clinics Großhadern; Dr. Gires
11/2002 – 02/2003 ***Townsville***	Australian Institute of Marine Science (AIMS); Dr. Hall, Dr. Bourne

List of Publications:

Fellinger K*, Meilinger D*, Bultmann S, Bonapace M, Klinkert WEF, Spada F, Leonhardt H (2009) Np95 interacts with *de novo* DNA methyltransferases Dnmt3a and3b and mediates epigenetic silencing. *EMBO Rep*, **under review**. *KF and DM contributed equally to this work.

Fellinger K, Rothbauer U, Felle M, Längst G, Leonhardt (2009) Dimerization of DNA methyltransferase 1 is mediated by ist regulatory domain. *J Cell Biochem,* **in production**.

Fellinger K, Leonhardt H, Spada F (2008) A mutagenesis strategy combining systematic alanine scanning with larger mutations to study protein interactions. *Anal Biochem* **373** (1): 176-178.

Munz M*, Fellinger K*, Hofmann T, Schmitt B, Gires O (2008) Glycosylation is crucial for stability of tumor and cancer stem cell antigen EpCAM. *Front Biosci* 13:5195-5201. *MM and KF contributed equally to this work.

Ruf P, Gires O, Jager M, Fellinger K, Atz J, Lindhofer H (2007) Characterisation of the new EpCAM-specific antibody HO-3: implications for trifunctional antibody immunotherapy of cancer. *Br J Cancer* **97**(3)**:** 315-321

Filipe-Santos O, Bustamante J, Haverkamp MH, Vinolo E, Ku CL, Puel A, Frucht DM, Christel K, von Bernuth H, Jouanguy E, Feinberg J, Durandy A, Senechal B, Chapgier A, Vogt G, de Beaucoudrey L, Fieschi C, Picard C, Garfa M, Chemli J, Bejaoui M, Tsolia MN, Kutukculer N, Plebani A, Notarangelo L, Bodemer C, Geissmann F, Israel A, Veron M, Knackstedt M, Barbouche R, Abel L, Magdorf K, Gendrel D, Agou F, Holland SM, Casanova JL (2006) X-linked susceptibility to mycobacteria is caused by mutations in NEMO impairing CD40-dependent IL-12 production. *J Exp Med* **203**(7)**:** 1745-1759